Institute of Thermoelectricity, Academy of Sciences and Ministry of Education and Science of Ukraine

Journal of THERMOELECTRICITY

International Research

Founded in December, 1993

published 6 times a year

No. 1 *2017*

Editorial Board

International Editorial Board

Founders – National Academy of Sciences, Ukraine
Institute of Thermoelectricity of National Academy of Sciences and Ministry of Education and Science of Ukraine

Certificate of state registration № КВ 15496-4068 ПР

Approved for printing by the Academic Council of Institute of Thermoelectricity of the National Academy of Sciences and Ministry of Education and Science, Ukraine

Address of editorial office:
Ukraine, 58002, Chernivtsi, General Post Office, P.O. Box 86.
Phone: +(380-372) 90 31 65.
Fax: +(380-3722) 4 19 17.
E-mail: jt@inst.cv.ua
http://www.jt.inst.cv.ua

Signed for publication 25.01.17. Format 70×108/16. Offset paper №1. Offset printing.
Printer's sheet 11.5. Publisher's signature 9.2. Circulation 400 copies. Order 5.

Printed from the layout original made by "Journal of Thermoelectricity" editorial board in the printing house of "Bukrek" publishers,
10, Radischev Str., Chernivtsi, 58000, Ukraine

CONTENTS

* – publication of the lectures presented at the XVII International Forum on Thermoelectricity

M. A. Korzhuev *cand. fiz.-mat. science*, **M. A. Kretova, I. V. Katin**

A. A. Baikov Institute of Metallurgy and Materials Science
Leninskiy prosp., 49, Moscow 119991, Russia,
e-mail: korzhuev@ultra.imet.ac.ru

CONTRIBUTION OF THE ACADEMICIAN E. CH. LENTZ TO THE DEVELOPMENT OF MODERN THERMOELECTRICITY

Considered the works of the academician of the St. Petersburg Academy of Sciences E. Ch. Lenz (1804-1865) and his students – Ch. E. Lenz (son) (1833-1903) and M. P. Avenarius (1835-1895), contributed to the development of modern thermoelectricity (TE). Bibl. 25, Fig. 9, Tabl. 4.
Key words: thermoelectricity; academician E. Ch. Lenz; the Lenz rule for induction; the Joule-Lens law; the Peltier efftct; maximum power mode of thermocouple; automobile thermoelectric generators.

Introduction

St. Petersburg Academy of Sciences (SPb AS) since its foundation (1724) specialized in natural-scientific research, many of which were carried out at the intersection of various sciences [1-3]. In particular, in 1745-1803 employees of St. Petersburg Academy of Sciences investigated the cross-effects "electricity-heat" observed in thermoelectric-active media as some dielectrics and liquid electrolytes [4-7]. Acad. G.-W. Rikhman (1711-1753) studied in detail the thermo-electric effect in sulfur and resins (1746). Acad. M. V.Lomonosov (1711-1765) described complex thermoelectric phenomena in the Earth's atmosphere that determine the charge of clouds (1753) [4, 5]. Acad. F. T. U. Aepinus (1724-1802), invited to work in St. Petersburg Academy of Sciences from Germany (1757), explained the pyroelectric effect in the tourmaline discovered by him in 1756 [6]. In turn, acad. V. V. Petrov (1763-1814) observed (1804) thermoelectric effects in galvanic cells (GC), which are metal-electrolyte-metal systems with mixed electron-ion conductivity [7].

At the beginning of the nineteenth century, the scientific and technological revolution in Europe covered energy, communications (telegraph) and transport (railways) [8]. Accordingly, the interest of researchers in the new fields of the electricity has increased especially to electromagnetism, electrodynamics, and electromagnetic induction. A new impulse of development was also received the theory of thermoelectricity [9, 10].

In 1821 T. I. Seebeck (1770-1831), working in Jena (Germany), discovered a thermoelectric effect in metallic thermocouples (*Bi-Cu* and *Bi-Sb*), which occurs when one of the junctions of thermocouples is heated or cooled. The discovery of thermoelectricity in conducting media[1] has increased the interest in further research in this field [8-13]. In 1834, J. Peltier (1785-1845) (France), investigating the *Bi-Sb* thermocouple, established that when the electric current was passed through a thermocouple, depending on the direction of the current, its working junction could not only be heated

[1] "This beautiful form of electricity" – according to M. Faraday [14]. In contrast to thermoelectrics – dielectrics and GC, operating in the "charge-discharge" mode, current sources based on metal thermocouples operate in a continuous mode, which is of considerable practical interest [13].

but also cooled [8-10]. Finally, in 1856W. Thomson (Kelvin) (1824-1907) discovered the third thermoelectric effect (Thomson effect) associated with the release (absorption) of additional heat in conductors with current in the presence of temperature gradients in them [8-10]. This work is a continuation of research on the history of thermoelectricity in Russia [4-7]. Below we consider the work in the field of thermoelectricity, carried out in 1833-1884 by acad. St. Petersburg Academy of Sciences E. Ch. Lenz (1804-1865) [15, 16] and his students – corresponding member of St. Petersburg Academy Ch. E. Lenz (son) (1833-1903) and M. P. Avenarius (1835-1895) [9. 12, 17].

1. A Brief Historical Reference

Emil Christianovich Lentz (Fig. 1) was born in the family of Christian Heinrich Friedrich Lenz († 1817), the Chief Secretary of the magistrate of Dorpat (Russian: Yuriev, now Tartu, Estonia). The family belonged to an old Germanic Ostsee family. After the death of his father, with the support of the Lutheran community of Dorpat, he entered the Natural Science Department of the Dorpat University, opened in 1802 by Emperor Alexander I [3, 12, and 15][2].

Fig. 1. Lenz Emily Christianovich (German: Heinrich Friedrich Emil Lenz) (1804, Dorpat – 1865, Rome). He studied at the University of Dorpat. In 1827 he completed a thesis at Heidelberg University. Since 1828 – adjunct, and since 1834 – Academician of St. Petersburg Academy of Sciences. Head of the Physical Cabinet of St. Petersburg Academy of Sciences (1830-1865). Professor of the Department of Physics and Physical Geography of St. Petersburg University. (1836), Dean of the Faculty of Physics and Mathematics (1840), Rector (1863) [11, 12]. The secret counselor [2]. (Official portrait of the RAS [3]).

Teacher and mentor of E. Ch. Lentz was the rector of the university – a well-known physicist, E. I. Parrot (Fig. 2), who was on friendly terms with Emperor Alexander I.[3] In 1823, Parrot, who evaluated Lentz's abilities for science, recommended him as a research physicist to the round-the-world expedition of Captain Otto Evstafievich (Otton Augustovich) von Kocebu (1788-1846) on the sloop "Enterprise" (1823-1826) [18]. For the needs of the expedition, Parrot and Lenz in a short time jointly developed new scientific instruments: a depth-gage and a bathometer (a device for taking water samples and determining its temperature at various depths) [15].[4]

During the expedition, Lenz conducted many oceanographic, meteorological and geophysical studies. He took samples of water from various depths, was engaged in determining its salinity, density, temperature, and studied ocean currents. As a result, he obtained the dependence of salinity of

[2] Dorpat University (formerly Academia Gustaviana) was founded in 1644 by the Swedish king Gustav I Adolf and ceased to exist after the Northern War in 1712. Restored by order (1799) of Emperor Paul I (1754-1801) in connection with the ban on Russian students to study abroad.

[3] E. I. Parrot first described the phenomenon of osmosis, developed the designs of medical thermometers widely used to date. Reorganized the *Physical Cabinet* of St. Petersburg Academy of Sciences (1830-1840) [1, 12].

[4] Known tip E. I. Parrot about E. Ch. Lenz: "For old age, it is encouraging to train young scientists who replace us and help us with the kind of art and courtesy that Mr. Lenz has repeatedly shown" (1840).

sea water on the strength of winds and the amount of sunlight: for example, at the equator, with the greatest amount of sunlight, the winds are not strong. The vapors formed during evaporation remain above the sea surface and prevent further evaporation. Therefore, at the equator, the salinity of the water is less than to the north and south of it, where the trade winds are blowing [15]. Lenz also established that the reason for the occurrence of ocean currents are not only winds, as previously thought, but also differences in the density of water in different latitudes. In addition, it was possible to show that deep waters can be cooled to temperatures below + 4°C. When studying the atmospheric processes, Lenz paid special attention to the action of the energy of sunlight, which they called the main reason [15].

Fig. 2. Parrot Egor Ivanovich (German: Parrot Georg Friedrich von) (1767, Duchy of Württemberg – 1852, Helsingfors), Rector of the Dorpatt (Yuryev) University (1801), corresponding member (1811) and academician of St. Petersburg Academy of Sciences in applied mathematics (1826) and in physics (1830), honorary member (1840). Head of the Physical Cabinet of St. Petersburg Academy of Sciences (1830-1840). Actual State Councilor. (The lithography in Yuriev University).

Lenz returned from the expedition by an experienced and skillful physicist-experimenter. He settled in St. Petersburg and devoted the next year to processing the results. The oceanographic studies of the scientist became the subject of a dissertation, which he successfully defended in 1827 at Heidelberg University. In February 1828 the scientist submitted a report to the St. Petersburg Academy of Sciences: “The physical observations made during the round-the-world trip under the command of Captain Otto von Kocebu in 1823, 1824, 1825 and 1826” [11, 15], as a result, in May 1828 Lenz unanimously Elected as an adjunct in physic of the St. Petersburg Academy of Sciences. In 1829-1830 Lenz took part in the expedition to Elbrus. Due to the deep snow cover, it was not possible to reach the summit (600 feet left). However, at the reached point of recovery, Lenz made measurements of atmospheric pressure, over which he established approximately the height of the peak (5642 m). In May 1830, Lents returned to St. Petersburg, where he was elected an extraordinary academician [11, 15].

The experimental investigations in the field of electrophysics E. Ch. Lents began in 1831; the work conducted in the Physical Cabinet of St. Petersburg Academy of Sciences [1, 11, and 15]. The main works of E. H. Lents in the field of electrophysics are presented in Table 1. The sign (*) in Table 1 indicates works directly related to thermoelectricity, others refer to current sources that are widely used for supplying thermocouples.

2. The main results of the work of E. H. Lentz in the field of electrophysics

2.1. Verification of Ohm's law

In 1831, Lenz constructed a sensitive galvanometer, which confirmed the validity of the basic law of electric circuits – Ohm's law, discovered by G. S. Ohm (1787-1854) in 1826 (1, Table 1). It is

believed that largely due to the results of high-precision measurements carried out by Lenz, Ohm's law received definitive recognition among physicists [12, 15].

2.2. Lenz's induction rule

In 1831, M. Faraday (1791-1887) discovered the phenomenon of electromagnetic induction [14]. Learning about this discovery, Lentz immediately began research, whose goal was to determine the general laws of this phenomenon. (2, Table 1) [15]. Lenz was interested in establishing a general rule for the direction of the induction current, which Faraday defined as applied to various particular cases of interaction of moving magnets with conductors, as well as conductors with current to each other.

Table 1

The main results of the work of E. Ch. Lentz (1804-1865) on electromagnetism and thermoelectricity[5]

№	Year	Works	Formula	Ref.
1	1831	Verification of Ohm's Law *	$I = U/R$	[15]
2	1833	The Lenz induction rule *	$E = -\Delta\Phi/\Delta t$	[8,15]
3	1833	The principle of equivalence of electrical machines	-	[11]
4	1835	Temperature dependence of the electrical resistivity of metals (*Cu*, brass, *Fe*, *Pt*, *Ag*, *Au*, *Pb*, *Sn*)*	$R \sim R_0\Delta T$	[8, 15]
5	1838	Confirmation of the Peltier effect and freezing of water with a thermocouple *Bi-Sb**	-	[16]
6	1842 1843	a) The Joule-Lenz law* b) The Lenz rule (½) for maximum heat release on the load*	$Q = I^2R$ $R = r$	[10, 15] [10, 15]
7	1847	The reaction of the armature of electromagnetic machines (Together with B. S. Jacobi (1801-1804))	-	[15]
8	1847	Experiments on the polarization of GE electrodes (Together with A. S. Savelyev (1820-1860))	-	[15]

Lentz repeated the experiments of M. Faraday (Fig. 3) and found a rule later named after him[6].

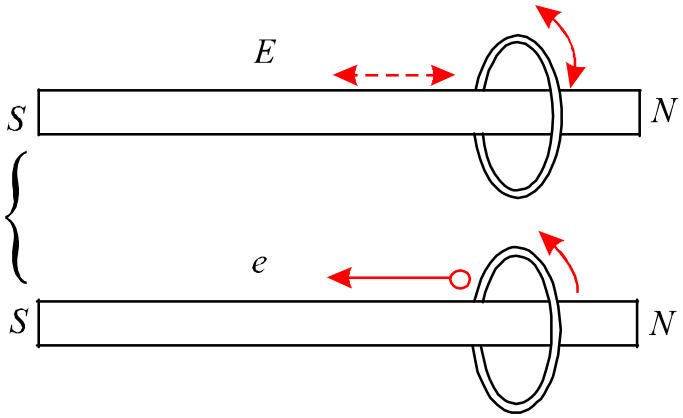

Fig. 3. Schemes of Lenz experiments by induction with permanent magnets and circular conductors consisting of 20 turns of braided copper wire [15].

[5] Here: *I, U* and *R* are current, voltage and resistance of the circuit; *E* is the induction voltage; Φ and *t* are the magnetic flux and time; R_0 is the resistance of the metal at room temperature; ΔT is the temperature change; *Q* is the heat released on the load; *r* is the internal resistance of the current source.

[6] M. Faraday never referred to the work of Lenz in his works on electromagnetic induction [14].

According to the Lenz rule (2, Table 1), the induction current has such a direction that the flux of magnetic induction created by it through the area bounded by the contour tends to compensate for the change in the flux $\Delta\Phi$ that causes this current. Later it was found out that Lenz's rule has a great degree of generality and is connected with the law of conservation and transformation of energy, as well as with the principle of stability of thermodynamic systems.

In 1847 the G. Helmholtz (1821-1894) mathematically substantiated the law of conservation of energy and showed that the Lenz rule is a consequence of this law in the field of electromagnetic phenomena. In 1884-1887 Lenz's rule was generalized by A. Le-Chatelier (1850-1936) to chemical reactions and by C. Brown (1850-1918) – on various physical phenomena [12]. According to the Le-Chatelier-Brown principle (LCB), if a system in stable equilibrium is influenced from outside by changing any of the equilibrium conditions (temperature, pressure, concentration, external electromagnetic field), then the processes aimed at compensation of external impact. The principle of LCB is applicable to an equilibrium of any nature – mechanical, thermal, chemical, electrical. It is also widely used in the field of thermoelectricity [9].

2.3. The principle of reversibility of electrical machines

In 1833 Lenz discovered the possibility of a reversible conversion of a magneto-electric machine into an electric motor (3, Table 1) [11]. Transformations of the electric machine (generator) into the electric motor are carried out by its simple connection to the current source, the reverse transformation – by mechanical rotation of the rotor of the electric motor. The reversibility of electric machines is explained by the same device of converters of electrical energy into mechanical energy and mechanical energy into electrical energy. Now this discovery of Lenz is widely used in electrical engineering, for example, for electrodynamic braking of trains.

2.4. Temperature dependence of electrical resistance of metals

In 1835, Lenz conducted a highly accurate measurement of the temperature dependence of the electrical resistance R of a number of metals. (Brass, *Cu*, *Fe*, *Pt*, *Ag*, *Au*, *Pb*, *Sn*) (4, Table 1) [8, 11]. He showed that when the temperature rises above room temperature, the resistance of R metals increases, and when cooled, it decreases linearly. According to M. Laue [8], the decrease in the resistivity R of metals with decreasing temperature, discovered by Lenz, was a new and unexpected discovery in the field of electrical conductivity, which stimulates subsequent studies in low-temperature physics. Later, Kamerling-Ones (1853-1926) showed that in *Au*, *Ag*, and *Cu* there is some "residual" resistance R_0 below which it does not decrease with decreasing temperature. On the other hand, in *Hg*, *Pb*, *Sn*, *Tl*, and some other metals, the phenomenon of superconductivity was discovered – the disappearance of the resistance to electric current ($R = 0$) below a certain critical temperature. On the other hand, in *Hg*, *Pb*, *Sn*, *Tl*, and some other metals, the phenomenon of superconductivity was discovered – the disappearance of the resistance to electric current ($R = 0$) below a certain critical temperature T_c (1913) [8, 10, 12].

2.5. Checking the Peltier effect

In 1834, Jean Charles Peltier (1785-1845) discovered a new thermoelectric effect, the reverse of the Seebeck effect. The effect consisted in simultaneous heating and cooling of various junctions of the thermocouple when electric current was passed through it [8, 10]. For the experiments, Peltier used a thermocouple in the form of a cross (Fig. 4a), welded from dissimilar metals *n-Bi* and *p-Sb*. (Here *n-* and *p-* denote the electron and hole types of conductivity of materials). Through the ends *A* and *C* of

the cross (Fig. 4a) Peltier passed an electric current, the change in the junction temperature he determined by the indications of the galvanometer *G*, connected to the free ends of the cross at the points *B* and *D*. Depending on the direction of the operating current in the AC circuit, the readings of the galvanometer *G* indicated either heating or cooling of the working junction.

Contemporaries Peltier – A. S. Becquerel (1788-1878), A. O. De La Reeve (1801-1873) and others reacted with distrust to his experiments [9]. Doubts caused a small effect (temperature difference $\Delta T \sim 1$ K), as well as a non-standard measurement scheme ΔT, assembled without the necessary electrical isolation of working and measuring circuits (Fig. 4a). Lenz decided to repeat the experiments of Peltier using a standard mercury thermometer (Fig. 4b). He described the results of his experiments (5, Table 1) in the journals of the St. Petersburg Academy of Sciences "Bulletin Scientifique de l'Academie Imperials des Sciences" [15] and "Libraries for reading" (Fig. 5) [16].

For his experiments, Lenz used rectangular samples of *Bi* and *Sb* with a length of 4½ inches (English), a width and height of 4 lines (10.16 mm), the mass of the thermocouple was 215.8 g. The thermoelectric characteristics of the branches of the *Bi-Sb* thermocouple are given in Table 2 [19]. At the first stage of the study, the Peltier measurement scheme was used (Fig. 4a), for which the branches of the *Bi* and *Sb* thermocouples were soldered by tin in the middle. The current source in this experiment was a galvanic element (GE) of Volts with *Zn* and *Pt* electrodes, similar in parameters to the GE used by Peltier (emf $E = 1.1$ V). The effects of cooling and heating the working junction of the thermocouple were fixed by a galvanometer, and also using a mercury thermometer of Reaumur with a ball of small diameter ($D = 2$ lines (~ 5, 12 mm)) (Fig. 4). The results of the studies (Table 3) showed that the cooling effect observed by Peltier with the aid of the circuit (Fig. 4a) does indeed exist, but it is sufficiently small ($\Delta T_{cool} \sim 0.84$ K). When the direction of the current *I* was changed, the working junction of the thermocouple was heated ($\Delta T_{heat} \sim 3.96$ K) (Table 3).

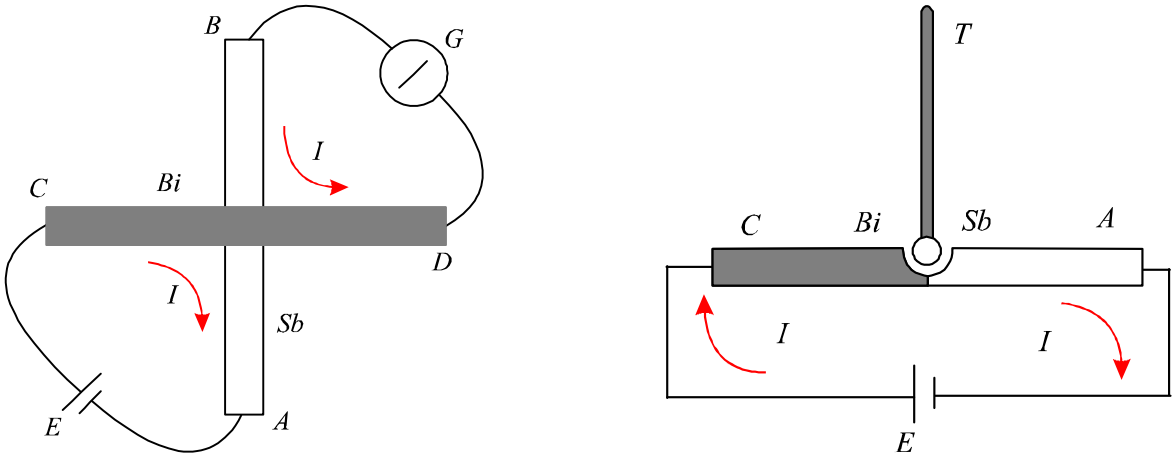

Fig. 4. The Peltier thermoelectric cross (Bi- Sb) (a) [9] and the Lenz scheme with the mercury thermometer T (b), which we reconstructed according to the verbal description given in [16]. The polarity of the voltages and the direction of the currents in the circuits (arrows) correspond to the cooling effect of the working junction of thermocouple.

Lenz explained the small values of ΔT_{cool} by supplying heat to the working junction of the thermocouple from the measuring ends of the cross (Fig. 4a). As a result, he abandoned the measurement scheme (Fig. 4a). And proposed his original scheme for measuring the Peltier effect, where the branches of the thermocouple were soldered at the ends (Fig. 4b). In the area of the working

junction of the obtained thermocouple, a hole for the thermometer was drilled (Fig. 4b). The circuit was powered by a Volta element with *Zn* and *Pt* electrodes of increased power (the area of the plates was 1 square foot (~ 900 cm^2)). With the help of the scheme (Fig. 4b), Lenz managed to increase ΔT_{cool} to ~ 3.5 K (Table 3) and to demonstrate for the first time the freezing of a drop of water with the help of the Peltier effect. To do this, a drop of water was placed in the deepen on the working junction of the thermocouple (Fig. 4b). The branches of the thermocouple were cooled with snow to a temperature T~ 0°R (°C) and held at this temperature for 10 min. Then the current of the necessary direction was turned on, the freezing time of the drop of water under the current was 3 min [16].

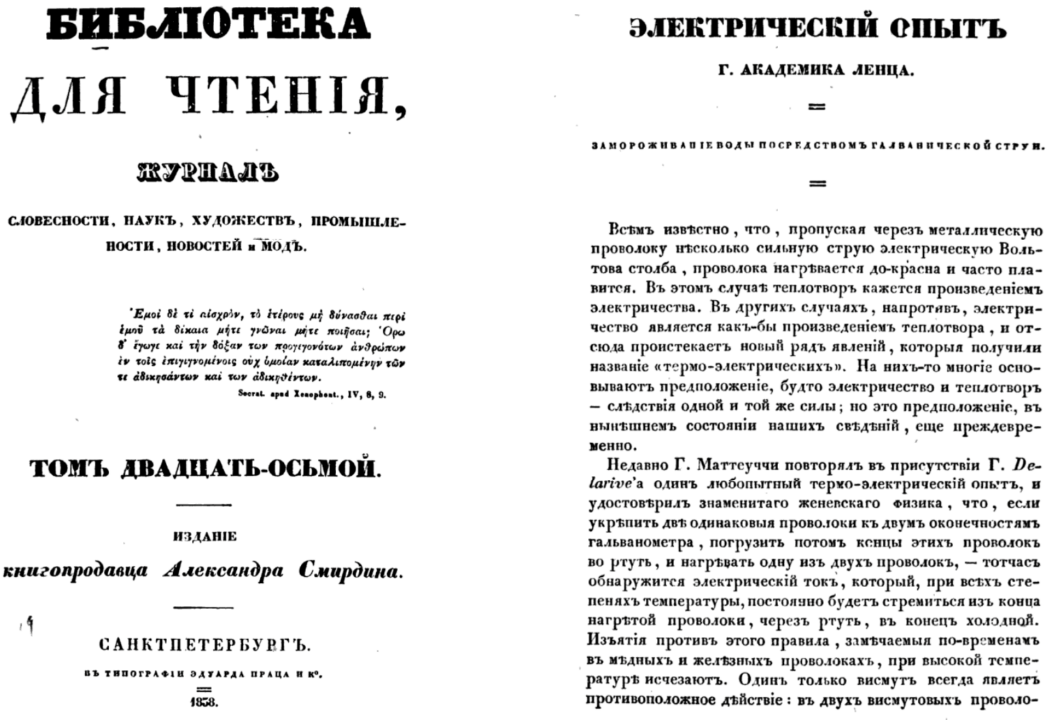

БИБЛІОТЕКА
ДЛЯ ЧТЕНІЯ,
ЖУРНАЛЪ
СЛОВЕСНОСТИ, НАУКЪ, ХУДОЖЕСТВЪ, ПРОМЫШЛЕ-
НОСТИ, НОВОСТЕЙ и МОДЪ.
Ἐμοὶ δὲ τί αἰσχρὸν, τὸ ἑτέρους μὴ δύνασθαι περὶ
ἐμοῦ τὰ δίκαια μήτε γνῶναι μήτε ποιῆσαι; Ὅρω
δ' ἴσως καὶ τὴν δόξαν τῶν προγεγονότων ἀνδρῶπων
ἐν τοῖς ἐπιγιγνομένοις οὐχ ὁμοίαν καταλιπομένην τῶν
τε ἀδικούντων καὶ τῶν ἀδικουμένων.
Socrat. apud Xenophont., IV, 8, 9.
ТОМЪ ДВАДЦАТЬ-ОСЬМОЙ.
ИЗДАНІЕ
книгопродавца Александра Смирдина.
САНКТПЕТЕРБУРГЪ.
ВЪ ТИПОГРАФІИ ЭДУАРДА ПРАЦА И К°.
1838.

ЭЛЕКТРИЧЕСКІЙ ОПЫТЪ
Г. АКАДЕМИКА ЛЕНЦА.
ЗАМОРОЖИВАНІЕ ВОДЫ ПОСРЕДСТВОМЪ ГАЛВАНИЧЕСКОЙ СТРУИ.
Всѣмъ извѣстно, что, пропуская черезъ металлическую проволоку нѣсколько сильную струю электрическую Вольтова столба, проволока нагрѣвается до-красна и часто плавится. Въ этомъ случаѣ теплотворъ кажется произведеніемъ электричества. Въ другихъ случаяхъ, напротивъ, электричество является какъ-бы произведеніемъ теплотвора, и отсюда проистекаетъ новый рядъ явленій, которыя получили названіе «термо-электрическихъ». На нихъ-то многіе основываютъ предположеніе, будто электричество и теплотворъ – слѣдствія одной и той же силы; но это предположеніе, въ нынѣшнемъ состояніи нашихъ свѣдѣній, еще преждевременно.
Недавно Г. Маттеуччи повторялъ въ присутствіи Г. *Delarive*'а одинъ любопытный термо-электрическій опытъ, и удостовѣрилъ знаменитаго женевскаго физика, что, если укрѣпить двѣ одинаковыя проволоки къ двумъ оконечностямъ гальванометра, погрузить потомъ концы этихъ проволокъ во ртуть, и нагрѣвать одну изъ двухъ проволокъ, – тотчасъ обнаружится электрическій токъ, который, при всѣхъ степеняхъ температуры, постоянно будетъ стремиться изъ конца нагрѣтой проволоки, черезъ ртуть, въ конецъ холодной. Изъятія противъ этого правила, замѣчаемыя по-временамъ въ мѣдныхъ и желѣзныхъ проволокахъ, при высокой температурѣ исчезаютъ. Одинъ только висмутъ всегда являетъ противоположное дѣйствіе: въ двухъ висмутовыхъ проволо-

Fig.5. The first pages of the article "The Electric Experience of Mr. Lenz. Freezing of water by means of a galvanic jet", published in the journal "Library for Reading" (1838) [16].

It is of interest to compare the results of Lenz's experiments with theoretical estimates of the magnitude of cooling effects (Fig. 4) in the framework of the modern theory of thermoelectric coolers [20]. The maximum value of ΔT_{cool} was calculated from formula $\Delta T_{cool}^{max} = ½Z_0T_1^2$, where $Z_0 = (\alpha_{Sb} - \alpha_{Bi}) / [(\rho_{Sb}\,\kappa_{Sb})^{½} + (\rho_{Bi}\,\kappa_{Bi})^{½}]^2$ is thermoelectric figure of merit of a thermocouple, α and ρ are thermo-EMF and the electrical resistivity of the branches, T_1 is absolute temperature of the cold junction (Table 1). The optimum operating current of the thermocouples was determined from relation $I_0 = \alpha T / R$, where $R_0 = L(\rho_{Sb} / S_{Sb} + \rho_{Bi}/S_{Bi})$ is electrical resistance of thermocouple, L is length of branches, S_{Sb} and S_{Bi} are their cross sections. The currents in the thermocouples (Fig. 4) were estimated according to Ohm's law: $I = E/R$. Here, E = 1.1 V is the EMF of the GE, $R = r_{GE} + R_0$ is the impedance of the electrical circuit, R_0 is the thermocouple resistance, $r_{GE} = l/(\sigma \cdot s)$ is the electrolyte resistance, l ~ 5 cm is the distance between the plates (*Zn* and *Pt*) of the GE, $\sigma = 1/\rho = 0.653$ Ohm·cm (20% H_2SO_4) is the specific conductivity of the electrolyte [21], s is the area of the GE plates, which was assumed equal to 20 cm^2 in the experiment (Fig. 4a) and was a square foot (929 cm^2) in the experiment (Fig. 4b) [16].

Table 2

The thermoelectric characteristics of the branches of the Bi-Sb thermocouple, investigated by Lenz [19]

Sample	Thermo-EMF α, μV/K	Specific resistance, $\rho \cdot 10^6$, Ohm·cm	Specific heat conductivity, κ, W/(m·K)	The thermoelectric figure of merit of materials, $Z \cdot 10^{-3}$, 1/K
Bi	– 68	110	7.9	0.53
Sb	35	39	24	0.13

Estimates show that the relatively small values of ΔT_{cool} observed by Lenz in the experiments (Fig. 4) are related to the violation of the optimization conditions for the thermocouples in the S_{Sb}/S_{Bi} cross section and the working current I (Table 3). According to Table 3, the operating current of thermocouples I, which was used by Lenz during cooling in the experiment (Fig. 4a), was smaller, and in the experiment (Fig. 4b) – more than optimal. In the latter case, the thermocouple operated in a "pulsed mode" [20], therefore, with time, the value of ΔT_{cool} decreased [16]. This explains why, during the freezing of a drop of water in the experiment (Fig. 4b), Lenz fixed the temperature of the junction near $T \sim 0$°R (°C). In turn, due to a violation of the optimization over the cross section (Table 3), the bismuth branch of the thermocouple was strongly heated in comparison with the antimony branch [16]. This reduced the value of ΔT_{cool} and substantially increased ΔT_{heat} (Table 3). All these effects were noticed and described by Lenz [16].

Table 3

The Peltier effects studied by Lenz on a Bi-Sb thermocouple [16], in comparison with the theory [20]

№	Experiment and theory	The cooling effect, ΔT_{cool}, °R (K)	The effect of heating, ΔT_{heat}, °R (K)	The thermoelectric figure of merit of thermocouple, $Z_0 \cdot 10^3$, 1/K	r_{GE}, Ohm	Optimization conditionsnull	
						Operating current, I, A	Cross section, S_{Sb}/S_{Bi}
1	The Lenz experiment using the Peltier scheme (Fig. 4a)	0.7 (0.84)	3.3 (3.96)	0.019	0.38	2.8	1
2	The Lenz experiment according to the scheme (Fig. 4b)	2.9 (3.48)	48 (57.6)	0.088	0.033	29.7	1
3	Theory [20]	10.7 (12.8)	-	0.284	-	17	0.35

During the experiments (Fig. 4), Lenz established the direction of current I, in which the effect of cooling or heating was observed on the working junction of the thermocouple [16]. According to [16], cooling of the working junction of the thermocouple was observed when the galvanic current was from bismuth (n-type) to antimony (p-type) (Fig. 4). When the current passes in the opposite direction, the working junction of the thermocouple is heated. In this case, the direction of the current I, necessary to observe the effect of cooling the working junction of the thermocouple (Fig. 4), coincided with the direction of the current arising in the closed circuit of the thermocouple when its working junction was heated. This coincidence was not accidental, it is explained by the Le-Chatelier-Brown

principle, according to which the current *I*, caused by heating the working junction of the thermocouple, causes cooling of this junction [22].

2.6. The law of Joule-Lenz

In 1842-1843 Lenz conducted a series of experiments to study the thermal action of electric current (6, Table 1). The experiments were carried out with copper, iron, platinum and neusilber wires using the installation (Fig. 6). The result of this work was an article: "On the laws of heat extraction by galvanic current", in which Lentz laid out the law of the thermal action of current established by him [15]. According to this law:

1. "Heating of the wire with galvanic current is proportional to the resistance of the wire".
2. "The heating of the wire by a galvanic current is proportional to the square of the current used for heating" ([15], p. 441).
3. "With the most advantageous heat release for the circuit device, the resistance of the heated wire *R* must be equal to the resistance of the galvanic battery *r*", which is ½ of the impedance of the circuit. ("Heat release in wires". Reported August 11, 1843, p.443).

$$R = r = ½(R + r). \quad (1)$$

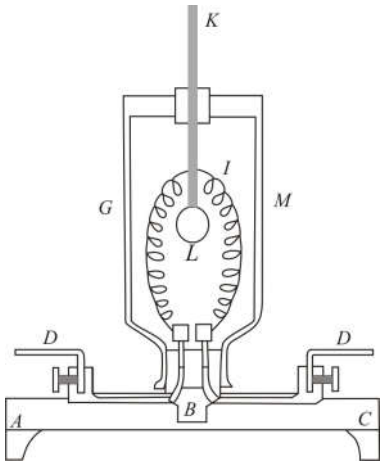

Fig. 6. Installation of Lenz for the study of heat generation in wires. A, B, C are the base parts; D are current leads (Pt); GM is a glass flask with alcohol; KL is a mercury thermometer; I is the wire being examined. The installation was powered by a Daniel battery (24 pairs) via a Volt-agometer (rheostat) [15] .

Conclusions of Lenz 1 and 2 on the thermal action of the current were already known to the scientific community, they were discovered in 1841 by the English physicist J. Joule (1818-1889) [8, 10]. These Joule's conclusions Lenz confirmed with high accuracy. For this reason, the law of thermal action of a current bears the name of both scientists [15]. In turn, the conclusion 3 and the relation (1), obtained by Lenz in the study of heat generation in the wires, were highly original [10]. Lenz suggested that rule of ½ (1) is universal and can be "proved for the entire region of galvanism" ([15], p. 443).

Later it was established that the Lenz rule (½) (1) is connected with the extreme principles of thermodynamics determining the maximum net power W_{max}, which can be obtained from a current source in a closed electric circuit (Fig. 7) [22]. In [23-24], the Lenz rule (½) was generalized to thermal chains ($\Psi = \zeta/\zeta_i = 1$, here ζ and ζ_i are the thermal load resistance and internal resistance of the heat source), and in [20-21] – simultaneously on the electrical and thermal circuits of thermoelectric generators (TEG). It was shown that when the TEG operates in the maximum power mode (W_{max}), the optimal ratios of their electrical and thermal resistances can deviate significantly from the Lenz rule (½) – ($R/r \geq 1$, $\zeta/\zeta_i \geq 1$) because of their interaction with each other. (Here $\zeta_i = \zeta_h + \zeta_{he} + \zeta_{ce}$; ζ_h, ζ_{he}, and

ζ_{ce}, are thermal resistance of the heater, hot and cold heat exchangers. As a result, both the electrical and thermal parameters of the TEG require additional optimization. In this case, in the optimized W_{max} mode, two invariants of the Lenz rule are conserved in the TEG: $U^{xx}/2$ and $\Delta T^{xx}/2$ – voltage and temperature drops on thermocouple branches corresponding to the idle mode[7]. The application of the generalized Lenz rule to automotive thermoelectric generators (ATEG) has made it possible to relate their low efficiency to the difficulties of heat exchange at the "exhaust gas / ATEG" boundary [25].

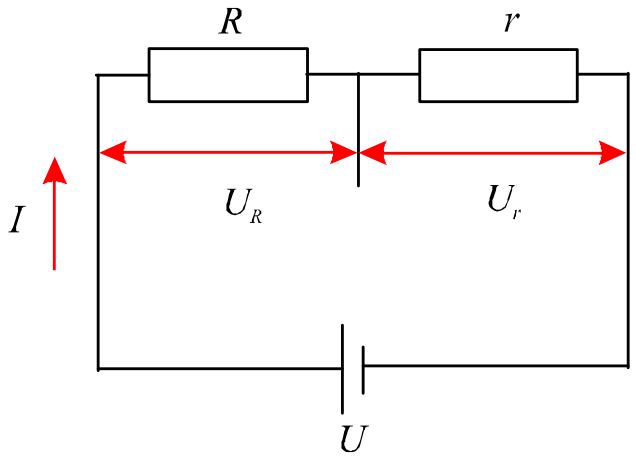

Fig. 7. An electrical diagram illustrating the application of the Lenz rule (½) to closed circuits operating in maximum power mode:R = r, $U_R = U_r = U/2$. Here: U and r are the internal resistance of the current source, R is the load resistance.

Table 4

Calculations of TEG parameters in various modes without taking into account (I) and taking into account (II) the Lenz thermal rule (½) [24, 25] [8]

№	Mode	$\Delta T'$	$M = R/r$	U_R	I	W
I	I.m.	ΔT	∞	U	0	0
	S.c.	ΔT	0	0	U/r	0
	W_{max}	ΔT	1	$U/2$	$U/(2r)$	$U^2/(4r)$
II	I.m.	$\Delta T_{xx} = ½\Delta T$	∞	U	0	0
	S.c.	$\Delta T_{xx} / A$	0	0	U/r	0
	W_{max}	$½\Delta T$	$A = \Psi = M_0$	$U/2$	$U/(2rM_0)$	$(U)^2/(4rM_0)$

[7] TEG operation modes: 1) "short circuit" (s.c.) ($R = 0$); 2) "idling move" (i.m.) ($R = \infty$); 3) "maximum power" W_{max} ($R = r$); 4) "maximum efficiency" (m.e.) $\eta_{max} = (W/Q_h)_{max}$. (Here W is the net power, Q_h is the input heat flux of the TEG).

[8] Calculations are made for $(ZT) = 1$, where Z is the thermoelectric figure of merit of the TEG; $\bar{M}_0 = (1+Z\bar{T})^{1/2}$; $\bar{T} = (T_h + T_c)/2$; $\Delta T = T_h - T_c$; T_h are the temperatures of hot and cold junctions; $r = \Sigma r_k$ is the total electrical resistance of the TEG (branches, contacts and fittings); U and U_R are the total voltage in the circuit and its part falling on the load; $A = 1 + ZT_h (\zeta_l + \zeta_{he}) / \zeta + ZT_c \zeta_{ce}/\zeta$; $\zeta = \zeta_l + \zeta_{he} + \zeta_{sc} + \zeta_{ce}$ is the total thermal resistance of the TEG; ζ_h, ζ_{he}, ζ_{ce} and ζ_{sc} are the thermal resistances of the heater, $\Psi = \zeta_{пп}/\zeta_i$; $\zeta_i = (\zeta_н + \zeta_{he} + \zeta_{ce})$ is the ratio of the thermal resistances of the load and the heat source with heat exchangers.

2.7. The reaction of the armature of electromagnetic machine

A special place in the scientific work of E. Ch. Lentz was engaged in cooperation with academician B. S. Yakobi, the result of which was their joint work "On the laws of electromagnets" (1838-1844), which describes methods for calculating electromagnets in electric machines (6, Table 1) [15]. Working together, the scientists established the existence in the magneto-electric machines of the so-called "anchor reaction effect" (ARE). The cause of ARE was the phenomenon of electromagnetic induction, which occurs when the collector of the electric generator opens [15]. As a result of the action of the ARE, the current produced by the generator turned out to be unstable, which made the generators less suitable for the purposes of electroforming, which was being actively developed at that time by B. S. Yakobi. To combat ARE, Lenz and Yacobi were suggested to move the generator brushes relative to the center of the collector plates. This allowed to significantly reduce the noise and bring the current produced to a constant one [15].

2.8. Experiments on the polarization of electrodes of galvanic cells

Until the seventies of the XIX century, the most common sources of current in physical studies were galvanic cells (GC), which are notable for their instability. The cause of instability was for a long time incomprehensible to contemporaries. Indeed, on the one hand, as a result of the chemical reaction, the voltage $U \sim 1$ V was set at the terminals of the open GC, which remained constant for a long time. However, when the GC circuit is closed to an external load, the magnitude of the EMF E was rapidly decreasing. As it turned out, hydrogen began to form within the GC, covering the surface of the plates with a layer of bubbles. This layer, as a result of the polarization of the plates, reduced the voltage at the terminals of the GC. It was shown that the larger the discharge current, the more polarization develops and the faster the GC voltage decreases. The first weakly polarized EC in 1829 was proposed by A. S. Becquerel (1788-1888) [12]. In 1847, E. Ch. Lenz together with A. Savelyev continued the study of the polarization of the GC. To eliminate polarization, it was proposed to introduce depolarizers capable of absorbing hydrogen in the GC. Now depolarizers are mandatory components of all chemical sources of current.

Conclusion

Academician E. Ch. Lenz considered as one of the most outstanding Russian scientists of the XIX century in the field of electricity and magnetism [1, 11]. The main results of his research presented in all textbooks of physics [10-12]. A number of factors determined Lenz success in scientific research. This is a high level of theoretical training combined with experimental skill, as well as pedagogical talent, which enabled Lents to present his works in an extremely concise and understandable form. Lentz was not a lone scientist; he attracted to his work the staff of the Physical Cabinet, professors of the University (A. S. Savelyev and others), academicians of St. Petersburg Academy of Sciences (E. I. Parrot, B. S. Yacobi, etc.) [1, 11, 12]. Lenz was not a lone scientist; he attracted to his work the staff of the Physics Cabinet, professors of the University (A. S. Savelyev and others), academicians of St. Petersburg Academy of Sciences (E. I. Parrot, B. S. Yacobi, etc.) [1, 11, and 12].

In the process of work, Lenz concentrated his efforts on a narrow field of research, which allowed him to penetrate deeply into the essence of the problem studied. As a result, many of the results of his research were of the nature of scientific discoveries, undoubtedly the priority of which was recognized not only in Russia but also abroad [8, 10, and 11]. A large number of friends and admirers of his scientific talent Lenz had in Germany, where he published his scientific articles in the journal "Annals of Physics and

Chemistry", published in Berlin by Academician of Berlin Academy of Sciences (1839) and Foreign member of St. Petersburg Academy of Sciences (1868) I. K. Poggendorff (1796-1877) [12, 15]. Being an excellent teacher, E. Ch. Lentz brought up a large number of students who worked in the most diverse fields of science. The most famous among them is chemist D. I. Mendeleev (1834-1907), naturalist K. A. Timiriazev (1843-1920), geographer and botanist N. N. Semenov-Tien-Shansky (1824-1914), and others [12, 15]. Appendix 1 contains the works of two students of E. Ch. Lenz - Ch. E. Lentz (son) and M. P. Avenarius, who continued the research of his teacher in the field of thermoelectricity [9, 17][9].

Appendix 1

Pupils and followers of E. Ch. Lenz in the field of thermoelectricity

R. E. Lenz (son) (Fig. 8) carried out high-precision studies the effect of temperature on the thermal conductivity of metals (1869) [3, 9]. In 1883, he showed the possibility of using thermocouples for remote measurement of temperatures at large distances (up to 5 km). The experiments were carried out with *Fe-Ag* wire thermocouples, the accuracy of measuring the temperature difference was of ~ 0.01 K. At present, a similar method is used, for example, for remote measurement of temperatures in deep mines and wells [9].

M. P. Avenarius (Fig. 9) in 1863 obtained empirically a formula for the EMF metallic thermocouples at large ΔT [9, 17]:

$$E = (t_2 - t_1)[b + c(t_1 + t_2)] = \alpha(t_2 - t_1) + \beta(t_2^2 - t_1^2). \quad (2)$$

Then he derived his formula theoretically, believing that the EMF E of the thermoelectric circuit is determined only by the contact differences of the metal potentials $e = a + bt + ct^2$ on the junctions of the differential thermocouple at various temperatures $t_1 < t_2$. (Here: $\alpha = \alpha_p - \alpha_n$, α_p and α_n are the Seebeck coefficients of the thermocouple and the branches of the *p*- and *n*-types of conductivity; *b*, *c*, β are the coefficients different for different materials).

Fig. 8. Lentz Robert Emilievich (1833-1903) – physicist, son of E. Ch. Lenz. He graduated from St. Petersburg University, read physics at the Institute of Technology and University. The degree of the master of physics was awarded for his thesis "On magnetic anomalies in the Gulf of Finland" (1862), the doctor's degree for "Studies on the effect of temperature on the thermal conductivity of metals" (1869). Corresponding member of St. Petersburg Academy of Sciences (1876). In 1889, he was appointed the manager of the expedition of preparing state securities. (Official portrait of the RAS [3].

[9] In the autumn of 1864, E. Ch. Lenz's eyesight deteriorated sharply. For treatment, he went to Rome. Vision began to recover and E. Ch. Lenz could already read and write. But on February 10, 1865, a scientist suddenly died of a cerebral hemorrhage. He is buried in one of the Lutheran cemeteries in Rome [15].

Later, in his work "On the electric excitation force of thermoelectric elements from the point of view of the mechanical theory of heat", Avenarius, in deriving formula (2), took into account the Thomson effect in the branches of thermocouples [17]. The need to consider this was first paid attention to (1874) by P. T. Thet (1831-1901) – a professor of the Royal College in Belfast (1854-1860).

Fig. 9. Avenarius Mikhail Petrovich (1835, Tsarskoe Selo – 1895, Kiev), physicist, graduated from St. Petersburg University in 1858. In 1862 – 1864, he trained at Magnus in Berlin and Kirchhoff in Heidelberg. In 1865, he defended his master's thesis: "On Thermoelectricity" and was appointed to the Department of Physics at the University of Kiev. In 1866, he defended his doctoral dissertation: "On the electrical differences of metals at different temperatures". Corresponding member of St. Petersburg Academy of Sciences (1876). The founder of the Kiev school of physicists [12, 17]. (Official portrait of the RAS [3]).

According to the Avenarius formula (2), depending on the magnitude and sign of the thermocouple coefficient β, the temperature dependences $E = f(T)$ of three types are observed. For $\beta = 0$, from Eq. (2) we obtain the linear dependence $E = \alpha(t_2 - t_1)$ that is the law of A. Becquerel (1788-1878) (for example, *Ni*, *Ir*, *Au-Fe* thermocouples near room temperature). For $\beta > 0$, for the function $E = f(T)$, we have an « ⌣ »-shaped curve (for example, thermocouples of non-silicon beams), and for $\beta < 0$, an « ∩ »-shaped curve with a maximum at temperature t_{tm}, and with a sign change E in the high-temperature region (thermocouples *Cu-Fe*, *Mo-Fe*, etc.). In the latter case, formula (2) could be transformed into the expression $E = \alpha(t_2 - t_1)[t_{tm} - (t_2 + t_1)/2]$, which shows that for $(t_2 + t_1)/2 \sim t_{tm}$ the value of E and the current direction I in a short-circuited thermocouple change sign.

The verification of the Avenarius formula and the determination of constants in it were carried out by many scientists in different countries of the world [9, 17]. As a result, it was established that the Avenarius formula (2) is valid for most thermoelectric circuits in the region of normal and high temperatures [9].

References

1. Вавилов С.В. Физический кабинет. Физическая лаборатория. Физический институт Академии Наук за 220 лет. / Вавилов С.В. // УФН. – 1947. – С. 1 – 28.
2. Модзалевский Б.Л. Список членов императорской Академии наук (1725 – 1907). / Модзалевский Б.Л.
   // – СПб: Типография АН, 1908. – 404 с.
3. Персональный состав АН СССР (1724-1917). Москва. 1974. 480 с.
4. Коржуев М.А. Исследования Рихмана и Ломоносова в области термоэлектричества (1745 – 1753). / Коржуев М.А., Темяков В.В. // Термоэлектричество. – 2014. – С. 90 – 104.
5. Коржуев М.А. Работа сотрудников Физического кабинета Петербургской академии наук по исследованию термоэлектрических эффектов в различных диэлектрических средах. Ч.I – Старт и выход на «мировой уровень». В сб.: Термоэлектрики и их применения. Под ред.

М.И. Федорова. / Коржуев М.А., Тихомирова О. Ф., Темяков В.В. // Санкт-Петербург – 2015. – С. 535–540.
6. Коржуев М.А., Тихомирова О. Ф., Темяков В.В. Работа сотрудников Физического кабинета Петербургской академии наук по исследованию термоэлектрических эффектов в различных диэлектрических средах. Ч. II – На «переднем фронте» науки. В сб.: Термоэлектрики и их применения. Под ред. М.И. Федорова, Л.Н.Лукьяновой. Санкт-Петербург. 2015. С. 541 – 546.
7. Коржуев М.А. Работа сотрудников Физического кабинета Петербургской академии наук по исследованию термоэлектрических эффектов в различных диэлектрических средах. Ч. III – Период застоя» и новый подъем. В сб.: Термоэлектрики и их применения. Под ред. М.И. Федорова, Л.Н.Лукьяновой. / Коржуев М.А., Тихомирова О. Ф., Темяков В.В. // Санкт-Петербург. – 2015. С. 547- 552.
8. Лауэ М. История физики. / Лауэ М. – Москва. 1956. – 232 с.
9. Буряк А.А. Очерки развития термоэлектричества / Буряк А.А., Карпова Н.Б. 1988. – С. 290.
10. Льоцци М. История физики. / Льоцци М. 1970. – 464 с.
11. Люди русской науки. Под ред. И.В. Кузнецова. Москва. 1961. 600 с.
12. Храмов Ю.А. Физики. Библиографический справочник. / Храмов Ю.А. – Москва. 1983. – 400 с.
13. Коржуев М.А. О последовательности открытия основных термоэлектрических явлений. / Коржуев М.А., Катин И.В. // Термоэлектричество. – 2011. – С. 79 – 90.
14. Фарадей М. Экспериментальные исследования по электричеству. Москва. Т.I. 1947. 848 с. Т.II. 1951. 539 с. Т.III. 1959. 831 с.
15. Ленц Э.Х. Избранные труды. / Ленц Э.Х. 1950. – 521 с.
16. Электрический опыт г. академика Ленца. Замораживание воды посредством гальванической струи. Библиотека для чтения. – Санкт-Петербург: А. Смирдина, 1838. – 44 с. – (Раздел «Науки и художества».). – (Т.28).
17. Гольдман А.Г. Михаил Петрович Авенариус и киевская школа экспериментальной физики / Гольдман А.Г. // УФН Т.44. – 1951. – С. 586–609.
18. Коцебу О.Е. Новое путешествие вокруг света в 1823 / Коцебу О.Е. – Москва, 1981. – 352 с.
19. Григорьев И.С., Физические свойства материалов. / Григорьев И.С., Мейликов Е.З., 1991. – 1232 с.
20. Анатычук Л.И. Термоэлементы и термоэлектрические устройства. / Анатычук Л.И. – Киев, 1979. – 767 с.
21. Перельман В.И. Краткий справочник химика. / Перельман В.И.. – Москва: "Химия", 1964. – 623 с.
22. Базаров И. П. Термодинамика. / Базаров И. П. – Москва, 1991. – 292 с.
23. Эйнштейн А. Эволюция физики / Эйнштейн А., Инфельд Л.. – Москва, 1948. – 268 с.
24. Коржуев М.А. Правило Ленца для термоэлектрических преобразователей энергии, работающих в режиме максимальной мощности / Коржуев М.А. – В сб.: Термоэлектрики и их применения: Под ред. М.И. Федорова. Л.Н.Лукьяновой., 2015. – (Санкт-Петербург.). – С. 447 – 452.
25. Коржуев М.А. Термодинамические ограничения полезной мощности автомобильных термоэлектрических генераторов и перспективы их использования на транспорте. / Коржуев М.А., Свечникова Т.Е. // Термоэлектричество. – 2013. – С. 58 – 75.

Submitted 20.02.17

Коржуєв М. А., *канд. фіз.-мат. наук***, Кретова М. А., Катін І. В.**

Інститут металургії й матеріалознавства ім. А.А. Байкова РАН,
Ленінський просп., 49, Москва 119991, Росія
e-mail: korzhuev@ultra.imet.ac.ru

ВНЕСОК АКАДЕМІКА Е. Х. ЛЕНЦА В РОЗВИТОК СУЧАСНОЇ ТЕРМОЕЛЕКТРИКИ

Розглянуті роботи академіка Петербурзької Академії Наук Е.Х. Ленца (1804 – 1865)і його учнів –Х.Е. Ленца (сина) (1833 – 1903) і М.П. Авенаріуса (1835 – 1895), що внесли вклад у розвиток сучасної термоелектрики (ТЕ). Бібл. 25, рис. 9, табл. 4.

Ключові слова: термоелектрика; академік Е.Х. Ленц; правило індукції Ленца, закон Джоуля- Ленца, ефект Пельтьє, максимальна потужність термопари, автомобільні термоелектричні генератори.

Коржуев М. А., *канд. физ.-мат. наук,* **Кретова М. А., Катин И. В.**

Институт металлургии и материаловедения им. А.А. Байкова РАН,
Ленинский просп., 49, Москва 119991, Россия
e-mail: korzhuev@ultra.imet.ac.ru

ВКЛАД АКАДЕМИКА Э. Х. ЛЕНЦА В РАЗВИТИЕ СОВРЕМЕННОГО ТЕРМОЭЛЕКТРИЧЕСТВА

Рассмотрены работы академика Петербургской Академии Наук Э.Х. Ленца (1804 - 1865) и его учеников - Х.Э. Ленца (сына) (1833-1903) и М.П. Авенариуса (1835-1895), внесшие вклад в развитие современного термоэлектричества (ТЭ). Библ. 25, рис. 9, табл. 4.

Ключевые слова: термоэлектричество, академик Э.Х. Ленца, правило индукции Ленца,, закон Джоуля-Ленца; эффект Пельтье, максимальная мощность термопары, автомобильные термоэлектрические генераторы.

Referens

1 Vavilov S.V. (1947). Fizicheskiy kabinet. Fizicheskaya laboratoriya. Fizicheskiy institut Akademii Nauk za 220 let [Physical cabinet. Physical laboratory. Physical Institute of the Academy of Sciences for 220 years]. *Uspekhi Fizicheskih Nauk -Physics-Uspekhi,* 28(1), 1 – 50 [in Russian].

2 Modzalevskii B.L. (1908). *Spisok chlenov imperatorskoi Akademii nauk* (1725-1907) [*List of Members of the Imperial Academy of Sciences (1725 – 1907)*]. St-Petersburg: Printing House of the Academy of Sciences [in Russian].

3 *Personalnyi sostav Akademii Nauk CCCP* (1724-1917) *[Personal Composition of the USSR Academy of Sciences (1724-1917)] (1974).* Moscow [in Russian].

4 Korzhuev M.A., Temyakov V.V. (2014). Issledovaniya Rikhmana i Lomonosova v oblasti termoelektrichestva (1745-1753) [Richmann's and Lomonosov's research in the field of thermoelectricity (1745 – 1753).] *J. Thermoelectricity,* 1, 90 – 104.

5 Korzhuev M.A., Tikhomirova O.F., Temyakov V.V. (2015). Rabota sotrudnikov Fizicheskogo kabineta Peterburgskoi Akademii nauk po issledovaniyu termoelektricheskih effektov v razlichnyh dielektricheskih sredah. Chast I – Start i vykhod na "mirovoi uroven" [The work of employees of the Physical cabinet of St.Petersburg Academy of Sciences to study thermoelectric effects in different dielectric media. Part I – The start and access to the "world level". *In.: Thermoelectrics and their applications.* Fedorov M.I., Lukyanova L.N. (Ed.). Saint-Petersburg: PNPI [in Russian].

6 Korzhuev M.A., Tikhomirova O.F., Temyakov V.V. (2015). Rabota sotrudnikov Fizicheskogo kabineta Peterburgskoi Akademii nauk po issledovaniyu termoelektricheskih effektov v razlichnyh dielektricheskih sredah. Chast II – Na "perednem fronte" nauki [The work of employees of the physical cabinet of St.Petersburg Academy of Sciences to study thermoelectric effects in different dielectric media. Part II – On the "forefront" of science]. *In: Thermoelectrics and their applications.* Fedorov M.I., Lukyanova L.N. (Ed.).Saint-Petersburg: PNPI [in Russian].

7 Korzhuev M.A., Tikhomirova O.F., Temyakov V.V. (2015). Rabota sotrudnikov Fizicheskogo kabineta Peterburgskoi Akademii nauk po issledovaniyu termoelektricheskih effektov v razlichnyh dielektricheskih sredah. Chast III – Period zastoia i novyi podjom [The work of employees of the Physical cabinet of St.Petersburg Academy of Sciences to study thermoelectric effects in different dielectric media. Part III – The period of stagnation and a new rise]. *In.: Thermoelectrics and their applications.* Fedorov M.I., Lukyanova L.N. (Ed.). Saint-Petersburg: PNPI [in Russian].

8 Laue M. (1956). *Istoriya fiziki [History of Physics]*. Moscow: GITTL [in Russian].

9 Buryak A.A., Karpova N.B. (1988). *Ocherki razvitia termoelektrichestva* [Essays on the development of thermoelectricity]. Kyiv: Naukova Dumka [in Russian].

10 Liozci M. *History of Physics*. Moscow: Mir, 1970 [Russian transl].

11 Kuznetzov I.V. (ed). (1961). *Liudi russkoi nauki [Persons of Russian science]*. Moscow: GIF-ML [in Russian].

12 Khramov Yu.A. (1983). *Fiziki. Bibliograficheskii spravochnik [Physicists. Bibliographical reference]*.
Moscow: Nauka [in Russian].

13 Korzhuev M.A., Katin I.V. (2011). *O posledovatelnosti otkrytia osnovnyh termoelektricheskih effektov [On the sequence of discovery of the basic thermoelectric effects]*. *J.Thermoelectriicty,* 3, 79 – 90.

14 Faraday M. (1947-1959). *Experimental Studies on Thermoelectricity. (Vols.I-III).* Moscow: AN SSSR [Russian transl.]

15 Lenz E.Ch. (1950). *Izbrannyie Trudy [Selected Works]*. Moscow: AN SSSR [in Russian].

16 *Elektricheskii opyt akademika Lenza. Zamorazhivanie vody posredstvom galvanicheskoi strui. Biblioteka dlia chtenia. Vol.28. Razdel "Nauki i khudozhestva" [Electric experience of academician Lenz. Freezing of water through a galvanic jet. Library for reading. Vol. 28. Section "Science and Art"]*. (1838). *St.Petersburg:* Smirdin Publ.

17 Goldman A.G. (1951). Mikhail Petrovich Avenarius i kievskaya shkola eksperimentalnoi fiziki [Mikhail Petrovich Avenarius and the Kiev school of experimental physics]. *Uspekhi Fizicheskih Nauk -Physics-Uspekhi,* 44(4), 586 – 609 [in Russian].

18 Kocebu O.E. (1981). *Novoe puteshestvie vokrug sveta v 1823-26 [A new journey around the world in 1823-26]*. Moscow: Nauka [in Russian].

19 Grigoryev I.S., Meilikov E.Z. (1991). *Fizicheskie svoistva materialov [Physical properties of materials]*. Moscow: Energia [in Russian].

20 Anatychuk L.I. (1979). *Termoelementy i termoelektricheskiye ustroistva [Thermoelements and*

thermoelectric devices]. Kyiv: Naukova Dumka [in Russian].

21 Perelman V.I. (1964). *Kratkii spravochnik khimika [Quick reference book of the chemist]*. Moscow-Leningrad: Khimia [in Russian].

22 Bazarov I.P. (1991). *Termodinamika [Thermodynamics]*. Moscow: Vysschaia Shkola [in Russian].

23 Einstein A., Infeld L. (1948). *Evolutsia fiziki [Evolution of Physics]*. Moscow-Leningrad: OGIZ.

24 Korzhuev M.A. (2015). *Pravilo Lenza dlia termoelektricheskikh preobrazovatelei energii, rabotaiushchih v rezhime maksimalnoi moshchnosti [The Lenz rule for thermoelectric energy converters operating in maximum power mode]*. *In: Thermoelectrics and their applications.* M.I.Fedorov, L.N.Lukyanova (Ed.). St.-Petersburg: PNPI.

25 Korzhuev M.A., Svechnikova T.E. (2013). Termodinamicheskie ogranichenia poleznoi moshchnosti avtomobilnyh termoelektricheskikh generatorov i perpectivy ikh ispolzovania na transporte [Thermodynamic restriction for useful power of the automotive thermoelectric generators and prospects of their use in transport]. *J.Thermoelectricity,* 3, 58 – 75.

Submitted 20.02.17

P.V. Gorskiy

P. V. Gorskiy

Institute of Thermoelectricity of the NAS and MES of Ukraine,
1, Nauky Str., Chernivtsi, 58029, Ukraine
e-mail: anatych@gmail.com

THE FIVAZ MODEL AND PREDICTION OF THERMOELECTRIC MATERIALS

This paper is concerned with the role of dimensionality reduction of thermoelectric material structure for increasing its thermoelectric figure of merit. It is shown that the thermoelectric figure of merit of a "purely two-dimensional" thermoelectric material can exceed that of a three-dimensional crystal only when the Fermi energy of a three-dimensional crystal at absolute zero temperature is significantly larger than the Fermi energy of a "purely two-dimensional" material, which is achievable only at sufficiently small distances between the layers and (or) quantum well widths. In traditional thermoelectric materials this condition is poorly satisfied or not satisfied at all. The way out can be in using layered (superlattice) materials described by the Fivaz model. For this purpose they must possess very narrow allowed bands describing motion of electrons between the layers, which assures high degree of openness of the Fermi surface of these materials. At the same time, forbidden bands of these materials must be sufficiently wide so as to prevent conversion of impurity conduction to intrinsic in the "generator" temperature range. Traditional layered and superlattice materials used in electronics and thermoelectricity possess an antipodal property: their allowed bands are wide, and forbidden bands are narrow. Moreover, the distances between their layers and, hence, corresponding quantum well widths, are rather large. The totality of these factors significantly limits the thermoelectric figure of merit of these materials.

On the basis of the analysis, possible optimal parameters of promising superlattice thermoelectric material are determined. Such material, if it were created, on the one hand would allow creating a thermoelectric generator with the efficiency of the order of 34% between temperatures 300 and 500 K, and on the other hand – a cooler providing single-stage cooling from 300 to 100 K with a coefficient of performance about 0.3.

Methods of search for promising thermoelectric materials described by the Fivaz model with the use of quantizing magnetic fields are proposed. Bibl. 32, Fig. 2.

Key words: Fivaz model, nonparabolicity, Fermi surface, thermoelectric figure of merit, efficiency, coefficient of performance, quantizing magnetic field, prediction of thermoelectric materials.

Introduction. Current status of the problem

For more than two decades, substantial hopes for an increase in the figure of merit of thermoelectric materials have been associated with the so-called dimensionality reduction of their structure. In particular, in one of the fundamental works [1] devoted to this problem, a thermoelectric material based on bismuth telluride with quantum wells was theoretically considered. In fact, it was a layered material, the layers of which were separated by quantum wells. Therefore, the motion of charge carriers in the plane of the layers was described by the traditional effective mass approximation, and the motion in the perpendicular direction, although described by a parabolic

dispersion law, was assumed to be dimensionally quantized due to the discreteness of the corresponding quasi-momentum component.

The discreteness was dictated by the condition that the carriers could not leave the well. There fore, the energy spectrum of charge carriers in the material was represented as

$$E\left(k_x, k_y, n\right) = \frac{\hbar^2}{2}\left(\frac{k_x^2}{m_1} + \frac{k_y^2}{m_2}\right) + \frac{\hbar^2 \pi^2 n^2}{2 m_3 d^2}. \quad (1)$$

In this formula, m_1, m_2, m_3 – components of the effective mass tensor, n – dimensional quantization subband number, d – quantum well width.

For this case calculations were made of the kinetic coefficients of a two-dimensional electron gas, following which the resulting expression was optimized with respect to chemical potential determined with regard to dimensional quantization of charge carrier energy spectrum. As a result, it was established that transition from a three-dimensional energy spectrum to a quasi-two-dimensional spectrum of the type (1) can increase considerably, namely by a factor of 4-6, the dimensionless thermoelectric figure of merit of such a structure, if quantum well width is, for example, 0.1 nm. However, the increase in the quantum well width results in a drastic drop of dimensionless thermoelectric figure of merit, and already at quantum well widths of the order of 4-8 nm it becomes equal to the thermoelectric figure of merit of a single-crystal bismuth telluride.

From this standpoint, other structures of reduced dimension were also considered. For example, in [2], structures consisting of layers or bismuth wires were considered. Since bismuth is a semimetal in the single-crystal state, the semimetal-semiconductor phase transition was considered to be the main mechanism for increasing its thermoelectric figure of merit with decreasing dimensionality of the structure, as a result of which the ratio between the contributions of electrons and holes to the kinetic coefficients and, consequently, to the thermoelectric figure of merit, changed radically. The reason for phase transition was dimensional quantization of free carrier energy spectrum, owing to which partial overlap of valence band and conduction band was removed, and a real gap appeared between them which eventually caused semiconductor properties of low-dimensional structures. In so doing, in the case of a structure consisting of wires, owing to dimensional quantization in two directions, the gap width was greater and, hence, the semiconductor properties were more expressed. That is why, according to calculations, the thermoelectric figure of merit of a "wire superlattice" was higher than the figure of merit of a layered superlattice. Thus, for instance, at quantum well width 2 nm and temperature gradient and electric field orientation along the trigonal axis, the dimensionless thermoelectric figure of merit of a layered superlattice at 300 K was about 2.5, and that of a wire superlattice – about 6. However, these results were not proved experimentally.

Superlattices consisting of *GaAs*/*AlGaAs*, *Si*-*Ge* layers and some others were considered as well. The properties of *GaAs*/*AlGaAs* superlattices widely used, for instance, in terahertz electronics, have been studied most thoroughly [3]. There are works on the use of superlattices based on gallium arsenide in thermoelectricity [4]. Superlattices based on *Si*-*Ge* have proved to be a good material for thermoelectric generators operating at higher temperatures than bismuth telluride [5, 6]. As generator medium- and high-temperature thermoelectric materials, the *ZnSb*/*CdSb* superlattices might also be of interest, although it is recommended to use them mainly in electronics, for example, for creating dynamic storage devices [7].

While studying the thermoelectric properties of superlattices, it was well established that, other things being equal, their thermoelectric figure of merit turns out to be considerably (sometimes even an order of magnitude) higher than the thermoelectric figure of merit of "ordinary" single crystals of

the same chemical composition. However, even this increased figure of merit does not exceed the figure of merit of traditionally used prevailing "ternary" and "quaternary" alloys based on *Bi*(*Sb*)-*Te*(*Se*) system. Such alloys, due to their layered structure and hexagonal symmetry, even by themselves, as we shall show later, can be considered as "superlattices".

Interest in "superlattice" materials, especially for generators, is also due to the fact that tellurium is expensive, toxic, its reserves in tellurium-containing polymetal ores are restricted, it is just a by-product of processing these ores and its main consumer is metallurgy, rather than thermoelectricity. At the same time, the need for thermoelectric modules is constantly increasing, so that high-efficient materials, including superlattice materials, could be worthy of competition with traditional materials without containing scarce, toxic and expensive components.

All of the above is the basis for setting the task of a more detailed theoretical consideration of factors that can both increase and reduce the thermoelectric figure of merit of "superlattice" materials. This is the purpose of the present article.

On the limitation of the figure of merit of "purely two-dimensional" superlattices

Let us consider and compare the figure of merit of "purely two-dimensional" superlattices and three-dimensional single crystals in the region of impurity conduction [8]. To clarify the role played by dimensionality reduction of the structure "in pure form", we will assume that both two-dimensional and three-dimensional electron gases are described by the isotropic effective mass approximation. By virtue of such approximation the relaxation time of free carrier momentum will be considered to be isotropic and depending on the kinetic energy ε of charge carriers as a whole by the power law with exponent r. For this exponent by virtue of general concepts of quantum mechanics the inequality $-0.5 \le r \le 3.5$ is valid.

We will also take into account that as long as the thermoelectric figure of merit *ZT* which is to be estimated is a dimensionless value, it must depend on certain dimensionless parameter or on the totality thereof. If as a first approximation we will consider lattice thermal conductivity of material to be low as compared to thermal conductivity of free carrier subsystem, in the case of isotropic and parabolic band spectrum of the latter the only such parameter (except for factor *r*) characterizing both material and its application conditions is the ratio of the Fermi energy ζ_0 of electron gas in material at the absolute zero temperature to the average energy $k_B T$ of thermal motion. Through this (or its reciprocal) ratio the reduced chemical potential $\eta = \zeta / k_B T$ is found from the following equations written for the two-dimensional and three-dimensional cases, respectively:

$$\eta = \ln\left[\exp\left(t_0^{-1}\right) - 1\right], \tag{2}$$

$$\frac{2}{3} t_0^{-1.5} = F_{0.5}(\eta). \tag{3}$$

In these formulae, $t_0 = k_B T / \zeta_0$.

The corresponding expressions for the thermoelectric figure of merit of a two-dimensional superlattice and a three-dimensional crystal are of the form:

$$ZT = \left[\frac{(2r+4)F_{r+1}(\eta)}{(2r+2)F_r(\eta)} - \eta\right]^2 \left[\frac{(r+3)F_{r+2}(\eta)}{(r+1)F_r(\eta)} - \frac{(r+2)^2 F_{r+1}^2(\eta)}{(r+1)^2 F_r^2(\eta)}\right]^{-1}, \tag{4}$$

$$ZT = \left[\frac{(2r+5)F_{r+1.5}(\eta)}{(2r+3)F_{r+0.5}(\eta)} - \eta\right]^2 \left[\frac{(r+3.5)F_{r+2.5}(\eta)}{(r+1.5)F_{r+0.5}(\eta)} - \frac{(r+2.5)^2 F^2_{r+1.5}(\eta)}{(r+1.5)^2 F^2_{r+0.5}(\eta)}\right]^{-1}. \quad (5)$$

Dependences described by Eqs. (2) – (5) are shown in Fig. 1.

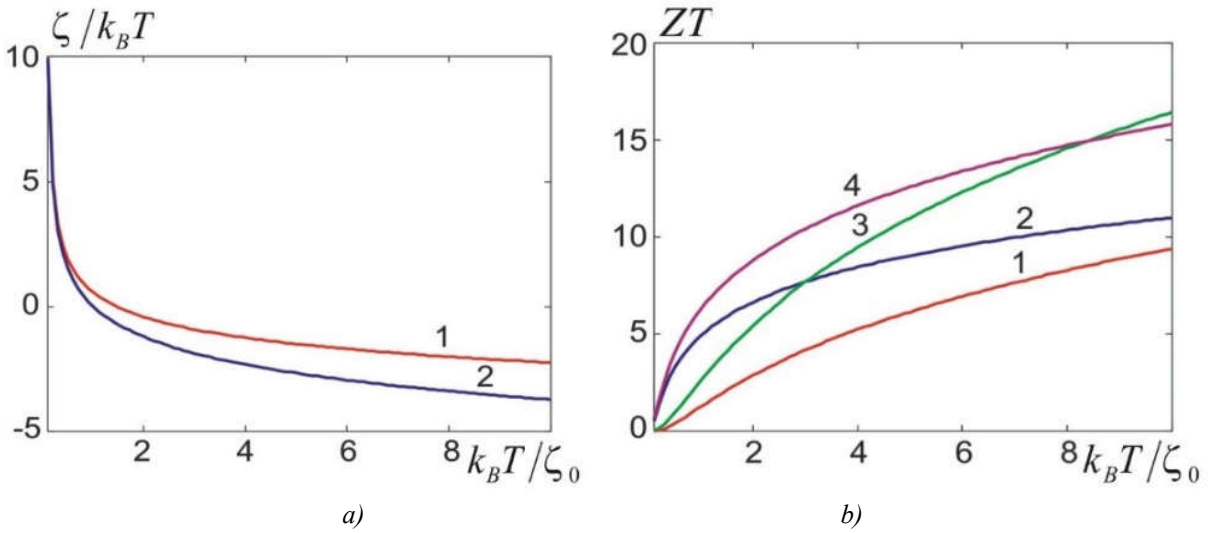

a) *b)*

Fig. 1. a) temperature dependences of reduced chemical potential: 1 – for a two-dimensional superlattice; 2 – for a three-dimensional crystal; b) dependences of the thermoelectric figure of merit on dimensionless temperature: 1, 2 – for a two-dimensional superlattice at r = – 0.5; 3.5 respectively; 3, 4 – for a three-dimensional crystal at the same r.

From the plots it follows that with the same values of dimensionless temperature and scattering factor the thermoelectric figure of merit of a three-dimensional crystal is much larger than that of a two-dimensional superlattice. Therefore, it is clear that at the same temperature the thermoelectric figure of merit of a "purely two-dimensional" superlattice can exceed the thermoelectric figure of merit of a three-dimensional crystal only when at absolute zero temperature the Fermi energy of electron gas in a "purely two-dimensional" superlattice will be much less than in a three-dimensional crystal. It can be shown that if scattering factor r, concentration n_0 and effective masses m^* of charge carriers in a "purely two-dimensional" superlattice and a three-dimensional crystal are identical, the above mentioned condition is equivalent to inequality $0.283\, n_0 a^3 << 1$. By virtue of this fact it is clear that increasing the distance a between superlattice layers, or, which is the same (at least for the simplest structure of identical layers), quantum well width, must significantly reduce the thermoelectric figure of merit of a "purely two-dimensional" superlattice. For instance, if typical for thermoelectric materials based on *Bi*(*Sb*)-*Te*(*Se*) system concentration of free charge carriers is assumed to be equal to $3 \cdot 10^{19} \text{cm}^{-3}$, then at the well width equal to 3 nm, the above inequality is satisfied relatively well, but already at a double width of the well it is not satisfied.

The situation can be slightly improved by such a combination of material parameters whereby not one but several quantum wells are involved in the processes of heat and electricity transfer, i.e. there is some dispersion of the energy of the interlayer motion of the charge carriers, by virtue of which the superlattices are not "purely two-dimensional". But exactly in the same way the situation can be improved by the use of sharply anisotropic layered materials in which the band spectrum of charge carriers is described by the Fivaz model, if their parameters are optimal [9, 10].

The figure of merit of superlattices described by the Fivaz model and optimization of their parameters

In the framework of the Fivaz model [11] the energy spectrum of charge carriers in material is determined as follows:

$$E\left(k_x, k_y, k_z\right) = \frac{\hbar^2}{2m^*}\left(k_x^2 + k_y^2\right) + \Delta\left(1 - \cos ak_z\right), \tag{6}$$

where k_x, k_y – quasi-momentum components in a plane parallel to layers, k_z – quasi-momentum component perpendicular to layers, m^* – effective mass of electron in a plane parallel to layers, Δ – half-width of a miniband describing the interlayer motion of electrons a – the distance between translation-equivalent layers. In the framework of such a model of energy spectrum on condition of electron mean free path independence of quantum numbers the dimensionless thermoelectric figure of merit of material is determined as follows:

$$ZT = 8\pi^3 \frac{A_0}{B_0 + \kappa_l \left(2k_B \zeta_{02D}^2 l\right)^{-1} ah^2 \sqrt{m^{*-1}\zeta_{02D}}}. \tag{7}$$

In so doing, the dimensionless functions A_0 and B_0 are of the form:

$$A_0 = \left\{\int_0^\infty\int_0^\pi \frac{y\left[y + K^{-1}\left(1-\cos x\right) - \gamma^*\right]\exp\left\{\left[y + K^{-1}\left(1-\cos x\right) - \gamma^*\right]/t_{2D}\right\}}{\left\{\exp\left\{\left[y + K^{-1}\left(1-\cos x\right) - \gamma^*\right]/t_{2D}\right\} + 1\right\}^2 \sqrt{2y + 4\pi K^{-2} n_0 a^3 \sin^2 x}} dxdy\right\}^2 \times$$
$$\left\{\int_0^\infty\int_0^\pi \frac{y\exp\left\{\left[y + K^{-1}\left(1-\cos x\right) - \gamma^*\right]/t_{2D}\right\}}{\left\{\exp\left\{\left[y + K^{-1}\left(1-\cos x\right) - \gamma^*\right]/t_{2D}\right\} + 1\right\}^2 \sqrt{2y + 4\pi K^{-2} n_0 a^3 \sin^2 x}} dxdy\right\}^{-1}, \tag{8}$$

$$B_0 = \int_0^\infty\int_0^\pi \frac{K^{-1}\left(1-\cos x\right) + y - \gamma^*}{t_{2D}^2} \cdot \frac{\exp\left\{\left[y + K^{-1}\left(1-\cos x\right) - \gamma^*\right]/t_{2D}\right\}}{\left\{\exp\left\{\left[y + K^{-1}\left(1-\cos x\right) - \gamma^*\right]/t_{2D}\right\} + 1\right\}^2} \times$$
$$\times \frac{y\left[y + K^{-1}\left(1-\cos x\right)\right]dxdy}{\sqrt{2y + 4\pi K^{-2} n_0 a^3 \sin^2 x}} +$$
$$+ \left\{\int_0^\infty\int_0^\pi \frac{y\left[y + K^{-1}\left(1-\cos x\right) - \gamma^*\right]\exp\left\{\left[y + K^{-1}\left(1-\cos x\right) - \gamma^*\right]/t_{2D}\right\}}{\left\{\exp\left\{\left[y + K^{-1}\left(1-\cos x\right) - \gamma^*\right]/t_{2D}\right\} + 1\right\}^2 \sqrt{2y + 4\pi K^{-2} n_0 a^3 \sin^2 x}} dxdy\right\} \times$$
$$\times \left\{\int_0^\infty\int_0^\pi \frac{y\exp\left\{\left[y + K^{-1}\left(1-\cos x\right) - \gamma^*\right]/t_{2D}\right\}}{\left\{\exp\left\{\left[y + K^{-1}\left(1-\cos x\right) - \gamma^*\right]/t_{2D}\right\} + 1\right\}^2 \sqrt{2y + 4\pi K^{-2} n_0 a^3 \sin^2 x}} dxdy\right\}^{-1} \times$$
$$\times \int_0^\infty\int_0^\pi \frac{K^{-1}\left(1-\cos x\right) + y - \gamma^*}{t_{2D}} \cdot \frac{\exp\left\{\left[y + K^{-1}\left(1-\cos x\right) - \gamma^*\right]/t_{2D}\right\}}{\left\{\exp\left\{\left[y + K^{-1}\left(1-\cos x\right) - \gamma^*\right]/t_{2D}\right\} + 1\right\}^2} \times$$
$$\times \frac{y\left[y + K^{-1}\left(1-\cos x\right)\right]dxdy}{\sqrt{2y + 4\pi K^{-2} n_0 a^3 \sin^2 x}}. \tag{9}$$

In formulae (7) – (9), the following notation is introduced: $K = \zeta_{02D}/\Delta, t_{2D} = k_B T/\zeta_{02D}, \gamma^* = \zeta/\zeta_{02D}$, ζ_{02D} – the Fermi energy of an ideal two-dimensional electron gas with a quadratic dispersion law, c_l – lattice thermal conductivity of material, l – mean free path of charge carriers in material. The normalized chemical potential of the free carrier subsystem $\gamma*$ was found from equation:

$$\frac{t_{2D}}{\pi}\int_0^{\pi} \ln\left[1+\exp\left(\frac{\gamma^* - 2\pi^{-2}K^{-1}x^2}{t_{2D}}\right)\right] - 1 = 0\,. \tag{10}$$

Note that in the calculation of the dimensionless thermoelectric figure of merit, the thermal conductivity was determined under condition of no current. The Peltier heat in this case was disregarded, as long as we considered the region of intrinsic conductivity.

The results of calculations of the dimensionless thermoelectric figure of merit of model superlattice thermoelectric material (SL TEM) with the effective electron mass $m^* = m_0$, the bulk carrier concentration $n_0 = 3\cdot 10^{19}$ cm^{-3}, the mean free path of charge carriers at 300 K $l = 20$ nm, the lattice thermal conductivity at 300 K $\kappa_l = 2$ W/(m·K) for different degrees of openness of the FS in the range of $0.01 \le K \le 1$ and temperatures $T = T_c = 300$ K, $T = T_h = 500$ K for two different values of *a*, as well as the generator efficiency between the above extreme temperatures are given in Fig. 2.

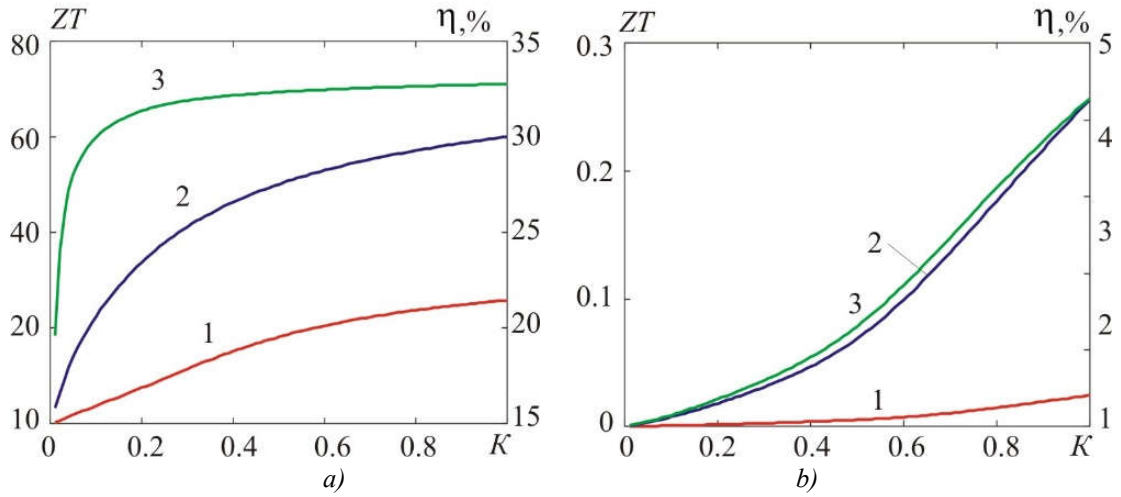

Fig. 2. Dependences of the dimensionless thermoelectric efficiency of SL TEM at T = 300 K (curves 1) and T = 500 K (curves 2), as well as generator efficiency at corresponding extreme temperatures (curves 3) for distances between SL TEM layers equal to 3 nm (a) and 15 nm (b), respectively.

Note that the values of $K < 1$ correspond to closed Fermi surfaces (FS), the value of $K = 1$ – to transient FS, the values of $K > 1$ – to open FS. The generator efficiency when constructing the plots in Fig. 2 was determined by the formula:

$$\eta = \frac{1}{1+2\sqrt{0.5\left(Z_c T_c + Z_h T_h\right)}\left(Z_h T_h\right)^{-1}} \cdot \frac{T_h - T_c}{T_h}\,. \tag{11}$$

From the figure it is seen that the figure of merit of SL TEM and the efficiency of generator significantly increase with increasing the degree of openness of the FS. For instance, for the considered model SL TEM at $a = 3$ nm the dimensionless thermoelectric figure of merit for transient

FS can reach 20 – 60, however, as the distance between the layers increases to 15 nm, it drops to the values not exceeding 0.25 even at 500 K. Accordingly, the generator efficiency between the corresponding extreme temperatures at $a = 3$ nm can reach 34%, or, in other words, 80% of the efficiency of the Carnot cycle, whereas at $a = 3$ nm it drops approximately to 4.2%, i.e. about 10% of the efficiency of the Carnot cycle.

The figures of merit of the same SL TEM as cooling material between temperatures $T = T_h = 300\,\text{K}$, $T = T_c = 230\,\text{K}$ and the coefficient of performance of the cooler were calculated in a quite similar fashion. To determine the latter, the following formula was used:

$$\varepsilon = \frac{\sqrt{1 + 0.5\left(Z_c T_c + Z_h T_h\right)} - T_h / T_c}{\sqrt{1 + 0.5\left(Z_c T_c + Z_h T_h\right)} + 1} \cdot \frac{T_c}{T_c - T_h}. \tag{12}$$

The results of these calculations are given in Fig. 3.

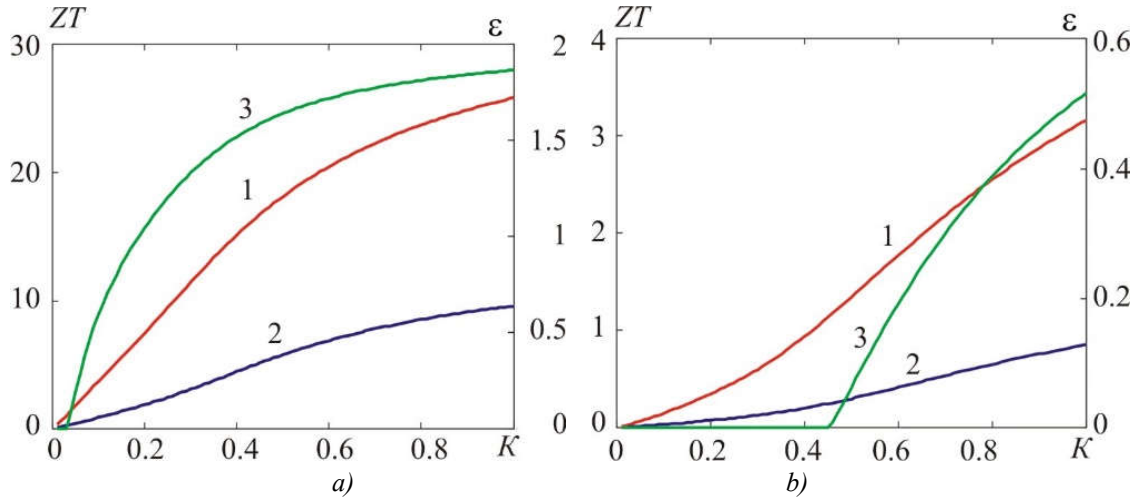

Fig. 3. Dependences of the dimensionless thermoelectric figure of merit of SL TEM at T = 300 K (curves 1) and T = 230 K (curves 2), as well as coefficient of performance of the cooler (curves 3) for corresponding extreme temperatures and the distances between SL TEM layers equal to 3 nm (a) and 6 nm (b), respectively.

From the plots it is seen that coefficient of performance at the hot side temperature equal to 300 K, drastically increases with increasing the degree of openness of the FS and with an optimal combination of SL TEM parameters for the transient surface it can reach 1.9 with temperature difference 70 K. However, as the distance between the layers increases from 3 to 6 nm, the maximum (for the range $0.01 \le K \le 1$) coefficient of performance decreases approximately to 0.52. Moreover, for each temperature difference there is a threshold degree of openness of the FS below which this difference with the use of one cooling stage is unattainable. This degree, as could be expected, increases rather drastically with increasing distance between the layers of SL TEM.

Thus, it turns out that to achieve high figure of merit of SL TEM, certain optimal combination of its parameters is needed, in particular, a combination of small distance between the layers and a high degree of openness of the FS. However, traditional SL TEM and layered materials based on *Al-Ga-As*, *Si-Ge*, *Bi*(*Sb*)-*Te*(*Se*) systems possess exactly the opposite property: the distance between their layers is sufficiently large, and the degree of openness of the FS is small. Such their feature is good for special, for instance, terahertz, electronics, but not very helpful for thermoelectric applications. Therefore, the correct approach in this case should not consist in the mechanical transfer of traditional

SL materials from electronics to thermoelectricity, but in the search for or the creation of "truly thermoelectric" SL materials, at least for the production of thermoelectric energy converters.

Our analysis showed that an "optimized" SL TEM might have, for instance, the following band parameters: $a = 30$ nm, $m^* = m_0$, $K = 1$, $\Delta = 2.16 \cdot 10^{-4}$ eV, and carrier concentration equal to $n_0 = 3 \cdot 10^{16}$ cm^{-3}. The energy gap of this material must be of the order of 1.74 eV. Such a wide energy gap is necessary in order that, in the "generator" temperature range, for example, at 500 K, the conductivity of the material does not change from impurity to intrinsic. The use of such material, if it were created, would allow increasing the generator efficiency between the temperatures 300 and 500 K to 37.5%, and the coefficient of performance on cooling from 300 to 230 K – to 2.92. However, the FS of such material should have the form shown in Fig. 4, and its band parameters – possess high temperature stability.

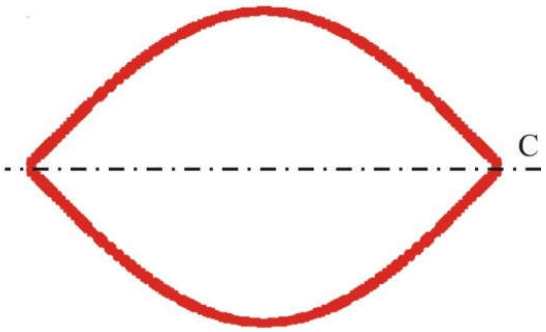

Fig. 4. The Fermi surface of possible SL TEM with a high figure of merit. The section of such FS with a plane parallel to layers is a circle, the C axis is perpendicular to the layers.

Calculations show that such SL TEM, if it were created, might be also applied for subsequent deeper cooling, for instance, from 200 to 100K, however, in this case the coefficient of performance would be 0.61. Even on condition of cooling from 300 to 100 K the coefficient of performance of such material would be about 0.3.

We see that our SL TEM, even though hypothetical at the moment, must have very narrow (at least in the direction of interlayer movement) allowed band, and, on the contrary, very wide forbidden band. Traditional thermoelectric materials, including those separately or together prone to formation of superlattices, for instance, gallium arsenide, bismuth telluride and alloys on its basis, silicon, germanium, zinc antimonide, cadmium antimonide and others in the overwhelming majority possess the opposite combination of band parameters, namely a narrow forbidden band and a wide allowed band. Exactly this fact determines the validity of using effective mass approximation in the theoretical calculation and description of the thermoelectric properties of the above materials.

It can be demonstrated that creation of SL TEM with so high figure of merit based on silicon, germanium or bismuth telluride is basically impossible. Indeed, for this to be possible, the distance between SL TEM layers must satisfy the condition $a \geq 4\pi m^* \Delta / n_0 h^2$. In so doing, Δ, in any case is a value of the order of forbidden band width E_g, and even larger, i.e. in traditional calculations Δ is assumed to be infinite, and FS seems to be consisting of identical ellipsoids. Therefore, substituting known parameters for silicon, namely $m^* = 1.26\, m_0$, $E_g = 1.12$ eV, $n_0 = 10^{15}$ cm^{-3}, we obtain

$a = 6.3$ mm. It is clear that such long-period superlattices cannot exist. The situation will not change too much, if we have, for instance, $n_0 = 3 \cdot 10^{19}$ cm^{-3}. In this case there should be $a = 210$ nm, whereas SL TEM based on *Si-Ge* have the highest a about 30 nm, and their highest thermoelectric figure of merit does not exceed 0.75 at $a = 7$ nm and $n_0 = 3 \cdot 10^{19}$ cm^{-3}, though this value is an order of magnitude higher than the dimensionless thermoelectric figure of merit of single crystals. In the former case the degree of openness of the FS is 0.16, and in the latter – 0.011, which, of course, is rather far from the required quasi-two-dimensionality value of highly efficient SL TEM equal to unity.

Likewise, if at $n_0 = 3 \cdot 10^{19}$ cm^{-3}, $a = 3$ nm, $m^* = m_0$ bismuth telluride were a single-valley SL TEM which obeys the Fivaz model, the degree of openness of its FS would be $K = 0.81\ \pi$ and the value of its dimensionless thermoelectric figure of merit at 300 K would be equal to 30.9. However, in reality, taking into account that the forbidden band width of this material is equal to 0.13 eV, and, hence, the allowed band width is of the order of 1.3 eV (it is necessary for the validity of traditional approaches based on parabolic band spectrum), we have $K = 0.017$, and, hence, the value of dimensionless thermoelectric figure of merit at 300 K equal to 0.531 which is completely correlated with the experimental data [12]. For cooling materials of *Bi*(*Sb*)-*Te*(*Se*) system the value of dimensionless thermoelectric figure of merit at 300 K is equal to 0.78 [13], which is matched by K = 0.024.

Based on the above, one can recommend the following four methods of finding promising SL TEM, including those described by the Fivaz model, by means of quantizing magnetic fields [14-16]:

1) study of Shubnikov-de-Haas oscillations in quasi-classical magnetic fields at helium temperatures, including study of the magnetic field dependence of oscillation amplitude;

2) selection of materials by the presence of negative longitudinal magnetoresistance section and its expressed minimum in ultra-quantum magnetic fields, if these are achievable;

3) selection of materials according to the degree of roundness of power factor peak in ultra-quantum magnetic fields;

4) selection of materials by the degree of manifestation of negative longitudinal magnetoresistance at higher temperatures.

The above methods should be supplemented with measurement of free carrier concentration by means of the Hall effect and X-ray diffraction control of interlayer distance.

Conclusions and recommendations

1. Conditions for the high figure of merit of quasi-two-dimensional thermoelectric materials are established.
2. Formulae for the figure of merit of thermoelectric materials described by the Fivaz model and the generator efficiency and the refrigerator coefficient of performance are derived depending on the degree of nonparabolicity of material band spectrum.
3. It is established that the generator efficiency and the refrigerator coefficient of performance drastically increase with increasing degree of nonparabolicity of material band spectrum, but drastically decrease with increasing distance between the layers.
4. Possible parameters of a promising high-figure-of-merit layered thermoelectric material described by the Fivaz model are evaluated.

A number of methods of search for promising layered thermoelectric materials with the use of quantizing magnetic fields are proposed.

References

1. Hicks L.D. Effect of quantum-well structures on the thermoelectric figure of merit. / Hicks L.D., Dresselhaus M.S.. // Phys. Rev. B.. – 1993. – P. 12727 – 12731.
2. Dresselhaus M.S. Low dimensional thermoelectric materials. / Dresselhaus M.S., Dresselhaus G., Sun X. [etc.]. // ФТТ.. – 1999. – P. 755 – 758.
3. Басс Ф.Г. Высокочастотные свойства полупроводников со сверхрешетками. / Басс Ф.Г., Булгаков А.А., Тетервов А.П. // Москва, 1989. – 288 с.
4. Zhang Y. Influence of doping concentration and ambient temperature on cross-plane Seebeck coefficient of *InGaAs/InAlAs* superlattices. / Zhang Y., Vashaee D., Singh R., Shakouri A.. // Mat. Res. Soc. Symp. Proc.. – 2004. – C. 59 – 65
5. Liu W.L. In-plane thermo- electric properties of *Si/Ge* superlattice. / Liu W.L., Borca-Tasciuk T., Liu J.L. [etc.]. // Proc. of 20th international conference on thermoelectrics. – 2001. – P. 340 – 343.
6. Venkatasubramanian R. In-plane thermoelectric properties of free-standing *Si/Ge* superlattice structures. / Venkatasubramanian R., Siivola E., Colpiits T.S. // Proc. of17th international conference on thermoelectrics. – 1998. – P. 191 – 197.
7. Берча Д.М. Зонная структура ромбических кристаллов *CdSb*, *ZnSb*, In_2Se_3 и моделирование сверхрешеток. / Берча Д.М., Митин О.Б., Раренко И.М. [та ін.]. // ФТП. – 1994. – С. 1249 – 1256.
8. Gorskyi P.V. Use of similarity criteria for evaluating the thermoelectric figure of merit of superlattices ArXiv: 1511.0557v1 [cond. mat. mes. hall] 2Nov / Gorskyi P.V. – 2015. – P. 1 – 3.
9. Gorskyi P.V. On conditions of high figure of merit and methods of search for promising superlattice thermoelectric thermoelectric materials. P.V. Gorskyi arXiv: 1509.01782 [cond.mat.mes.hall]. / Gorskyi P.V. – 2015. – 9 p.
10. Горский П.В. Об условиях высокой добротности и методиках поиска перспективных сверхрешеточных термоэлектрических материалов. / Горский П.В.. // Термоэлектричество. – 2015. – С. 5–14.
11. Fivaz R.F. Theory of layered structures. / Fivaz R.F.. // J. Phys. Chem. Sol. – 1967. – P. 839 – 845.
12. Гольцман Б.М. Полупроводниковые термоэлектрические материалы на основе Bi_2Te_3 / Гольцман Б.М., Кудинов В.А., Смирнов И.А. // 1972. – 320 с.
13. Ivanova L.D. Influence of purity and perfection of Czochralsky-growth single crystals of bismuth and antimony chalcogenides solid solution on their thermoelectric properties Proc / Ivanova L.D., Granatkina Yu.V., Dausher A. [etc.]. // Of 5th European Workshop on Thermoelectrics. Pardubice, Czech Republic. – 1999. – P. 175 – 178.
14. Gorskyi Peter V. Layered structure effects as realization of anisotropy in magnetic, galvanomagnetic and thermoelectric phenomena. / Gorskyi Peter V. – 352 p. – (ISBN 978-1-62808-875-5. xiv.).
15. Горський П.В. Діагностика функціональних матеріалів, описуваних моделлю Фіваза та деякі аспекти їх застосування. / Горський П.В.. // Доповіді Національної Академії наук України. – 2014. – С. 77 – 85.
16. Gorskyi P.V. Gigantic negative magnetoresistance of nanoheterostructures described by Fivaz model. arXiv: 1503.02863 [cond.mat.mes.hall]. / Gorskyi P.V.., 2015. – 3 p.

Submitted 16.03.2017

Горський П. В., докт. фіз.-мат. наук

Інститут термоелектрики НАН і МОН України,
вул. Науки, 1, Чернівці, 58029, Україна,
e-mail: anatych@gmail.com

МОДЕЛЬ ФІВАЗА Й ПЕРЕДБАЧЕННЯ ТЕРМОЕЛЕКТРИЧНИХ МАТЕРІАЛІВ

У роботі розглянута роль зниження розмірності структури термоелектричного матеріалу в підвищенні його термоелектричної ефективності. Показано, що термоелектрична ефективність «чисто двовимірного» термоелектричного матеріалу може перевищувати термоелектричну ефективність тривимірного кристалу лише тоді, коли енергія Фермі тривимірного кристалу при абсолютному нулі температури суттєво більша, ніж енергія Фермі «чисто двовимірного» матеріалу, що здійсненне тільки при досить малих відстанях між шарами й (або) ширинах квантових ям. У традиційних термоелектричних матеріалах ця умова виконується погано або не виконується зовсім. Вихід зі становища може полягати у використанні шаруватих (надграткових) матеріалів, описуваних моделлю Фіваза. Для цього вони повинні мати досить вузькі дозволені зони, що описують рух електронів між шарами, що забезпечує високий ступінь відкритості поверхні Фермі цих матеріалів. У той же час заборонені зони цих матеріалів повинні бути досить широкими для того, щоб перешкодити перетворенню домішкової провідності у власну в «генераторному» діапазоні температур. Традиційні шаруваті й надграткові матеріали, використовувані в електроніці та термоелектриці, мають діаметрально протилежну властивість: їх дозволені зони широкі, а заборонені – вузькі. Окрім того, відстані між їх шарами, і, отже, відповідні ширини квантових ям, досить великі. Зазначені фактори в сукупності суттєво обмежують термоелектричну ефективність цих матеріалів. На підставі проведеного аналізу визначені можливі оптимальні параметри перспективного надграткового термоелектричного матеріалу. Такий матеріал, якби він був створений, дозволив би з одного боку створити термоелектричний генератор з ККД порядку 34 % між температурами 300 і 500 К, а з іншого – охолоджувач, що забезпечує однокаскадне охолодження з 300 до 100 К з охолоджувальним коефіцієнтом близько 0.3. Запропоновано методики пошуку перспективних термоелектричних матеріалів, описуваних моделлю Фіваза, із застосуванням квантуючих магнітних полів. Бібл. 15, рис. 4.
Ключові слова: модель Фіваза, непараболічність, поверхня Фермі, термоелектрична добротність, коефіцієнт корисної дії,холодильний коефіцієнт, квантуюче магнітне поле, передбачення термоелектричних матеріалів.

Горский П. В., *докт. физ.-мат. наук*

Институт термоэлектричества, ул. Науки, 1,
Черновцы, 58029, Украина,
e-mail: anatych@gmail.com

МОДЕЛЬ ФИВАЗА И ПРЕДСКАЗАНИЕ ТЕРМОЭЛЕКТРИЧЕСКИХ МАТЕРИАЛОВ

В работе рассмотрена роль понижения размерности структуры термоэлектрического материала в повышении его термоэлектрической эффективности. Показано, что термоэлектрическая эффективность «чисто двумерного» термоэлектрического материала может превышать термоэлектрическую эффективность трехмерного кристалла лишь тогда, когда энергия Ферми трехмерного кристалла при абсолютном нуле температуры существенно больше, чем энергия Ферми «чисто двумерного» материала, что осуществимо только при достаточно малых расстояниях между слоями и (или) ширинах квантовых ям. В традиционных термоэлектрических материалах это условие выполняется плохо либо не выполняется вовсе. Выход из положения может состоять в использовании слоистых (сверхрешеточных) материалов, описываемых моделью Фиваза. Для этого они должны обладать весьма узкими разрешенными зонами, описывающими движение электронов между слоями, что обеспечивает высокую степень открытости поверхности Ферми этих материалов. В то же время запрещенные зоны этих материалов должны быть достаточно широкими с тем, чтобы воспрепятствовать превращению примесной проводимости в собственную в «генераторном» диапазоне температур. Традиционные слоистые и сверхрешеточные материалы, используемые в электронике и термоэлектричестве, обладают диаметрально противоположным свойством: их разрешенные зоны широки, а запрещенные узки. Кроме того, расстояния между их слоями, и, следовательно, соответствующие ширины квантовых ям, достаточно велики. Указанные факторы в совокупности существенно ограничивают термоэлектрическую эффективность этих материалов. На основании проведенного анализа определены возможные оптимальные параметры перспективного сверхрешеточного термоэлектрического материала. Такой материал, будь он создан, позволил бы с одной стороны создать термоэлектрический генератор с КПД порядка 34% между температурами 300 и 500К, а с другой – холодильник, обеспечивающий однокаскадное охлаждение с 300 до 100К с холодильным коэффициентом около 0.3. Предложены методики поиска перспективных термоэлектрических материалов, описываемых моделью Фиваза, с применением квантующих магнитных полей. Библ. 32, рис. 2.

Ключевые слова: модель Фиваза, непараболичность, поверхность Ферми, термоэлектрическая добротность, коэфициент полезного действия, холодильный коэфициент, квантующее магнитное поле, прогнозирование термоэлектрических материалов.

References

1. Hicks L.D., Dresselhaus M.S. (1993). Effect of quantum-well structures on the thermoelectric figure of merit. *Phys. Rev. B*, 47(19), 12727 – 12731.
2. Dresselhaus M.S., Dresselhaus G., Sun X., Zhang Z., Cronin S.B., Koga T. (1999). Low dimensional thermoelectric materials. *Solid State Physics*, 41(5), 755 – 758.
3. Bass F.G., Bulgakov A.A., Tetervov A.P. (1989). *Vysokochastotnye svoistva poluprovodnikov so sverhreshetkami [High-frequency properties of semiconductors with superlattices]*. Moscow: Nauka [in Russian].
4. Zhang Y., Vashaee D., Singh R., Shakouri A. (2004). Influence of doping concentration and ambient temperature on cross-plane Seebeck coefficient of *InGaAs/InAlAs* superlattices. *Proc. Mat. Res. Soc. Symp.* Vol.793. (P. 59 – 65).
5. Liu W.L., Borca-Tasciuk T., Liu J.L., Taka K., Wang K.L., Dresselhaus M.S., Chen G. (2001).In-plane thermoelectric properties of *Si/Ge* superlattice. *Proc. of 20th International Conference on Thermoelectrics*. (pp. 340 – 343).

6. Venkatasubramanian R., Siivola E., Colpiits T.S. (1998). In-plane thermoelectric properties of free- standing *Si*/*Ge* superlattice structures. *Proc. of 17th International Conference on Thermoelectrics*. (pp. 191 – 197)
7. Bercha D.M., Mitin O.B., Rarenko I.M., Kharkhalis L.Yu., Bercha A.I. (1994). Zonnaya struktura rombicheskikh kristallov *CdSb*, *ZnSb*, In_2Se_3 i modelirovanie sverhreshetok [Band structure of *CdSb*, *ZnSb*, In_2Se_3 rhombic crystals and simulation of superlattices]. *Fizika i tekhnika poluprovodnikov – Semiconductors*, 28(7), 1249 – 1256 [in Russian].
8. Gorskyi P.V. Use of similarity criteria for evaluating the thermoelectric figure of merit of superlattices ArXiv: 1511.0557v1 [cond. mat. mes. hall] 2Nov. 2015. P. 1 – 3.
9. Gorskyi P.V. On conditions of high figure of merit and methods of search for promising superlattice thermoelectric thermoelectric materials. P.V. Gorskyi arXiv: 1509.01782 [cond.mat.mes.hall]. 2015. 9p.
10. Gorskiy P.V. (2015). Ob usloviakh vysokoi dobrotnosti i metodikah poiska perpektivnyh sverhreshetochnyh termoelektricheskikh materialov [On the conditions of high figure of merit and methods of search for promising superlattice thermoelectric materials]. *Termoelektrichestvo - J.Thermoelectricity,* 3, 5 – 14 [in Russian].
11. Fivaz R.F. (1967). Theory of layered structures. *J. Phys. Chem. Sol*., 26(5), 839 – 845.
12. Goltsman B.M., Kudinov V.A., Smirnov I.A. (1972). Poluprovodnikovye termoelektricheskie materialy na osnove Bi_2Te_3.*[Semiconductor thermoelectric materials based on* Bi_2Te_3*.* Moscow: Nauka. [in Russian].
13. Ivanova L.D., Granatkina Yu.V., Dausher A., Lenoir B., Sherrer H. (1999). Influence of purity and perfection of Czochralsky-growth single crystals of bismuth and antimony chalcogenides solid solution on their thermoelectric properties Proc. *of 5th European Workshop on Thermoelectrics.* (Pardubice, Czech Republic, September 20-21, 1999) (pp.175-178).
14. Gorskyi P. V. Layered structure effects as realization of anisotropy in magnetic, galvanomagnetic and thermoelectric phenomena. Nova Publishers. New York-2014. ISBN 978-1-62808-875-5. xiv. 352 p.
15. Gorskyi P.V. (2014). Diagnostyka funktsionalnyh materialiv, opysuvanykh modelliu Fivaza ta deiaki aspekty yikh zastosuvannia [Diagnostics of functional materials described by the Fivaz model and some aspects of their use]. *Dopovidi Natsionalnoi Akademii nauk Ukrainy – Reports of the National Academy of Sciences of Ukraine,* 12, 77 – 85 [in Ukrainian].
16. Gorskyi P.V. Gigantic negative magnetoresistance of nanoheterostructures described by Fivaz model.arXiv: 1503.02863 [cond.mat.mes.hall]. 2015. 3p.

Submitted 16.03.2017

T. A. Ismailov *Doctor of Technical Sciences*,
T. A. Ragimova *Candidate of Technical Sciences*,
M. A. Khazamova *Candidate of Technical Sciences*

Federal State Budgetary Educational Institution of Higher Professional Education
"Dagestan State Technical University"70, Imam Shamil avenue,
Makhachkala, 367015, Russia, *e-mail: dstu@dstu.ru*

RESEARCH ON A THERMOELECTRIC DEVICE FOR THERMOPUNCTURE

The paper deals with a thermoelectric device for thermopuncture. The results of mathematical simulation of the work of device for thermopuncture are presented. Single-dimensional theoretical plots of temperature distribution in heating and cooling modes are given. Bibl. 9, Fig. 5
Key words: biologically active point, thermoelectric system, thermopile, thermal impact, thermal field, mathematical model, prototype, experiment.

Introduction

In contemporary context, the priority is the impact on the human body of natural physical factors. Among them, a widely used and effective method of medical rehabilitation is a local thermal effect. [1].

The mechanism of thermotherapy is quite complex and consists of local and general reactions. With the impact on biologically active points, of interest is local focal reaction which is manifested in improving blood and lymph circulation and neurotrophic processes. Cold and thermal effects act on the skin, most closely associated with the central nervous system. By irritating peripheral receptors in this way, the temperature factor affects the entire body. The thermal effect on the reflexogenic zones of the human body, which is defined as puncture physiotherapy, has the following therapeutic effect on the body [2]: pain killing (gipalgesia, less often analgesia); more intensive formation of certain types of neurohumoral substances; normalization of many components of the mediator exchange; normalization of vegetoendocrinic functions; improvement of microcirculation in many organs and systems; normalization of arterial and venous pressure; antidepressant and sedative action.

Currently used means for cold impact on the biologically active points are represented by cryoprobes of various configurations which outperformed the reaction of classical acupuncture: from cryoreflexotherapy 84% of improvements, from a needle – 52.3% [3].

In most cases, the method of heating the biologically active points of the body is used, which, with reduced body resistance, often gives a more pronounced therapeutic effect compared with acupuncture at the same indications. Warming can be used alone or in combination with acupuncture. There are two main types of thermal effects: remote and contact. Remote thermopuncture is carried out with the help of wormwood cigars. Contact thermopuncture is very consistent with most areas of alternative medicine and is effective in conjunction with finger point massage. To cool or heat a limited area of the skin, various skin-temperature instruments are also used [1, 4].

The methods and tools cited have various drawbacks. Thus, the supply of temperature stimuli with the help of skin-temperature instruments ("temperature boxes") and other devices used for this

purpose – thermodes filled with water or ice, does not provide an accurate dosage of thermal irritation and requires further improvement. In addition, all of the above methods do not have the possibility of combined exposure to various physical factors, the consequence of which is the lack of modern tools that would ensure the effectiveness of treatment.

Taking into account these aspects, the thermoelectric method of creating a local thermal effect, in comparison with other methods, has proved to be out of competition [5, 6], since the thermopuncture technique requires both cold and thermal effects with pulses of certain duration. The required contrast mode of action is possible by simply switching the current direction [7, 8].

In this connection, the purpose of the work is to investigate the thermoelectric device for thermopuncture, to study the processes taking place in it taking into account the influence of the object parameters and the characteristics of thermopiles.

The design of a thermoelectric device for thermopuncture comprises a cylindrical housing equipped with a threaded lid sealing the housing with a rubber gasket. The housing is divided into sections by the finning of a sleeve made of high-heat-conducting metal and pressed into the opposite end of the housing. A threaded hole is made in the sleeve into which the working head is screwed, also made of high-heat-conducting metal in the form of a screw with a flat cap in contact with the first junctions of the thermopile. A washer with a thread on which a hemispherical nozzle is mounted is connected to the second junctions of the thermopile in thermal contact with them. The thermopile is electrically connected to the voltage polarity switch and an adjustable current source [9].

Mathematical simulation of a thermoelectric device for local thermal effect on the reflex zones of human body

A mathematical model of a device for local thermal effect on the reflex zones of human body was developed. This mathematical model considers the device as a set of elements – heat-exchange devices assuring the temperature of effect on the biological object within the required time to the necessary value.

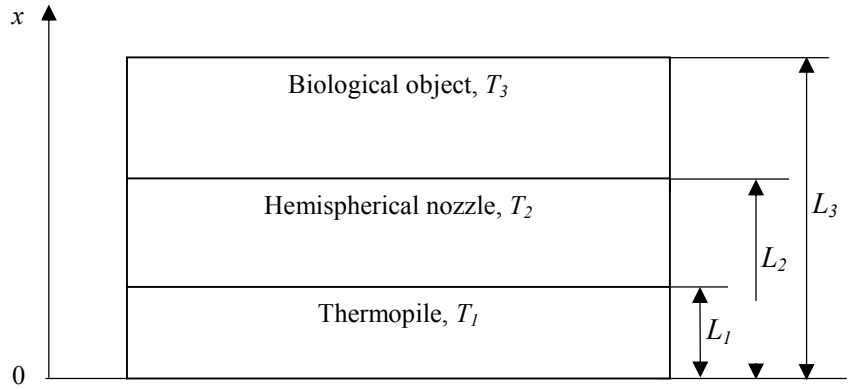

Fig. 1. Physical model of TE device.

A physical model of the device consisting of adjoining layers is shown in Fig 1. Layer 1 of thickness L_1 is a thermopile brought into thermal contact with a hemispherical nozzle. Layer 2 of thickness $L_2 - L_1$ is a nozzle, layer 3 of thickness is a biological object. It is assumed that this system is isolated from the lateral and top surfaces.

Mathematical formulation of the problem of heat exchange calculation for such a model is of the form:

$$\frac{d^2T_1}{dx^2}+\frac{r_1I_1^2}{\lambda_1}=0, \tag{1}$$

$$\frac{d^2T_0}{dx^2}=0, \tag{2}$$

$$\frac{d^2T_3}{dx^2}+\frac{q_{\text{ext}}}{\lambda_3}=0\,, \tag{3}$$

with the boundary conditions

$$T_1\big|_{x=0}=T_{1.\text{ext}}\,, \tag{4}$$

$$\lambda_2\frac{dT_2}{dx}\bigg|_{x=L_1}=\lambda_1\frac{dT_1}{dx}\bigg|_{x=L_1}-q_{0.1}\,, \tag{5}$$

$$\lambda_2\frac{dT_2}{dx}\bigg|_{x=L_2}-fv\rho=\lambda_3\frac{dT_3}{dx}\bigg|_{x=L_2}\,, \tag{6}$$

$$\lambda_3\frac{dT_3}{dx}\bigg|_{x=L_3}=0\,, \tag{7}$$

$$T_1\big|_{x=L_1}=T_2\big|_{x=L_1},\ T_2\big|_{x=L_2}=T_3\big|_{x=L_2}\,, \tag{8}$$

where $T_1,\ T_2,\ T_3$ is temperature distribution across the thickness of the thermopile, nozzle, biological object; r_1, I_1 is resistance and supply current of the thermopile; $\lambda_1, \lambda_2, \lambda_3$ is thermal conductivity coefficient of the thermopile, nozzle, biological object, respectively; q_{ext} is the amount of heat release per unit time in the biological object; $T_{1.\text{ext}}$ is the temperature of the thermopile external junctions; $q_{0.1}$ is heat flux on the internal thermopile junctions arising due to (absorption, release) of the Peltier heat; f is friction coefficient in case of displacement of the nozzle along the surface of the biological object; ν is travel speed of the nozzle; P is nozzle pressure on the biological object.

Calculations were performed at $T_1=T_{1.\text{ext}}=T_2=20\,^{\circ}\text{C}$, $T_3=36.6^{\circ}\text{C}$, $\lambda_1=0.6$ W/(m·K), $\lambda_2=10$ W/(m·K), $\lambda_3=0.25$ W/(m·K), $q_{\text{ext}}=40$ W/m^2, $f=0.5$, $\nu=0.01$, $P=1000$ N/m^2, $q_{0.1}=-3000$ W/m^2 (in cooling mode), $q_{0.1}=4000$ W/m^2 (in heating mode).

Solution of system (1)-(3) with the boundary conditions (4)-(8) can be presented as follows:

$$T_1=-\frac{r_1I_1^2}{2\lambda_1}x^2+C_{11}x+C_{21},, \tag{9}$$

$$T_2=C_{12}x+C_{22}, \tag{10}$$

$$T_3=-\frac{q_{\text{ext}}}{2\lambda_3}x^2+C_{13}x+C_{23}, \tag{11}$$

where integration constants C_{11}, C_{12}, C_{13}, C_{21}, C_{22}, C_{23} are found from the solution of the system of equations

$$C_{21}=T_{1.\text{ext}};\ C_{12}\lambda_2=r_1I_1^2L_1+C_{11}\lambda_1-q_{0.1};\quad -\frac{r_1I_1^2}{2\lambda_1}L_1^2+C_{11}L_1+C_{21}=C_{12}L+C_{22};$$

$$C_{12}\lambda_2-fvP=-q_{\text{ext}}L_2+C_{13}\lambda_3;\quad C_{12}L_2+C_{22}=-\frac{q_{\text{ext}}}{2\lambda_3}L_3^2+C_{13}L_2+C_{23}; \tag{12}$$

$$-q_{\text{ext}}L_3+C_{13}\lambda_3=0.$$

Equations (9)-(11) describe temperature distribution across the thickness of each layer in the system, with regard to heat fluxes on the internal thermopile junctions, parameters of the biological object and the nozzle.

The results of calculations using these dependences are shown in Figs. 2-5.

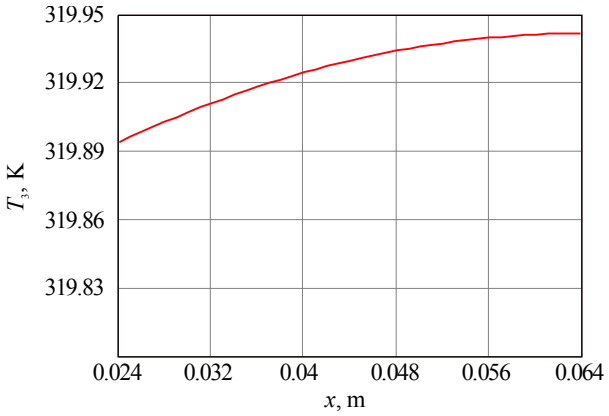

Fig. 2. Temperature distribution across the thickness of the biological object at q_{01} = 4000 W/m^2 in heating mode.

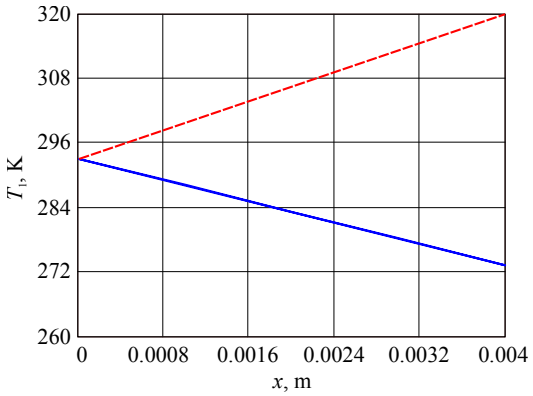

Fig. 3. Temperature distribution in thermopile at q_1 = 4000 W/m^2 in heating mode and q_{01} = –3000 W/m^2 in cooling mode.

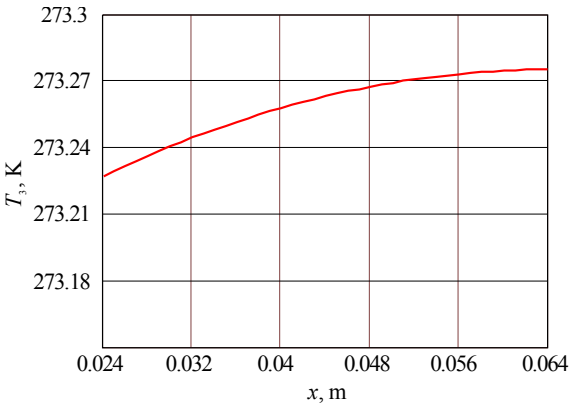

Fig. 4. Temperature distribution across the thickness of the biological object at q_{01} = –3000 W/m^2 in cooling mode.

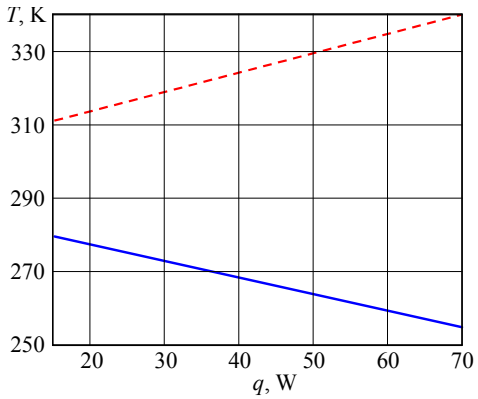

Fig. 5. Dependence of biological object temperature at the depth of 0.025 m on thermopile cooling capacity in cooling and heating mode.

Of greatest interest are the dependences which determine temperature distribution across the thickness of the biological object (Fig. 2). In this case, there is practically no temperature difference across the thickness of the biological object. This is due to the availability of intensive heat removal from the biological object and its own, low specific heat release of the biological object as compared to heat flux from its surface, as well as consideration of steady-state mode of the "device-biological object" system.

For the model under consideration Fig. 5 shows a plot of the biological object temperature at the depth of 0.025 m (the lower skin boundary) on thermopile cooling capacity.

According to the plot, the dependence is practically linear, and the necessary range of thermal effect corresponds to thermopile cooling capacity of the order of 30 W, which determines quite acceptable value of energy consumption.

Conclusions

Based on the calculations performed, the following conclusions can be made:

1. One of the efficient physiotherapeutic methods of prophylaxis, treatment and rehabilitation of various diseases is local thermal impact on the biologically active points of human body. This procedure can be implemented due to the use of a thermopile as a source of heat and cold.
2. A design of thermoelectric device for thermopuncture has been developed consisting of current source and control unit which supply to thermopile current of the necessary value and polarity depending on the assigned temperature of hemispherical nozzle.
3. A mathematical model of thermoelectric system has been proposed which considers a device as a unified set of elements – heat-exchange devices assuring the temperature of impact on the biological object within the required time to the necessary value.
4. It has been established that under a local temperature effect on the biological object there is no essential temperature drop across its thickness. This aspect makes it possible to assert that the proposed device is safe to use, since at a temperature effect on a biologically active point there is no parasitic thermal field affecting the nearby organs and tissues.
5. The developed device has low energy consumption, since the necessary range of thermal impact corresponds to cooling capacity and heat production of thermopile.
6. The results of theoretical studies of the thermoelectric device for thermopuncture showed its undeniable advantages when used in practice.

References

1. Александров В.В. Основы восстановительной медицины и физиотерапии. / Александров В.В., Алгазин А.И., 2010. – 144 с.
2. Физическая реабилитация. – Ростов н/Д.: Под ред. С.Н.Попова., 2004.
3. Баранов А.Ю. Криогенная физиотерапия Физиотерапия, бальнеология и реабилитация / Баранов А.Ю.. – 2005. – №3.
4. Physiological and clinical changes after therapeutic massage of the neck and shoulders. / Sefton JoEllen M., Yarar Ceren, Carpenter David M., Berry Jack W.. // Manual Therapy.. – 2011 October Vol. 16. Iss. 5. P. 487 – 494.
5. Исмаилов Т.А. Термоэлектрические полупроводниковые устройства и интенсификаторы теплопередачи: монография Политехника. 2005. 533 с.
6. Twaha Ssennoga. A comprehensive review of thermoelectric technology: Materials, applications, modelling and performance improvement. / Twaha Ssennoga, Zhu Jie, Yuying, Bo Li. // Renewable and Sustainable Energy Reviews.. – 2016. – С. 698 – 726.
7. Патент РФ № 2312647. Термоэлектрическое полупроводниковое устройство для температурного воздействия на ухо человека // Исмаилов Т.А., Аминов Г.И., Хазамова М.А., Рагимова Т.А., 2007.
8. Патент РФ № 2326625. Термоэлектрическое полупроводниковое устройство для аурикулярного температурного массажа // Исмаилов Т.А., Аминов Г.И., Хазамова М.А., Рагимова Т.А. 2008.
9. Патент РФ №2146511. Полупроводниковое устройство для термопунктуры // Исмаилов Т.А., Гаджиев Х.М., Зарат А.У. 2001.

Submitted 18.03.17

Ісмаїлов Т. А. *докт. техн. наук*, **Рагімова Т. А.** *канд. техн. наук*,
Хазамова М. А. *канд. техн. наук*

ФДБОУ В «Дагестанський державний технічний університет»,
Росія, м. Махачкала, пр. Імама Шаміля, буд.70, 367015
e-mail: dstu@dstu.ru

ДОСЛІДЖЕННЯ ТЕРМОЕЛЕКТРИЧНОГО ПРИСТРОЮ ДЛЯ ПРОВЕДЕННЯ ТЕРМОПУНКТУРИ

У роботі розглянуто термоелектричний пристрій для термопунктури. Представлені результати математичного моделювання роботи пристрою для термопунктури. Наведені одновимірні теоретичні графіки розподілу температури в режимах нагрівання й охолодження. Бібл. 9, рис. 5

Ключові слова: біологічно активна точка, термоелектрична система, термоелектрична батарея, тепловий вплив, теплове поле, математична модель, дослідний зразок, експеримент.

Исмаилов Т. А. *докт. техн. наук*, **Рагимова Т. А.** *канд. техн. наук*,
Хазамова М. А. *канд. техн. наук*

ФГБОУ ВО «Дагестанский государственный технический университет»,
пр. Имама Шамиля, 70, 367015, Махачкала, Россия
e-mail: dstu@dstu.ru

ИССЛЕДОВАНИЕ ТЕРМОЭЛЕКТРИЧЕСКОГО УСТРОЙСТВА ДЛЯ ПРОВЕДЕНИЯ ТЕРМОПУНКТУРЫ

В работе рассмотрено термоэлектрическое устройство для термопунктуры. Представлены результаты математического моделирования работы устройства для термопунктуры. Приведены одномерные теоретические графики распределения температуры в режимах нагрева и охлаждения. Библ. 9, рис. 5

Ключевые слова: биологически активная точка, термоэлектрическая система, термоэлектрическая батарея, тепловое воздействие, тепловое поле, математическая модель, опытный образец, эксперимент.

References

1. Aleksandrov V.V., Algazin A.I. (2010). *Osnovy vosstanovitelnoi meditsiny i fizioterapii [Fundamerntals of rehabilitation medicine and physiotherapy]*. Moscow: GEOTAR-Media [in Russian].
2. Popova S.N. (Ed.) (2004). *Fizicheskaia reabilitatsia [Physical rehabilitation]*. Rostov-on-Don [in Russian].
3. Baranov A.Yu. (2005). Kriogennaia fizioterpia [Cryogenic Physiotherapy]. *Fizioterapia, balneologia i reabilitatsia –Physiotherapy, Balneology and Rehabilitation*, 3 [in Russian].

4. Sefton JoEllen M., Yarar Ceren, Carpenter David M., Berry Jack W. (2011). Physiological and clinical changes after therapeutic massage of the neck and shoulders. *Manual Therapy,* 16(5), 487 – 494.
5. Ismailov T.A. (2005). *Termoelektricheskie poluprovodnikovye ustroistva i intensifikatory teploperedachi: monografia [Thermoelectric semiconductor devices and heat transfer intensifiers: Monograph]*. St.-Peterburg: Politechnika.
6. Twaha Ssennoga, Zhu Jie, Yuying Bo Li. (2016). A comprehensive review of thermoelectric technology: Materials, applications, modelling and performance improvement. *Renewable and Sustainable Energy Reviews,* 65, 698 – 726.
7. *Patent of RF № 2312647*. (2007). Ismailov T.A., Aminov G.I., Khazamova M.A., Ragimova T.A. Thermoelectric semiconductor device for temperature effect on human ear [in Russian].
8. *Patent of RF № 2326625*. (2008). Ismailov T.A., Aminov G.I., Khazamova M.A., Ragimova T.A. Thermoelectric semiconductor device for auricular temperature massage [in Russian].
9. *Patent of RF* №2146511. (2001). Ismailov T.A., Gadzhiev Kh.M., Zarat A.U. [in Russian].

Submitted 18.03.17

Касіян А.І.

A. I. Casian, *Doctor of Technical Sciences*,
I. I. Sanduleac

Technical University of Moldova, Av. Stefan cel Mare 168, MD-2004, Chisinau, Rep. of Moldova,
e-mail: acasian@mail.utm.md

Сандуляк І.І.

THERMOELECTRIC EFFICIENCY OF A *p-n*-MODULE FORMED FROM ORGANIC MATERIALS

We analyze the thermoelectric properties of p-type tetrathiotetracene-iodide crystals, TTT_2I_3 and of n-type tetrathiotetracene-tetracyanoquinodimethane crystals, $TTT(TCNQ)_2$ in the frame of a more complete 3D physical model. It is shown that in order to increase the thermoelectric efficiency it is necessary to decrease the carrier concentration in crystals of p-type and to increase in those of n-type in comparison with the stoichiometric ones. Considered crystals admit nonstoichiometric composition. Optimal parameters are determined in order to achieve as high as possible values of thermoelectric figure of merit ZT. The thermoelectric efficiency of a p-n-module is modelled as function of crystal parameters. Bibl. 17, Tab. 1.

Key words: organic crystals, thermoelectric efficiency, thermoelectric figure of merit, *p-n*-module, tetrathiotetracene-iodide, tetrathiotetracene-tetracyanoquinodimethane.

Introduction

The search and investigation of more efficient thermoelectric materials continue to be an important and timely problem of solid-state physics. In the last years, organic compounds attract more and more attention as materials that are less expensive, have more diverse and often unusual properties in comparison with their inorganic counterparts. The molecular structure of these compounds can be easily modified to tune the desirable physical and chemical properties. Besides, the organic materials usually have low thermal conductivity and are friendly with the environment. Therefore, organic materials are good candidates for applications in cooling systems and in conversion of enormous waste heat into electrical energy.

The main parameter that determines the thermoelectric performance of a given material is the dimensionless thermoelectric figure of merit ZT, where T is the operating temperature. Now the largest commercially applied thermoelectric materials on the basis of Bi_2Te_3 have $ZT \sim 1$ near room T. It is a rather low value. Therefore, now the commercialization of thermoelectric devices has still limited applications. Nevertheless, one can mention the mass production of miniature thermoelectric modules destined to maintain constant temperatures in the laser diodes [1], climate control seats installed in hundreds of thousands of vehicles each year [2], portable beverage coolers [3] and other applications, including cosmic ones.

A value of $ZT \geq 3$ would make the solid-state convertors economically competitive with the ordinary used ones. Important progress in the growth of ZT has been obtained in low dimensional inorganic structures. A value of $ZT \sim 3$ has been reported in *PbTeSe* quantum dot superlattices [4] and even $ZT \sim 3.5$ [5]. However, these values have been realized in very sophisticated,

technologically complicated and very expensive structures. Nevertheless, it is demonstrated that such high values of *ZT* are possible.

The thermoelectric parameters of organic materials are improved, too. In poly (3, 4-ethylenedioxythiophene) (PEDOT) doped by poly(styrenesulphonate) (PSS) thin films of *p*-type a value of $ZT = 0.42$ at room temperature has been measured [6]. Even $ZT \sim 1$ has been reported in PP-PEDOT/Tos [7] films. We have predicted high values of *ZT* in some quasi-one-dimensional (Q1D) organic crystals, including those of *p*-type tetrathiotetracene-iodide, TTT_2I_3 [8] and of *n*-type tetrathiotetracene-tetracyanoquinodimethane, $TTT(TCNQ)_2$ [9].

In this paper, we study the thermoelectric properties of *p*-type crystals, TTT_2I_3 and of *n*-type, $TTT(TCNQ)_2$ in the frame of a more complete three-dimensional (3D) physical model. This model becomes rather cumbersome, but it permits to perform realistic modeling and to determine the optimal crystal parameters in order to achieve the maximum values of the thermoelectric figure of merit. In addition, it permits to determine the limitation of the improvement of thermoelectric proprieties that impose the carrier scattering on neighboring conductive chains.

Crystals with improved degree of perfection are considered. Due to the violation of the Wiedemann-Franz law and the diminution of the Lorentz number, in these crystals the growth of electrical conductivity is accompanied with a reduced growth of the electronic thermal conductivity. This is favorable for the increase of thermoelectric figure of merit *ZT*. Optimal parameters are determined in order to achieve as high as possible values of *ZT*. The thermoelectric efficiency of a *p*-*n*-module is modelled as function of crystal parameters.

Efficiency of a thermoelectric convertor in the regime of electricity generation

The efficiency of a thermoelectric convertor for electricity generation is determined by the parameter η, defined as:

$$\eta = E / Q , \tag{1}$$

where *E* is the energy provided to the load and *Q* is the heat energy absorbed at hot junction. Usually, η is measured in percents and its value depends on *ZT* of both *p*- and *n*-type materials used. The dimensionless figure of merit $ZT = \sigma S^2 T/\kappa$, where σ is the electrical conductivity, *S* is the Seebeck coefficient and κ is the thermal conductivity of the considered material. The thermal conductivity $\kappa = \kappa^{ph} + \kappa^{e}$, where κ^{ph} is the phonon contribution and κ^{e} is the electronic contribution to κ. Values of *ZT* as high as possible are needed. One may think that for this it is sufficiently to increase simultaneously σ and *S* and to decrease κ. However, σ, *S* and κ are independent of each other. The increase of σ leads to decrease of *S* and to increase of κ^{e} and vice versa. Therefore, ordinary commercial thermoelectric devices made of Bi_2Te_3/Sb_2Te_3 for near room temperature applications and of *PbTe* for higher temperature applications have a *ZT* of around one. New, more sophisticated materials are needed in order to overcome the interdependence of σ, *S* and κ^{e}.

The thermoelectric convertors are formed from a series of thermocouples, each made of two legs of *n*-and *p*-type materials [10]. As an example, HZ-14 module developed by Hi-Z Company, has 6.27 cm by 6.27 cm ceramic area with 49 *p*-*n* pairs of bismuth telluride based semiconductors and a thickness of about 5 mm (see [11] available at http://www.hi-z.com/hz-14.html.) The module provides 25 W (5% efficiency) output for a temperature difference of 300°C.

The maximum efficiency η_{max} is given by

$$\eta_{\max} = \frac{T_h - T_c}{T_h} \frac{\sqrt{1+ZT_{av}} - 1}{\sqrt{1+ZT_{av}} + T_c / T_h}, \tag{2}$$

where T_h is the temperature at hot side, T_c is the temperature at the surface of cooled side and T_{av} is the average temperature $T_{av} = (T_h + T_c)/2$. The first factor in (2) is the efficiency of the Carnot cycle. ZT_{av} is the dimensionless figure of merit of the device, which takes into consideration the thermoelectric figures of merit of both of *n*-and *p*-type materials. Geometrical optimization with respect to legs sections yields [12]:

$$ZT_{av} = \frac{(S_p - S_n)^2 T_{av}}{[(\sigma_n^{-1}\kappa_n)^{1/2} + (\sigma_p^{-1}\kappa_p)^{1/2}]^2}, \tag{3}$$

where σ_n, σ_p, S_n, S_p, κ_n, and κ_p are the electrical conductivities, Seebeck coefficients and thermal conductivities of *n*-and *p*-type materials, respectively.

Organic material of *p*-type

In the previous publications [8, 13 – 17] we have demonstrated that the nanostructured crystals of TTT_2I_3 are very promising thermoelectric materials of *p*-type. The crystals have needle-like form of the length of 6-12 mm and thickness of 30 – 60 μm almost ready for thermoelectric legs. The lattice constants a = 18.35 Å, b = 4.96 Å, c = 18.46 Å show a pronounced quasi-one-dimensional structure of the crystal. As a result, the electrical conductivity along conductive *TTT* chains σ_p is almost three orders of magnitude higher than in transversal directions. The carriers are holes. The width of conduction band along *TTT* chains is $4w_1$ = 0.64 eV (~ 25 k_0T_0, T_0 = 300 K), where w_1 is the transfer energy of hole from a given molecule to the nearest one in the *b* direction. The matrix element of electron-phonon interactions takes into account two main interactions. The first interaction is caused by the variation of transfer energies w_1, w_2 and w_3 of a hole from the given molecule to the nearest ones along lattice vectors, due to molecular vibrations and is similar to that of deformation potential. Three coupling constants of this mechanism are proportional to the derivatives w_1', w_2', w_3' with respect to the intermolecular distance of the transfer energies. The second interaction is determined by the variation, due to the same molecular vibrations, of polarization energy of molecules surrounding the conduction hole and is similar to that of polaron, but is determined by induced polarization. The coupling constant is proportional to the mean polarizability of the molecule α_0. It is very important to consider both these interactions together, because the interference between them leads to their compensation for some states in the conduction band. As a result, the conductivity σ increases considerably, especially in crystals with high degree of purity. The thermopower S grows too, however the electronic thermal conductivity κ^e grows in a smaller degree.

The electrical conductivity σ_p, Seebeck coefficient S_p and electronic thermal conductivity κ_e have been modelled in a more complete 3D model as functions of the dimensionless Fermi energy ε_F in unities of $2w_1$ for crystals with different degrees of perfection described by the parameter D_0. For D_0 the following values were chosen: 0.1 which corresponds to crystals grown by gas phase method with stoichiometric electrical conductivity $\sigma_p \sim 10^6\ \Omega^{-1}m^{-1}$; 0.02 which correspond to purer crystals grown also by gas phase method with somewhat higher $\sigma_p \sim 3\cdot10^6\ \Omega^{-1}m^{-1}$, not obtained yet, and 0.004 which corresponds to even more perfect crystals with $\sigma_p \sim 6.2\cdot10^6\ \Omega^{-1}m^{-1}$. For these three sets

of crystals, the impurity concentrations are expected to be $5\cdot10^{18}$ cm^{-3}, 10^{18} cm^{-3} and $2\cdot10^{17}$ cm^{-3}, respectively, or crystal purity: 99.6 %, 99.92 % and 99.98 %. These values of purity are achievable.

Some sets of values for σ_p, S_p and κ_p are presented below in the Table 1 with $\kappa^L = 0.6$ Wm^{-1}K^{-1}.

Organic material of n-type

Organic crystals of *n*-type $TTT(TCNQ)_2$ [9] have the aspect of dark-violet needles of the length of 3 – 6 mm. The internal crystal structure consists of molecular chains of *TTT* and *TCNQ* arranged along one highly conducting direction, *c*-axis. The lattice constants are $c = 3.75$ Å, $b = 12.97$ Å and $a = 19.15$ Å. The crystal has also a quasi-one-dimensional structure. The conductivity of *TCNQ* chains is much higher than that of *TTT* chains and the carriers are electrons.

The overlap of molecular orbitals of nearest molecules along the *TCNQ* chain generates a narrow conduction band of the width $4w_1 = 0.5$ eV ($\sim 19k_0T_0$, $T_0 = 300$ K), where w_1 is the transfer energy of an electron from a given molecule to the nearest one in the *c* direction. In transversal to chains directions the transfer energies are small and the transport mechanism is of hopping-type. The internal structure of $TTT(TCNQ)_2$ crystals is similar to that of TTT_2I_3. As in the case of TTT_2I_3, two electron-phonon interactions are considered: one of the type of deformation potential and other similar to that of polaron. The scattering on impurities and defects is described by the parameter D_0. The numerical calculations of thermoelectric coefficients were performed for crystals with different degrees of purity and respectively $D_0 = 0.1$, 0.04, 0.02 at room temperature. Some sets of values for σ_n, S_n and κ_n are presented below in the Table, where $\kappa^L = 0.4$ Wm^{-1}K^{-1}.

Let us consider a thermoelectric module constructed of a *n*-leg formed from a *n*-type $TTT(TCNQ)_2$ and a *p*-leg from TTT_2I_3, working in a regime of power generation.

In Table numerical data for σ_n, σ_p, S_n, S_p, κ_n, and κ_p are extracted from the previous calculations. The figure of merit ZT_{av} of the *p-n*-module and maximum efficiency η_{max} are calculated after (2) and (3).

Table

Calculations of ZT_{av} and of maximum efficiency η_{max} of the p-n-module

σ_n, Ω^{-1}m^{-1}	ε_F *n*-leg	S_n μVK^{-1}	$\kappa_n = \kappa^e + \kappa^L$ Wm^{-1}K^{-1}	σ_p Ω^{-1}m^{-1}	ε_F *p*-leg	S_p μVK^{-1}	$\kappa_p = \kappa^e + \kappa^L$ Wm^{-1}K^{-1}	ZT_{av}	η_{max} %
3.0×10^5	0.90	-170	4.4	7.5×10^5	0.09	300	3.1	2.53	13
7.0×10^5	1.00	-181	6.5	8.0×10^5	0.10	280	3.3	3.2	14
7.5×10^5	1.05	-183	7.8	12×10^5	0.15	226	4.3	2.5	13
11×10^5	1.10	-182	8.5	21×10^5	0.20	200	5.8	2.9	14
13×10^5	1.15	-177	9.2	26×10^5	0.25	145	7.3	2.1	12
19×10^5	1.20	-161	9.8	48×10^5	0.30	110	8.6	2.2	12
25×10^5	1.25	-146	10.2	54×10^5	0.35	60	9.6	1.5	9.8
11×10^5	1.10	-182	8.5	8.0×10^5	0.10	280	3.3	3.6	15
13×10^5	1.15	-177	9.2	8.0×10^5	0.10	280	3.3	3.7	15.7

The efficiency is not high, because these organic materials admit the highest temperature T_h = 480 K. We have put T_c = 300 K, so that the temperature difference is only ΔT = 180 K. For such small ΔT, the ideal Carnot efficiency is only 37.5%. Nevertheless, efficiencies ~ 12 – 15% for thermoelectric modules are predicted. Even if it will be possible to realize only one-half of predicted values, efficiencies ~ 6 – 8% for the conversion of low-temperature waste heat are very good results. These values are higher than those realized in a *p*-*n*-module on the basis of bismuth-telluride materials for ΔT = 300 K [11]. Moreover, considered here organic materials could be used in the low-temperature cascade of TE generators working at a larger ΔT in order to improve the overall efficiency.

From Table it is seen that the highest efficiency is achieved when both *n*- and *p*-legs have optimal parameters.

Conclusions

The maximum thermoelectric efficiency η_{max} has been calculated for a *p*-*n*-module formed from *p*-type tetrathiotetracene-iodide crystals, TTT_2I_3 and of *n*-type tetrathiotetracene-tetracyanoquinodimethane quasi-one-dimensional crystals, $TTT(TCNQ)_2$. Two electron-phonon interactions are considered: one is of the type of deformation potential and the other is similar to that of polaron. The scattering on impurities and defects is described by the parameter D_0. Crystals with improved degree of perfection are considered. Due to the violation of the Wiedemann-Franz law and the diminution of the Lorentz number, in these crystals the growth of electrical conductivity is accompanied with a reduced growth of the electronic thermal conductivity. In Table different values of the electrical conductivity σ_n, σ_p, Seebeck coefficient S_n, S_p, and electronic thermal conductivity κ_n, κ_p for *n*- and *p*-type materials are presented. The dimensionless figure of merit of the *p*-*n*-module ZT_{av} and the maximum thermoelectric efficiency η_{max} are presented, too. Efficiencies of the order of 12 – 15% are predicted, very promising for the conversion of low-temperature waste heat into electrical energy. Considered here organic materials could be also used in the low temperature cascade of TE generators working in larger temperature intervals ΔT in order to improve the overall efficiency.

The authors gratefully acknowledge the support form EU Commission FP7 program under the grant no. 308768 and the support of the scientific program of the Academy of Sciences of Moldova under the project no. 14.02.116F.

References

1. MARLOW INC., “Transmission Lasers (DWDM)”, доступно на сайте: http://www.marlow.com/industries/telecommunications/transmission-lasers-dwdm.html .
2. GENTHERM, “Climate Seats”, доступно на сайте: http://www.gentherm.com/page/climate-seats .
3. “KOOLATRON”, доступно на сайте: http://www.koolatron.com/.
4. Dresselhaus M.S., Heremans J.P. Recent Developments in Low-Dimensional Thermoelectric Materials in: *Thermoelectric Handbook, Macro to Nano, Ed. by D. M. Rowe*, CRC Press, 2006, Chap. 39 (and references therein).
5. Vining C.B. ZT~ 3.5: Fifteen years progress and things to come. *Proc. of 5th Europe Conf. on Thermoel., Odessa.* 2007. P. 5 – 10.

6. Kim G-H., Shao L., Zhang K. and Pipe K. P. Engineered Doping of Organic Semiconductors for Enhanced Thermoelectric Efficiency, *Nat. Mater*. 2013. 12. P. 719.
7. Troni P.J., HOCES I., et al., Thermoelectric Materials: A Brief Historical Survey from Metal Junctions and Inorganic Semiconductors to Organic Polymers. *Isr. J. Chem*. 2014. 54. P. 534.
8. Касіян А.І., Пфлаум Й., Сандуляк І.І. Перспективи низькорозмірних органічних матеріалів для термоелектричних застосувань. *Термоелектрика.* 2015. 1. С. 16 – 26.
9. Sanduleac I., Casian A. Nanostructured $TTT(TCNQ)_2$ Organic Crystals as Promising Thermoelectric *n*-Type Materials: 3D Modeling. *J. Electron. Mater*. 2015. 45. P. 1316 – 1320.
10. Анатычук Л.И., Термоэлектричество, Том. 2. Термоэлектрические преобразователи мощности (Киев, Черновцы: *Институт термоэлектричества.* 2003). 376 с.
10. Hi-Z14 Thermoelectric Module. Доступно на сайте http://www.hi-z.com/hz-14.html
11. Snyder G. J., Soto M., Alley R., Koester D., Conner B. Hot Spot Cooling Using Embedded Thermoelectric Coolers. *22nd IEEE SEMI-THERM symposium* (Dallas, TX. 2006. P.135 – 143).
12. Casian A., Sanduleac I.. Effect of Interchain Interaction on Electrical Conductivity in Quasi-One-
Dimensional Organic Crystals of Tetrathiotetracene-Iodide, *J. Nanoelectronics and Optoelectronics.* 2012. 7. P. 706 – 711.
13. Casian A., Sanduleac I. Organic Thermoelectric Materials: New Opportunities, *J. Thermoelectricity* 3. 2013. P. 11 – 20
14. Sanduleac I. I., Casian A. I., Pflaum J. Thermoelectric Properties of Nanostructured Tetrathiotetracene Iodide Crystals in a Two-Dimensional Model, *J.Nanoelectronics and Optoelectronics* 9. 2014. P. 247 – 252.
15. Casian A., Sanduleac I.. Thermoelectric properties of tetrathiotetracene iodide crystals: modeling and experiment, *J. Electron. Mat*. 2014. 43. P. 3740.
16. Casian A., Sanduleac I. Thermoelectric Properties of Nanostructured Tetrathiotetracene Iodide Crystals: 3D Modeling, *Mat. Today Proc*. 2. 2015. P. 504 – 509.

Submitted 9.03.2017

Касіян А. І. *докт. техн. наук,* **Сандуляк І. І.**

Технічний університет Молдови,
проспект Штефана чел Маре, 168,
Кишинів, MD-2004, Республіка Молдова,
e-mail: acasian@mail.utm.md

ТЕРМОЕЛЕКТРИЧНИЙ ККД *p-n*-МОДУЛЯ, ОТРИМАНОГО З ОРГАНІЧНИХ МАТЕРІАЛІВ

Нами проаналізовано термоелектричні властивості кристалів йодида тетратіотетрацену
p-типу, TTT_2I_3, і кристалів тетратіотетрацену-тетрацианохінодиметану n-типу, $TTT(TCNQ)_2$, у рамках більш повної 3D фізичної моделі. Показано, що для підвищення термоелектричного ККД концентрацію носіїв необхідно зменшити в кристалах p-типу й

збільшити в кристалах n-типу в порівнянні зі стехіометричними. Розглянуті кристали можуть мати нестехіометричний склад. Визначено оптимальні параметри для досягнення якомога більш високих значень термоелектричної добротності. Термоелектричний ККД p-n-модуля моделюється як функція параметрів кристалу. Бібл. 17, табл. 1.

Ключові слова: органічні кристали, термоелектричний ККД, термоелектрична добротність,
p-n-модуль, йодид тетратіотетрацену, тетратіотетрацен-тетрацианохінодиметан.

Касиян А. И. *докт. техн. наук,* **Сандуляк И. И.**

Технический университет Молдовы,
проспект Штефана чел Маре, 168,
Кишинев, MD-2004, Республика Молдова
e-mail: acasian@mail.utm.md

ТЕРМОЭЛЕКТРИЧЕСКИЙ КПД *p-n*-МОДУЛЯ, ПОЛУЧЕННОГО ИЗ ОРГАНИЧЕСКИХ МАТЕРИАЛОВ

Нами проанализированы термоэлектрические свойства кристаллов иодида тетратиотетрацена p-типа, TTT_2I_3, и кристаллов тетратиотетрацена-тетрацианохинодиметана n-типа, $TTT(TCNQ)_2$, в рамках более полной 3D физической модели. Показано, что для повышения термоэлектрического КПД концентрацию носителей необходимо уменьшить в кристаллах p-типа и увеличить в кристаллах n-типа по сравнению со стехиометрическими. Рассмотренные кристаллы могут иметь нестехиометрический состав. Определены оптимальные параметры для достижения как можно более высоких значений термоэлектрической добротности. Термоэлектрический КПД p-n-модуля моделируется как функция параметров кристалла. Библ. 17, табл. 1.

Ключевые слова: органические кристаллы, термоэлектрический КПД, термоэлектрическая добротность, *p-n*-модуль, иодид тетратиотетрацена, тетратиотетрацен-тетрацианохинодиметан.

References

1. MARLOW INC. “Transmission Lasers (DWDM)”. Retrieved from: http://www.marlow.com/industries/telecommunications/transmission-lasers-dwdm.html .
2. GENTHERM. “Climate Seats”. Retrieved from: http://www.gentherm.com/page/climate-seats .
3. “KOOLATRON”. Retrieved from: http://www.koolatron.com/.
4. Dresselhaus M.S., Heremans J.P. (2006). Recent developments in low-dimensional thermoelectric materials. Chapter 39. In: *Thermoelectric Handbook, Macro to Nano. D. M. Rowe (Ed.).* Boca-Raton: CRC Press.
5. Vining C.B. (2007) ZT~ 3.5: Fifteen years progress and things to come. *Proc. of 5th Europe Conf. on Thermoelectrics.* (Odessa, Ukraine, September 10-12, 2007) (pp. 5 – 10).
6. Kim G-H., Shao L., Zhang K., Pipe K. P. (2013). Engineered Doping of Organic Semiconductors for Enhanced Thermoelectric Efficiency. *Nat. Mater*., 12, 719.
7. Troni P.J., HOCES I., et al. (2014). Thermoelectric Materials: A brief historical survey from metal junctions and inorganic semiconductors to organic polymers. *Isr. J. Chem*., 54, 534.

8. Casian A.I., Pflaum J., Sanduleac I.I. (2015). Prospects of low-dimensional organic materials for thermoelectric applications. *J.Thermoelectricity,* 1, 16 – 26.
9. Sanduleac I., Casian A. (2015). Nanostructured $TTT(TCNQ)_2$ Organic Crystals as Promising Thermoelectric *n*-Type Materials: 3D Modeling. *J. Electron. Mater*., 5, 1316 – 1320.
10. Anatychuk L.I.. (2003). *Thermoelectricity. Vol.2. Thermoelectric power converters*. Kyiv, Chernivtsi: Institute of Thermoelectricity.
11. Hi-Z14 Thermoelectric Module. Retrieved from: http://www.hi-z.com/hz-14.html
12. Snyder G. J., Soto M., Alley R., Koester D., Conner B. (2006). Hot spot cooling using embedded thermoelectric coolers. *22nd IEEE SEMI-THERM symposium.* (Dallas, TX. 2006)(pp.135 – 143).
13. Casian A., Sanduleac I. (2012). Effect of interchain interaction on electrical conductivity in quasi-one-dimensional organic crystals of tetrathiotetracene-iodide. *J. Nanoelectronics and Optoelectronics,* 7, 706 – 711.
14. Casian A., Sanduleac I. (2013). Organic Thermoelectric Materials: New Opportunities. *J. Thermoelectricity,* 3. P. 11 – 20
15. Sanduleac I. I., Casian A. I., Pflaum J. (2014). Thermoelectric properties of nanostructured tetrathiotetracene iodide crystals in a two-dimensional model. *J.Nanoelectronics and Optoelectronics,* 9, 247 – 252.
16. Casian A., Sanduleac I.. (2014). Thermoelectric properties of tetrathiotetracene iodide crystals: modeling and experiment. *J. Electron. Mat*. , 43, 3740.
17. Casian A., Sanduleac I. (2015). Thermoelectric properties of nanostructured tetrathiotetracene iodide crystals: 3D modeling. *Mat. Today Proc*., 2, 504 – 509.

Submitted 9.03.2017

V. G. Deibuk

V. G. Deibuk[1,2]

[1]Institute of Thermoelectricity of the NAS and MES Ukraine,
Nauky str., Chernivtsi, 58029, Ukraine;
Yu.Fedkovich Chernivtsi National University,
[2]Kotsyubynsky str., Chernivtsi, 58012, Ukraine,
e-mail: v.deibuk@chnu.edu.ua

THERMODYNAMIC STABILITY OF THIN *CdZnSb* EPITAXIAL FILMS

The diagrams of spinodal decomposition and critical temperatures of decomposition of epitaxial thin films of Cd-Zn-Sb semiconductor substitution solid solutions are calculated in the delta lattice parameter model with account of both deformation energy and plastic relaxation effects due to misfit dislocations. Within the framework of the proposed model it was shown that compared to the bulk samples, in the films there is a reduction of spinodal decomposition range and, as a rule, a reduction of critical temperature of decomposition. The effect of substrate on the above processes was investigated by the example of CdSb, ZnSb and $Cd_{0.5}Zn_{0.5}Sb$ substrates. The emergence of various kinds of biaxial strains in pseudomorphic films leads to a different character of the composition dependence of critical thickness of thin films. From the perspective of the use of these thin films in thermoelectric devices, the most promising films, in the author's opinion, are $Cd_xZn_{1-x}Sb/Cd_{0.5}Zn_{0.5}Sb$, where spinodal decomposition range and critical decomposition temperature are below the temperature of technological growth. Creation and widespread use of such materials opens up new possibilities for thin-film thermoelectric energy converters. Bibl. 20, Fig. 3

Key words: thin films, *CdZnSb*, thermodynamic stability, spinodal decomposition, biaxial deformation, thermoelectric converters.

Introduction

Extensive study of the thermoelectric properties of the bulk materials based on V-VI compounds and IV-VI, IV-IV semiconductor alloys has led to a striking progress in the design of various thermoelectric devices [1, 2]. The efficiency of thermoelectric devices is expressed by the dimensionless figure of merit given by:

$$ZT = S^2 \sigma T / k\,, \tag{1}$$

where S is the Seebeck coefficient, σ is electric conductivity, k is thermal conductivity, T is absolute sample temperature. In turn, thermal conductivity k can be regarded as additive value caused by electron (k_e) and lattice (k_l) components:

$$k = k_e + k_l\,. \tag{2}$$

Improvement in the thermoelectric figure of merit of thermoelectric materials, as follows from (1), is due to increase in electric conductivity and decrease in thermal conductivity of materials. This task is mutually contradictory, since, according to the Wiedemann-Franz law the electron thermal conductivity k_e is directly proportional to electric conductivity value. Therefore, ZT can be improved by reducing the lattice component of thermal conductivity k_l. At the same time, increasingly strict requirements to miniaturization and cheapening of such devices dictate the need for a search for new approaches to solving said problem.

Increasing attention has been paid recently to such promising objects as topological dielectrics, thin films, superlattices, etc. [3 – 5]. Such materials can be particularly relevant in connection with solving very important problem of cooling components of microprocessor devices of modern computer equipment. The idea of using thin films for thermoelectric devices is not new [3]. To improve the thermoelectric figure of merit *ZT*, several groups of scientists have studied thin films and superlattices Bi_2Te_3/Sb_2Te_3, *PbTe*/*PbSe*, *Si*/*Ge*, *Bi*/*Sb* and others [3 – 5]. It was shown that reduction of phonon thermal conductivity in such materials due to reflection at film boundaries and electric conductivity increase due to peculiarities of electron density, internal thermionic emission, etc, can result in significant *ZT* increase as compared to the bulk materials. Vast technological opportunities of obtaining a variety of composition, thickness and orientation of thin films on various substrates open up truly unlimited opportunities for improving their thermoelectric properties.

At the same time, such important class of strongly anisotropic thin films of solid solutions based on II-V [6 – 11] stays out of the attention of researchers. Among thermoelectric materials, *CdSb* and *ZnSb* are ecologically clean and economically efficient in the temperature range of 473 K – 673 K and can substitute toxic and rare *Pb*-*Te* metal alloys. While thermoelectric properties of bulk materials have been studied in considerable detail [12, 13], thin films and superlattices on their basis are still waiting for their research and use in thermoelectricity. There are several reasons for this, and perhaps one of the basic is the problem of thermodynamic stability of *CdZnSb* thin films. It is known that bulk crystals *CdZnSb* form a continuous series of substitution solid solutions [14]. Despite this fact, the phenomenon of thermal instability of melt structure was experimentally revealed which is manifested in the possibility of crystallization of different stability phases (*CdSb*, Cd_3Sb_2, Cd_4Sb_3, *ZnSb*, Zn_4Sb_3) [14 – 16]. At the same time, growing of epitaxial films is accompanied with formation of various structural defects, mechanical strains caused by mismatch between crystal lattices of substrate and film (misfit dislocations, islets of other phases, etc). The latter factors change free energy of solid solution, which in turn leads to a change in solubility limits of components and has a definite impact on the thermodynamic stability of the resulting thin films [17 – 19]. Thermoelectric properties of thin films are directly related to phase transformations in such thin films. In particular, it is shown in [6] that thin films with different phases *ZnSb* and Zn_4Sb_3 have larger values of the Seebeck coefficient than single-phase films. Discussion of these issues will be the subject of the present paper.

Account of elastic energy in the calculation of spinodal decomposition

Semiconductor compounds II-V, in particular, *CdSb*, *ZnSb* and their solid solutions $Cd_xZn_{1-x}Sb$, are crystallized as orthorhombic structure $D_{2h}^{15} - Pbca$ with 16 atoms in the unit cell, forming two identical, though translation-shifted relative to each other, sublattices [20]. For the thermodynamic description of pseudobinary ternary solid solutions we will consider the Gibbs free energy of mixing (ΔG) based on mole:

$$\Delta G = \Delta H - T\Delta S\,, \tag{3}$$

where ΔH is enthalpy of mixing, T is absolute temperature, ΔS is entropy of mixing which in the approximation of a regular solid solution can be written [18]:

$$\Delta S = -R\left\{x\ln x + (1-x)\ln(1-x)\right\}. \tag{4}$$

To describe the enthalpy of mixing, two models are most commonly used – regular solution model and "delta lattice parameter" (DLP) model [17]. It is known that regular solution model describes well the thermodynamic properties of liquid phase and has restrictions for the case of solid phase, since interaction parameters in regular solution model depend on the alloy composition (x). In the DLP model the enthalpy

of mixing ΔH depends only on lattice parameter (a), so it is assumed that the difference between the dimensions of atoms having common sublattice is a decisive factor which controls free energy of mixing. For $A_{1-x}B_xC$ solid solutions ΔH can be written as [18, 19]:

$$\Delta H = E(alloy) - xE(BC) - (1-x)E(AC) = \Omega x(1-x), \tag{5}$$

$$\Omega = K\Delta a^2 / a_{avg}^{4.5}, \tag{5′}$$

where K is model parameter, a_{avg} is averaged lattice parameter, Δa is the difference between lattice parameters of components of solid solution compounds. As long as lattice components of *CdSb-ZnSb* solid solution under study are rather close [20], the solid solution can be considered to be almost perfect, and the interaction parameter Ω and enthalpy of mixing ΔH are always positive values. The solid solution will be subject to spinodal decomposition on condition that the curve of the composition dependence of free energy has a bend point [18]. The products of spinodal decomposition are two solid solutions with different composition. Stability criterion of pseudobinary alloys can be written as $\partial^2 G/\partial x^2 > 0$. The instability area is determined as a geometrical place of points for which the condition $\partial^2 G/\partial x^2 = 0$ is met.

The Gibbs free energy of forming *CdSb-ZnSb* solid solutions, as was experimentally shown [16], varies significantly from the ideal form, changing the sign with composition x. The existence of positive region of $\Delta G(x)$ dependence can cause solid solution decomposition in certain range at temperatures lower than critical T_c. For the bulk solid solution, apart from the chemical part of free energy, one must also take into account the elastic component which follows from the requirement of coherent phase conjugation [18] with account of crystal anisotropy. In [17, 18], on the basis of a model of regular solid solution it is shown that in semiconductor solid solutions with the positive enthalpy of their formation, at certain temperatures there occurs a coherent phase separation with formation of elastic concentration domains with a variable composition of solid solution.

In the case when a solid solution is a thin epitaxial film and the thermodynamic process occurs by formation of misfit dislocations due to the mismatch between film lattice constants with substrate material, biaxial tensile or compression strains will occur in the film. In the general case the energy of elastic strain of the unit volume of deformed film can be written as [20]:

$$E_S = \frac{1}{2}\left(\sigma_x\varepsilon_x + \sigma_y\varepsilon_y + \sigma_z\varepsilon_z + \tau_{xy}\gamma_{xy} + \tau_{yz}\gamma_{yz} + \tau_{xz}\gamma_{xz}\right), \tag{6}$$

where σ_x, σ_y, σ_z are normal stresses; τ_{xy}, τ_{yz}, τ_{xz} are shear stresses; ε_x, ε_y, ε_z are normal strains; γ_{xy}, γ_{yz}, γ_{xz} are shear strains. It is commonly assumed that with the epitaxial growth due to mismatch between lattice constants of substrate-film only normal strains and stresses occur along two perpendicular axes in the film plane (001). Taking into account the relation between normal strains and stresses based on Hooke's law, we obtain:

$$\begin{aligned} \sigma_x &= c_{11}\varepsilon_x + c_{12}\varepsilon_y + c_{13}\varepsilon_z \\ \sigma_y &= c_{12}\varepsilon_x + c_{22}\varepsilon_y + c_{23}\varepsilon_z \end{aligned}, \tag{7}$$

where in the case of equal symmetry of film and substrate material, the relative strain components

$$\varepsilon_x = \frac{a_{alloy} - a_{sub}}{a_{sub}}, \qquad \varepsilon_y = \frac{b_{alloy} - b_{sub}}{b_{sub}}. \tag{8}$$

For orthorhombic crystals the array of elastic moduli comprises 9 independent components:

$$\begin{pmatrix} c_{11} & c_{12} & c_{13} & 0 & 0 & 0 \\ c_{12} & c_{22} & c_{23} & 0 & 0 & 0 \\ c_{13} & c_{23} & c_{33} & 0 & 0 & 0 \\ 0 & 0 & 0 & c_{44} & 0 & 0 \\ 0 & 0 & 0 & 0 & c_{55} & 0 \\ 0 & 0 & 0 & 0 & 0 & c_{66} \end{pmatrix} \quad (9)$$

Stress tensor component in perpendicular (z) direction can be written:

$$\sigma_z = c_{13}\varepsilon_x + c_{23}\varepsilon_y + c_{33}\varepsilon_z . \quad (10)$$

Taking into account for free (growth) direction of the film that $\sigma_z = 0$, from (10) we obtain:

$$\varepsilon_z = -\frac{C_{13}}{C_{33}}\varepsilon_x - \frac{C_{23}}{C_{33}}\varepsilon_y . \quad (11)$$

Hence, the elastic strain energy of the unit volume of epitaxial film (6), with regard to (10) – (11) can be written as:

$$E_s = \frac{1}{2}\left(\sigma_x\varepsilon_x + \sigma_y\varepsilon_y\right) = \frac{1}{2}\left(\left(c_{11} - \frac{c_{13}^2}{c_{33}}\right)\varepsilon_x^2 + \left(c_{22} - \frac{c_{23}^2}{c_{33}}\right)\varepsilon_y^2 + 2\left(c_{12} - \frac{c_{13}c_{23}}{c_{33}}\right)\varepsilon_x\varepsilon_y\right). \quad (12)$$

Thus, full Gibbs free energy of the system based on the unit volume is a sum of chemical energy (ΔG) and elastic strain energy (E_s):

$$G = N_v\Delta G + E_s , \quad (13)$$

where N_v is the number of moles of the unit volume of homogeneous solid solution to decomposition. Analysis of the Gibbs free energy as a function of solid solution composition and epilayer thickness together with stability criterion allows calculating solubility limits. Parameters used for calculations were taken from [20]. The dependence of lattice constants on the composition x was taken into account by the Vegard rule which is met for $Cd_xZn_{1-x}Sb$ semiconductor solid solutions with high precision [20].

The above situation is observed only in the case when film thickness (h) is smaller than critical thickness (h_c). On condition of $h > h_c$, plastic relaxation processes take place in the film with formation of misfit dislocations, and the thicker the film, the smaller is its strain. To determine the influence of said effects on the thermodynamic stability of chosen solid solutions, note that according to the model of balance of forces [19] acting on the dislocations, it can be written:

$$\varepsilon_z = A/h , \quad (14)$$

that is, as the thickness of epitaxial film increases, the value of relative decreases and the film gradually relaxes. Parameter A in (14) will be found from continuity condition of function $\varepsilon(h)$ at point $h = h_c$, then from relations (8), (11) i (14) we obtain $A = \varepsilon_{zmax}h_c$. The majority of semiconductor heteroepitaxies are grown on (001) substrate surface, so exactly this orientation will be considered. Theoretical expression for critical thickness h_c can be obtained on the basis of two different approximations, known as equilibrium theories of critical thickness. The former approximation is based on the minimum energy principle and was pioneered by Frank and Van der Merwe; the latter, known as theory of the balance of forces, belongs to

Matthews and Blakeslee (see review [19]). The said two approaches are equivalent and give equal values of critical film thickness. In our calculations we have used the model of balance of forces in which critical epilayer thickness can be estimated according to [19]:

$$h_c = \left(\frac{b}{\varepsilon_m}\right)\frac{1}{8\pi(1+\nu)}\left[\ln\left(\alpha\frac{h_c}{b}\right)+\beta\right], \tag{15}$$

where, ν is the Poisson coefficient, α = 4, β = 1, b – is the Burgers vector modulus. As long as in semiconductor epilayers 60° misfit dislocations are most common in (001) plane, the Burgers vector can be written as $(a_{avg}/2)<110>$, then $b = a_{avg}/\sqrt{2}$. The stresses in the region of dislocation centre are too high to be correctly described within the linear elasticity theory, so we have introduced a phenomenological parameter β as a measure of this deviation.

$Cd_xZn_{1-x}Sb/CdSb$ system

Let us consider $Cd_xZn_{1-x}Sb$ epitaxial layer on $CdSb$ substrate in the framework of the above described model. At low temperatures an unstressed alloy has additional free energy, which with a rise in temperature is reduced with formation of two minima indicating the possibility of spinodal decomposition. Phase diagram of spinodal decay of non-elastic film in this case is represented in Fig. 1*a* showing the existence of critical temperature (T_c = 1015 K at x_c = 0.5) above which the spinodal decomposition will not take place.

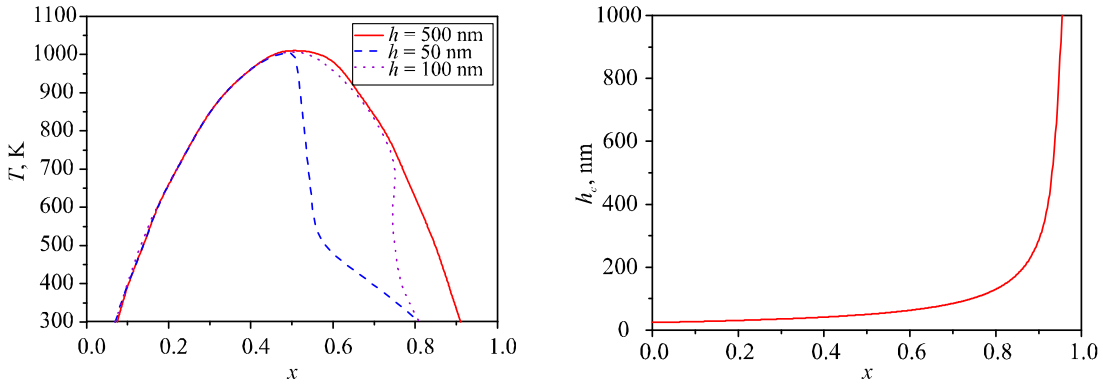

a) *b)*

Fig. 1. Phase diagrams of spinodal decomposition (a) and composition dependence of critical thickness (b) of $Cd_xZn_{1-x}Sb/CdSb$ epitaxial films.

If epitaxial film is fully strained, quick growth of elastic energy E_s (as compared to a change in chemical energy – the first term in formula (8)) with increasing *Cd* content in the film leads to the fact that two minima on the composition dependence of free energy merge into one. This testifies to elastic stabilization of film in terms of spinodal decomposition [17] and takes place for thin pseudomorphous films with less than critical thickness ($h < h_c$). However, when epilayer thickness exceeds critical ($h > h_c$), the film starts to relax, that is, the elastic energy of the film (4) – (6) decreases with increasing film thickness. In so doing, the area of existence of spinodal decomposition ($\partial^2 G/\partial x^2 < 0$) remains, though becomes narrower (Fig. 1*a*). The asymmetric narrowing of spinodal decomposition range can be explained taking into account the composition dependence of critical thickness of $Cd_xZn_{1-x}Sb$ film grown in *CdSb* substrate (Fig. 1*b*). The boundary of immiscibility area from higher *Cd* concentrations is rather responsive to a change in film thickness. The opposite boundary, where *Cd* concentration is lower, slightly changes with the film thickness, which is attributable to a greater mismatch between film –substrate (*CdSb*) lattice constants, hence, to a less critical thickness (close to several angstroms). Therefore, films with almost

arbitrary thickness in this composition range fully relax, and residual stresses in them are very low. However, from higher *Cd* concentrations due to strong dependence $h_c(x)$ the stresses are rather sensitive to epilayer thickness. $Cd_xZn_{1-x}Sb/CdSb$ films with thickness greater than 200 Å almost completely relax and in their thermodynamic properties approach the bulk samples. The spinodal decomposition range of unstressed $Cd_xZn_{1-x}Sb$ solid solution, calculated by us at $T = 640$ K is $0.2 < x < 0.7$ and agrees well with the experimental region of positive values of the Gibbs free energy [16].

$Cd_xZn_{1-x}Sb/ZnSb$ system

A similar dependence can be observed in $Cd_xZn_{1-x}Sb$ layers grown on *ZnSb* substrates. In particular, for the unstressed $Cd_xZn_{1-x}Sb$ we calculated critical temperature $T_c = 1015$ K at $x_c = 0.5$. From lower *Cd* concentrations the film is rather sensitive to internal stresses, which, in contrast to the above epitaxial films in this case are due to biaxial compression strain, since substrate lattice constants (*ZnSb*) are higher than lattice constants of pseudomorphous film ($Cd_xZn_{1-x}Sb$). The latter is manifested in considerable change of respective solubility limit (Fig. 2*a*) of films of different thicknesses.

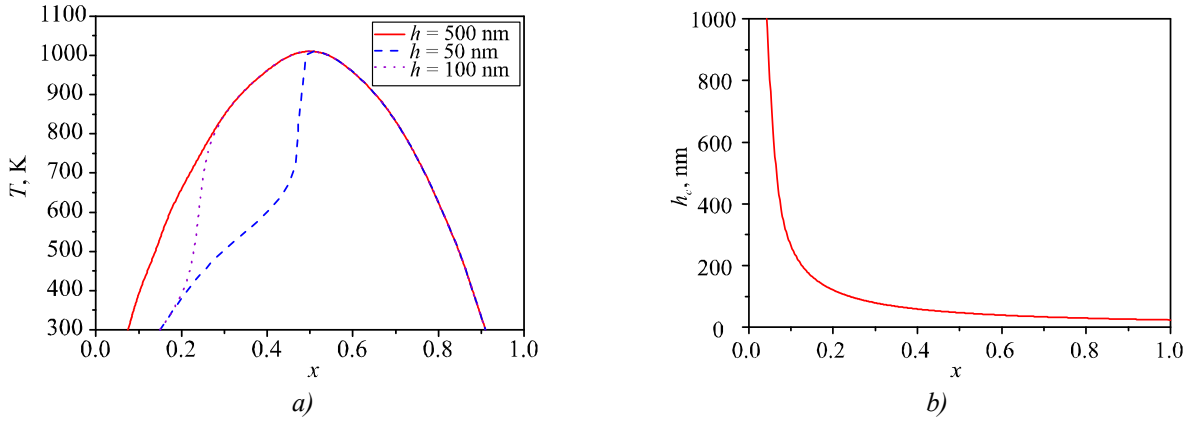

Fig. 2. Phase diagrams of spinodal decomposition a) and composition dependence of critical thickness (b) of $Cd_xZn_{1-x}Sb/ZnSb$ epitaxial films.

For instance, if for a film 100 nm thick the immiscibility interval at 600 K according to our calculations is $0.24 < x < 0.81$, then for a film 50 nm thick this interval is $0.41 < x < 0.81$. Considerable narrowing of spinodal decomposition range falls on technological temperature range 600 – 900 K. The nonmonotonous change in decomposition limit with a change of temperature is due to competition between chemical and elastic components of film free energy. For $h > 500$ nm the composition diagram practically coincides with the diagram of the bulk unstressed solid solution, that is, residual stresses in the film are close to zero. The composition dependence of critical film thickness is represented in Fig. 2*b*.

$Cd_xZn_{1-x}Sb/Cd_{0.5}Zn_{0.5}Sb$ system

High-performance $Cd_xZn_{1-x}Sb$ films, necessary for creation of new thermoelectric devices, are imposed with the requirements of almost complete matching between film-substrate lattice constants in order to assure their enhanced properties. From this standpoint, in our opinion, $Cd_xZn_{1-x}Sb/Cd_{0.5}Zn_{0.5}Sb$ system is interesting. In this case such requirements are met by $Cd_{0.5}Zn_{0.5}Sb$ substrate which is fully matched with the film at $x = 0.5$, whereas in the region $0 < x < 0.5$ in pseudomorphous film there is biaxial tensile strain, and at $0.5 < x < 1$ – biaxial compression strain. The composition dependence of critical thickness of such films that we calculated is represented in Fig. 3*b*.

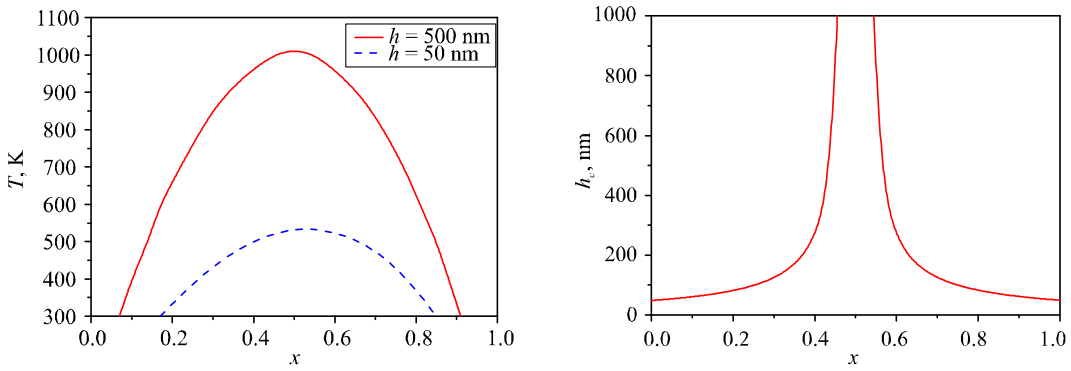

a) *b)*

Fig. 3. Phase diagrams of spinodal decomposition (a) and composition dependence of critical thickness (b) of $Cd_xZn_{1-x}Sb/Cd_{0.5}Zn_{0.5}Sb$ epitaxial films.

As can be seen from our diagrams of spinodal decomposition (Fig. 3*a*), as compared to a completely relaxed film (the bulk case) for the film 50 nm thick critical temperature decreases considerably (T_c = 550 K, x_c = 0.53), which holds out a hope of possible obtaining high-performance films in the technological temperature range. Films of thickness 500 nm and higher are almost completely relaxed, where the residual stresses are close to zero, but decomposition range becomes sufficiently large. Reduction of epitaxial films thickness leads to narrowing of immiscibility region. In particular, for films 50 nm thick the latter is $0.17 < x < 0.85$ at $T = 300$ K.

Conclusions

This paper presents a theoretical analysis of the effect of biaxial strains from the substrate on spinodal decomposition range of $Cd_xZn_{1-x}Sb$ pseudomorphous films on *CdSb*, *ZnSb*, $Cd_{0.5}Zn_{0.5}Sb$ substrates. The composition dependences of critical thickness of thin films were estimated on the basis of the Matthews-Blakeslee model. Intervals of immiscibility and critical temperature of spinodal decomposition of ternary semiconductor system *Cd-Zn-Sb* were calculated with regard to strain energy and plastic relaxation effect due to misfit dislocations. It is shown that account of elastic energy leads to narrowing of spinodal decomposition region and critical temperature reduction. In particular, for $Cd_xZn_{1-x}Sb/Cd_{0.5}Zn_{0.5}Sb$ pseudomorphous films 50 nm thick the delamination area totally disappears in the technological temperature range (600 – 900 K). The results of the work are prognostic for the experimental investigations of thin films for their application in thermoelectric devices.

The author is grateful to academician L. Anatychuk for the approval of research subject and interest in the work.

References

1. Анатычук Л.И. Термоэлементы и термоэлектрические устройства / Анатычук Л.И.. – Киев, 1979. – 768 с.
2. X.Zang. Thermoelectric Materials Energy Conversion Between Heat and Electricity / X.Zang, L.-D.Zhao. // J. of Materiomics. – 2015. – P. 92–105.
3. H.Böttner. Aspects of Thin-Film Superlattice Thermoelectric Materials, Devices, and Applications / H.Böttner, G.Chen, R.Venkatasubramanian. // MRS Bulletin. – 2006. – C. 211 – 217.
4. L.Müchler, F.Casper, B.Yan, S.Chadov, and C.Felser, Topological Insulators and Thermoelectric Materials, *Phys. Status Solidi RRL* 2013. **7**(1 – 2) P. 91 – 100.
5. Recent Progress in Electrodeposition of Thermoelectric Thin Films and Nanostructures / F.Xiao,

C.Hangarter, B.Yoo [etc.]. // Elecrochimica Acta. – 2008. – №53. – P. 8103 – 8117.
6. Enhanced Thermoelectric Properties of Mixed Zinc Antimonide Thin Films Via Phase Optimization. / Z.Zheng et al. // Appl. Surf. Sci. – 2014. – **292**. – P. 823 – 827.
7. On the Formation of Phases and Their Influence on the Thermal Stability and Thermoelectric Properties of Nanostructured Zinc Antimonide / P.Balasubramanian, M.Battabyal, D.Sivaprahasam, R. Gopalan. // J. Phys. D: Appl. Phys. – 2017. – №50. – P. 015 – 602.
8. M.Komatsu. Preparation and Properties of *Cd-Sb* Thin Films / M.Komatsu. // Mat. Res. Bull.. – 1978. – №13. – P. 835 – 840.
9. High-Performance Zinc Antimonide Thin Films for Thermoelectric Applications / Y.Sun, M.Christensen, S.Johnsen [etc.]. // Adv. Mater. – 2012. – №24. – P. 1693 – 1696.
10. Thermoelectric Properties of Zn_4Sb_3 Thin Films Prepared by Magnetron Sputtering, / L.T.Zhang, M.Tsutsui, K.Ito, M.Yamaguchi. // Thin Solid Films. – 2003. – 443(1-2). – P. 84 – 90.
11. Properties of *CdSb* Thin Films Obtained by RF Sputtering / A.I.Savchuk, V.V.Strebezhev, G.I.Kleto [etc.]. // Surf. Coat. Technol. – 2016. – №295. – C. 8–12.
12. L.Štourač. The Thermoelectric Efficiency of *CdSb* and Solid Solutions of $Zn_xCd_{1-x}Sb$ with Hole Conductivity / L.Štourač. // Czech. J. Phys. B. – 1967. – №17. – P. 543 – 550.
13. Thermal and Vibrational Properties of Thermoelectric *ZnSb* – Exploring the Origin of Low Thermal Conductivity / A.Fisher, E.-W.Scheidt, W.Scherer [etc.]. // Phys. Rev. B. – 2015. – №91. – P. 224 – 309.
14. Дремлюженко С.Г. Системы на основе *CdSb*: диаграммы состояния, получение и свойства сплавов. Справочник. / Дремлюженко С.Г. – Черновцы, 2002. – 127 с.
15. M.C.Record. Phase Transformations in *Zn-Cd-Sb* System. / M.C.Record, V.Izrad, M.Bulanova, and J.-C.Tedenac // Intermetallics. 2003. – **11**(11-12). – P. 1189 – 1194.
16. V.L.Goncharuk Thermodynamic Properties of Some Solid Solutions Formed by *A*II*B*VI and *A*II*B*V Semiconductor Compounds. / V.L.Goncharuk, V.R.Sidorko // Powder Metallurgy and Metal Ceramics – 1996. – **35**(7 – 8). – P. 392 – 396.
17. G.Stringfellow Thermodynamic Considerations for Epitaxial Growth of III-V Alloys. / G.Stringfellow // J. Cryst. Growth. – 2017. – **468**. – P.11–16.
18. Фистуль В.И. Распад пересыщенных твердых растворов. / Фистуль В.И. – Москва, 1977. 240с.
19. R.Beanland. Plastic Relaxation and Relaxed Buffer Layers for Semiconductor Epitaxy / R.Beanland, D.J.Dunstan, P.J.Goodhew // Adv. Phys. – 1996. – **45**(2). – P. 87 – 146.
20. Паранський М.Д. Пружні властивості та динаміка кристалічної ґратки деяких напівпровідникових монокристалів. / Паранський М.Д., Балазюк В.Н., Ковалюк З.Д. – Чернівці – 2012. – 200 с.

Submitted 15.03.2017

Дейбук В. Г.[1,2] *докт. фіз.-мат. наук*

[1]Інститут термоелектрики НАН і МОН України,
вул. Науки, 1, Чернівці, 58029, Україна;
[2]Чернівецький національний університет ім. Ю.Федьковича,
вул. Коцюбинського, 2, Чернівці, 58012, Україна
e-mail: v.deibuk@chnu.edu.ua

ТЕРМОДИНАМІЧНА СТАБІЛЬНІСТЬ ТОНКИХ ЕПІТАКСІАЛЬНИХ ПЛІВОК *CdZnSb*

У статті наведено результати розрахунку діаграм спінодального розпаду та критичні температури розпаду епітаксіальних тонких плівок напівпровідникових твердих розчинів заміщення $Cd_xZn_{1-x}Sb$ в моделі дельта-параметр ґратки з урахуванням як деформаційної енергії, так і ефектів пластичної релаксації, зумовлених дислокаціями невідповідності. В рамках запропонованої моделі показано, що порівняно з об'ємними зразками у плівках має місце звуження інтервалу спінодального розпаду та, як правило, пониження критичної температури розпаду. Досліджено вплив підкладки на вищезазначені процеси на прикладі підкладок CdSb, ZnSb, $Cd_{0.5}Zn_{0.5}Sb$. Виникнення різного роду біаксіальних деформацій у псевдоморфних плівках веде до різного характеру композиційної залежності критичної товщини тонких плівок. З точки зору перспектив використання вказаних тонких плівок у термоелектричних пристроях, на думку автора, найбільш перспективними є плівки $Cd_xZn_{1-x}Sb/Cd_{0.5}Zn_{0.5}Sb$, в яких область спінодального розпаду та критична температура розпаду лежать нижче технологічних температур вирощування. Створення й широке застосування таких матеріалів відкриває нові можливості тонкоплівкових термоелектричних перетворювачів енергії. Бібл. 20, рис. 3
Ключові слова: тонкі плівки, *CdZnSb*, термодинамічна стабільність, спінодальний розпад, біаксіальні деформації, термоелектричні перетворювачі.

Дейбук В. Г[1,2] *докт. физ.-мат. наук*

[1]Институт термоэлектричества, ул. Науки, 1, Черновцы, 58029, Украина
[2]Черновицкий национальный университет им. Ю.Федьковича,
ул. Коцюбинского, 2, Черновцы, 58000, Украина
e-mail: v.deibuk@chnu.edu.ua

ТЕРМОДИНАМИЧЕСКАЯ СТАБИЛЬНОСТЬ ТОНКИХ ЭПИТАКСИАЛЬНЫХ ПЛЕНОК *CdZnSb*

В работе рассчитаны диаграммы спинодального распада и критические температуры распада эпитаксиальных тонких пленок полупроводниковых твердых растворов замещения CdxZn1-xSb в модели дельта-параметра решетки с учетом как деформационной энергии, так и эффектов пластической релаксации, обусловленных дислокациями несоответствия. В рамках предложенной модели показано, что по сравнению с объемными образцами в пленках имеет место сужение интервала спинодального распада и, как правило, понижение критической температуры распада. Исследована роль подложки на вышеупомянутые процессы на примере подложек CdSb, ZnSb, $CdxZn_{1-x}Sb/Cd_{0.5}Zn_{0.5}Sb$. Возникновение разного рода биаксиальных деформаций в псевдоморфных пленках ведет к разному характеру композиционной зависимости критической толщины тонких пленок. С точки зрения перспектив использования указанных тонких пленок в термоэлектрических устройствах, по мнению автора, наиболее перспективными есть пленки$CdxZn_{1-x}Sb/Cd_{0.5}Zn_{0.5}Sb$, в которых область спинодального распада и критическая температура распада лежат ниже технологических температур выращивания. Создание и широкое применение таких материалов открывает новые возможности тонкопленочных термоэлектрических преобразователей энергии. Библ. 20, рис. 3
Ключевые слова: *тонкие пленки, CdZnSb, термодинамическая стабильность, спинодальный распад, биаксиальные деформации, термоэлектрические преобразователи.*

References

1. Anatychuk L.I. (1979). *Termoelementy i termoelektricheskiye ustroistva [Thermoelements and thermoelectric devices]*. Kyiv: Naukova Dumka [in Russian].

2. Zang X., Zhao L.-D. (2015). Thermoelectric materials energy conversion between heat and electricity. *J. of Materiomics,* 1(1), 92 – 105.
3. Böttner H., Chen G., Venkatasubramanian R.(2006). Aspects of thin-film superlattice thermoelectric materials, devices and applications. *MRS Bulletin,* 31(3), 211 – 217.
4. Müchler L., Casper F., Yan B., Chadov S., Felser C. (2013).Topological insulators and thermoelectric materials. *Phys. Status Solidi RRL,* **7**(1–2), 91 – 100.
5. Xiao F., Hangarter C., Yoo B., Rheem Y., Lee K.-H, Myung N.V. (2008). Recent progress in electrodeposition of thermoelectric thin films and nanostructures. *Elecrochimica Acta,* 53(28), 8103 – 8117.
6. .Zheng Z. et al. (2014). Enhanced thermoelectric properties of mixed zinc antimonide thin films via phase optimization. *Appl. Surf. Sci*.**,** 292**,** 823 – 827.
7. Balasubramanian P., Battabyal M., Sivaprahasam D., Gopalan R. (2017). On the formation of phases and their influence on the thermal stability and thermoelectric properties of nanostructured zinc antimonide. *J. Phys. D: Appl. Phys*., 50(1), 015602.
8. Komatsu M. (1978). Preparation and properties of *Cd-Sb* thin films. *Mat. Res. Bull*., 13(8), 835 – 840.
9. Sun Y., Christensen M., Johnsen S., Nong N.V., Sillassen Y.Ma., Zhang E., et al. (2012). Low-cost high-performance zinc antimonide thin films for thermoelectric applications. *Adv. Mater*., 24(13), 693 – 1696.
10. Zhang, L.T., Tsutsui M., Ito K, Yamaguchi M. (2003). Thermoelectric properties of Zn_4Sb_3 thin films prepared by magnetron sputtering. *Thin Solid Films,* 443(1-2), 84 – 90.
11. Savchuk A.I., Strebezhev V.V., Kleto G.I., Khalavka Y.B., Yuriychuk I.M., Fochuk P.M. , et al. (2016). Properties of *CdSb* thin films obtained by RF sputtering, *Surf. Coat. Technol*., 295**,** 8 – 12.
12. Štourač L. (1967). The thermoelectric efficiency of *CdSb* and solid solutions of $Zn_xCd_{1-x}Sb$ with hole conductivity. *Czech. J. Phys*. *B*, 17(6), 543 – 550.
13. Fisher A., Scheidt E.-W., Scherer W., Benson D., Wu Y, Ekloöf D., et al. (2015). Thermal and vibrational properties of thermoelectric *ZnSb* – exploring the origin of low thermal conductivity. *Phys. Rev. B,* 91(22), 224309.
14. Dremliuzhenko S.G. (2002). *Sistemy na osnove CdSb: diagrammy sostoiania, poluchenie I svoistva splavov. Spravochnik [CdSb based systems: diagrams of state, preparation and properties of alloys. Reference book]*. Chernivtsi: Ruta [in Russian].
15. Record M.C., Izrad V., Bulanova M., Tedenac J.-C. (2003). Phase transformations in *Zn-Cd-Sb* system. *Intermetallics,* 11(11-12), 1189 – 1194.
16. Goncharuk V.L., Sidorko V.R. (1996). Thermodynamic properties of some solid solutions formed by *A*II*B*VI and *A*II*B*V semiconductor compounds. *Powder Metallurgy and Metal Ceramics,* 35(7 – 8), 392 – 396.
17. G.Stringfellow, Thermodynamic Considerations for Epitaxial Growth of III-V Alloys, *J. Cryst. Growth*. 2017. **468**. P.11–16.
18. Fistul V.I. (1977). *Raspad peresyshchennykh tverdyh rastvorov [Breakdown of oversaturated solid solutions*]. Moscow: Metallurgia [in Russian].
19. Beanland R., Dunstan D.J., Goodhew P.J. (1996). Plastic relaxation and relaxed buffer layers for semiconductor epitaxy. *Adv. Phys*., 45(2), 87 – 146.
20. Raranskyi M.D., Balaziuk V.N., Kovaliuk Z.D. (2012). Pruzhni vlastyvosti ta dynamika krystalichnoi
21. gratky deiakykh napivprovidnykovykh monokrystaliv [Elastic properties and dynamics of crystal lattice of some semiconductor single crystals]. Chernivtsi: Zoloti Lytavry [in Ukrainian].

Submitted 15.02.2017

M. V. Maksymuk

M. V. Maksymuk

Institute of Thermoelectricity of the NAS and MES of Ukraine,
1, Nauky Str., Chernivtsi, 58029, Ukraine,
e-mail: anatych@gmail.com

ON THE OPTIMIZATION OF THERMOELECTRIC GENERATOR MODULES OF AUTOMOBILE STARTING PRE-HEATER

The results of computer design and experimental research on creation of a new design of thermoelectric thermocouple generator module Altec-1061 for increasing heat production of thermoelectric automobile starting pre-heater are presented. The design is carried out with regard to temperature dependences of material parameters, thermal and electric losses on the contacts and module interconnects. Bible. 13, Fig. 10, Table 1.

Key words: starting pre-heater, thermoelectric generator, computer design, physical model, thermoelement.

Introduction

To overcome the problem of discharging automobile battery during the operation of starting pre-heaters, at the Institute of Thermoelectricity an experimental sample of thermoelectric generator of electric power 70-90 W was created which operates from the heat of starting pre-heater and provides for autonomous power supply to its components [1-5]. Moreover, the excess energy of thermal generator can be used for recharging the battery and power supply to other automobile equipment (regular heating fan, warning systems, navigators, etc).

Experimental tests of the heater under test-bed conditions proved the efficiency of the design and confirmed the rationality of theoretical calculations performed in [3]. However, research on the sample under low temperatures has shown that thermal power which is "pumped" by thermoelectric modules is insufficient for engine heating to the temperature optimal for its start [4]. The point is that at negative air temperatures the viscosity of the engine oil increases, so before automobile start the engine must be heated to temperature not less than 70°C, prior to complete lubrication of the parts of cylinder-piston group occurs [6]. During full-scale tests of thermoelectric heater it was established that maximum temperature of engine in "preheating" mode is 50°C, in "preheating + passenger compartment heating" mode – 30°C. Hence, the relevance of the research aimed at further optimization of the design of the developed thermoelectric heater.

The temperature of warming up the engine cooling liquid (heat carrier) can be raised in two ways. The first one is to use the total thermal power of the heat source. As is shown in [4], only such operating modes are realized in the heater whereby the thermal power of the burner does not exceed 2.3 kW. Otherwise, the hot side of the thermopile is overheated and, as a result, the main functional units of the device fail. Therefore, to increase the thermal power of the heat source to maximum 4 kW, a thermopile used in the heater design must be created on the basis of medium-temperature or high-temperature thermoelectric materials [7-8]. It is also worthwhile to use combined segmented, cascade and permeable structures [9-10]. However, in our opinion, such approach is not quite rational, since for its

implementation it is necessary to change radically the proven design of the heater, namely to perform a search for optimal operation algorithms of the device itself and new operation algorithms of its components, to create a new design of electronic unit, etc.

The thermal power of the heater can be increased in a different fashion. The idea is to reduce the height of legs of thermoelectric modules and in this way to decrease their thermal resistance and, accordingly, to increase the thermal flux from the source to the heat carrier.

Competing factors that interfere with continuous reduction of leg height are contact thermal and electric resistances. Thus, as a leg is decreased, the losses in temperature differences in thermal contacts increase considerably, and the negative influence of the Joule heat released in electric contact junctions of thermopile becomes much more pronounced [11].

Therefore, the purpose of this work is to analyze the effect of thermoelectric module design on its energy characteristics and on the basis of the research performed to create a new variant of a thermopile for thermoelectric starting pre-heater.

Physical model of thermoelectric module and its description

As a thermopile, the heater design employed 12 generator thermocouple modules Altec-1061 developed at the Institute of Thermoelectricity [12], with their characteristics shown in Fig.1.

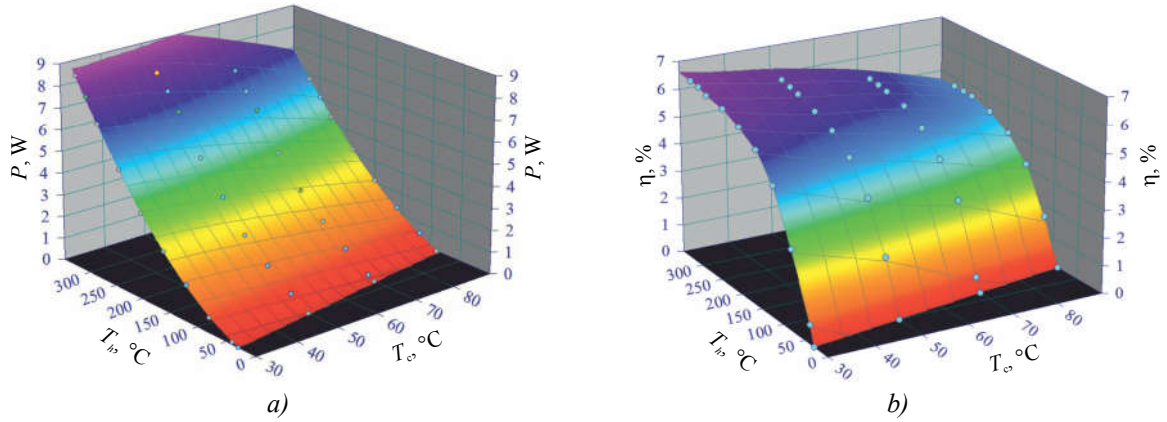

Fig. 1. Three-dimensional dependences of electric power P (a) and efficiency η (b) on the hot side T_h and cold side T_c temperatures of thermoelectric module Altec-1061 [6].

Using the above dependences in [4] it was shown that thermal power of the heater Q which is spent on heating automobile engine from 0°C to 50°C is on the average 1500 W (125 W as per one thermoelectric module). Accordingly, to heat the engine to temperature 70°C, it is necessary to determine such leg height whereby the level of module thermal power will be at least 180 W. This assumption is valid, as long as an equation which describes heating process is of a linear nature:

$$Q = cm\Delta T, \quad (1)$$

where Q is the amount of heat obtained by a body in heating, m is the mass of a body which is heated, $\Delta T = T_1 - T_0$ is the difference between final T_1 and initial T_2 body temperature.

For the calculations of the optimal height of leg of thermoelectric generator module Altec-1061 (Fig. 2a), a structural unit of module was used, namely a thermoelement, the physical model of which is shown in Fig. 2b. The model comprises n-type legs 1 and p-type legs 2 connected into a series electric circuit by interconnects 3 and 4 on the hot and cold side, respectively. Electric contacts 7 and 8 between the legs and connecting plates are characterized by electric contact resistances. The reinforced base of

thermoelectric module is made by electrically insulating heat conducting plates 5 and 6 that are in thermal contact 9 and 10 with the thermostat.

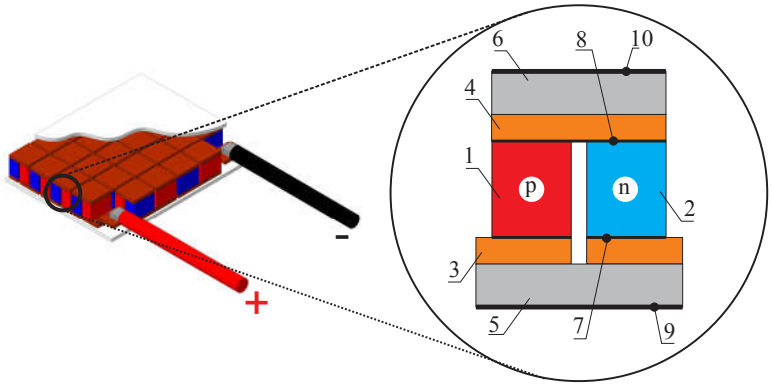

a) *b)*

Fig. 2. Schematic of thermoelectric module Altec-1061 (a) and physical model of its elementary structural unit (b): 1 – n-type leg; 2 – p-type leg; 3, 4 – electric interconnects; 5, 6 – ceramic plates; 7, 8 – electric contacts between the legs and connecting plates; 9 – thermal contact between electrically insulating plate and cold thermostat; 10 – thermal contact between ceramic plate and hot thermostat.

To find the distributions of temperature in the thermoelement, the law of conservation of energy is used.

$$\operatorname{div}\vec{w}=0, \tag{2}$$

$$\vec{w}=\vec{q}+U\vec{j}\,. \tag{3}$$

In (2) and (3), $\vec{w}$ is the density of energy flux, $\vec{q}$ is the density of heat flux, U is electrochemical potential, $\vec{j}$ is the density of electric current,

$$\vec{q}=-\kappa\nabla T+\Pi\vec{j}\,, \tag{4}$$

where Π is the Peltier coefficient, κ is thermal conductivity.

$$\Pi=\alpha T\,, \tag{5}$$

where α is the Seebeck coefficient, T is temperature.

The density of electric current is found from equation

$$\vec{j}=-\sigma\nabla U-\sigma\alpha\nabla T\,, \tag{6}$$

where σ is electric conductivity.

Substituting (3), (4) into (2), we obtain

$$-\nabla(\kappa\nabla T)+(\nabla\Pi+\nabla U)\vec{j}=0\,. \tag{7}$$

From equation (7), using (5) and (6), we obtain an equation for finding temperature distribution

$$-\nabla\left(\left(\sigma\alpha^2T+\kappa\right)\nabla T\right)-\nabla\left(\sigma\alpha T\nabla U\right)=\sigma\left(\left(\nabla U\right)^2+\alpha\nabla T\nabla U\right). \tag{8}$$

The distribution of electric potential is found using the law of conservation of electric charge

$$\operatorname{div}\vec{j}=0\,. \tag{9}$$

Substituting (5) into (8) we obtain the equation:

$$-\nabla\left(\sigma\alpha\nabla T\right)-\nabla\left(\sigma\nabla U\right)=0\,. \tag{10}$$

Equations (8), (10) are a system of differential equations with variable second order coefficients in partial derivatives describing the distribution of temperature and potential in the inhomogeneous thermoelectric medium.

Computer model of thermoelement

Solution of the system of equations (8) and (10) was realized in Comsol Multiphysics software environment [13] by the numerical finite element method. In the process of computer design the following values were used as the input data:

– temperature dependences of thermoelectric parameters $\alpha_n(T)$, $\alpha_p(T)$, $\sigma_n(T)$, $\sigma_p(T)$, $\kappa_n(T)$, $\kappa_p(T)$ (standard for materials based on n- and p-Bi_2Te_3 (Figs.3-5));

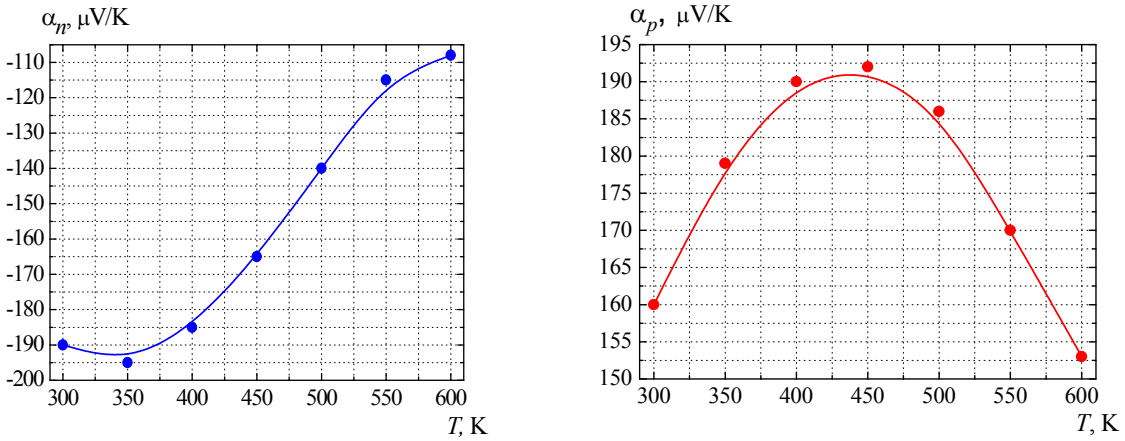

a) *b)*

Fig. 3. Temperature dependence of the Seebeck coefficient: a) n-Bi_2Te_3; b) p-Bi_2Te_3.

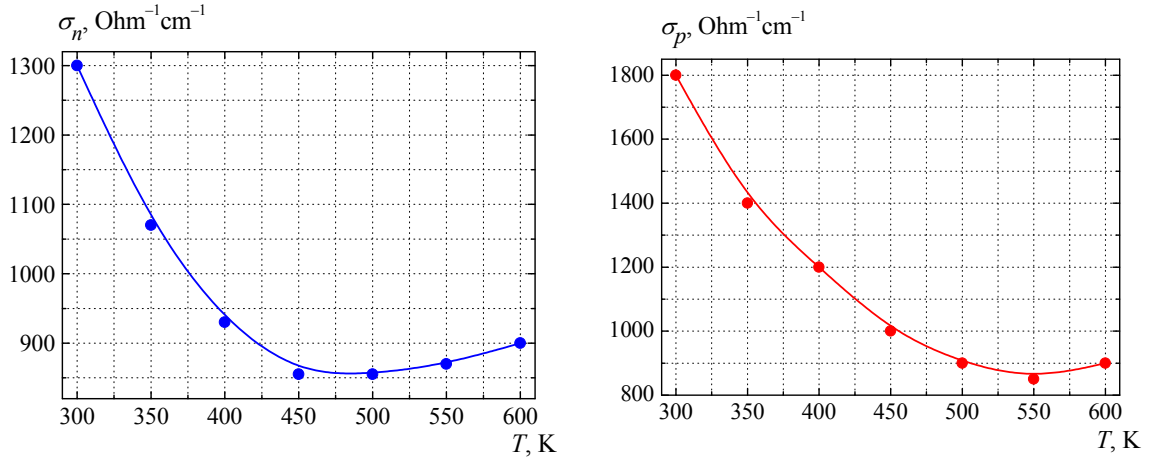

a) *b)*

Fig. 4. Temperature dependence of electric conductivity coefficient: a) n-Bi_2Te_3; b) p-Bi_2Te_3.

– cross-section of the legs ($a \times b$) = (1.8 × 4.2) mm;
– distance between the legs = 0.4 mm;
– the height of connecting plates h_{com} = 0.25 mm;
– the height of insulating plates h_{ins} = 0.65 mm;
– the number of leg couples in a module N = 56 pcs;

– thermal contact resistance between the thermostat and insulating plates $R = 4$ K/W;

– contact electric resistance between the legs and connecting plates $r = 10^{-5}$ Ohm·cm^2.

Fig. 6 shows the geometry and finite element mesh built in Comsol for thermoelement simulation.

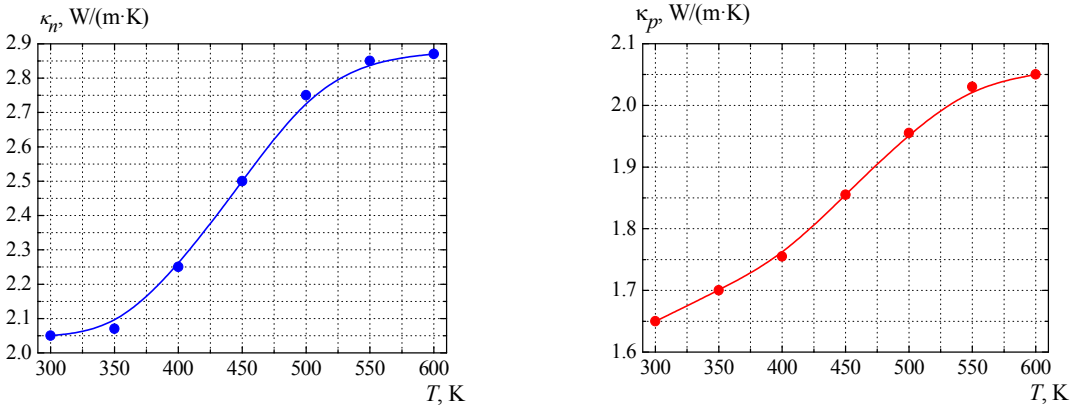

a) *b)*

Fig. 5. Temperature dependence of thermal conductivity coefficient: a) n-Bi_2Te_3; b) p-Bi_2Te_3.

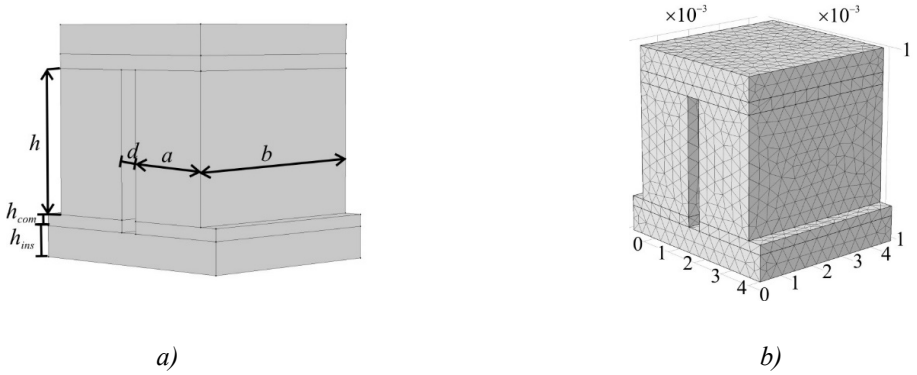

a) *b)*

Fig.6. Geometry (a) and finite element method (b) built in Comsol as applied to thermoelement model.

Design was carried out at the height h of thermoelement leg which was consecutively changed in the range from 3 mm to1 mm with increments of 0.5 mm.

The boundary conditions for the solution of equations (8) and (10) were chosen as follows. The temperatures of heat-absorbing and heat-releasing thermoelement surfaces were recorded as $T_h = 280^oC$ and $T_c = 50^oC$. Conditions of adiabatic thermal insulation were imposed on the rest of the boundaries. The zero potential value on the connecting plate of n-type leg was assigned. On the other connecting plate of p-type leg the value U was assigned which is half of thermopower generated by the thermoelement. In turn, the value of generated thermopower was determined by the system of equations (8) and (10) in the absence of current flow through the thermoelement.

On the boundaries of legs and contact layer, contact layer and connecting plates, insulating and connecting plates, conditions of the equality of temperatures and thermal flows were taken into account.

Research results

As a result of simulation, we obtained the distributions of temperature and electric potential in the thermoelement of generator module Altec-1061 (Fig. 7).

Figs. 8, 9 show the dependences of the energy characteristics of thermoelectric module Altec-1061 on the height of thermoelement leg.

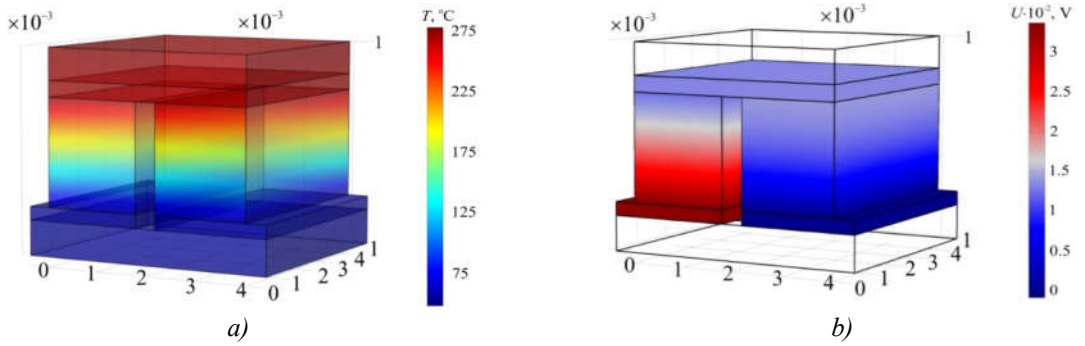

a) *b)*

Fig. 7. Distribution of temperature (a) and electric potential (b) in thermoelement of generator module Altec-1061. Leg height h = 2 mm.

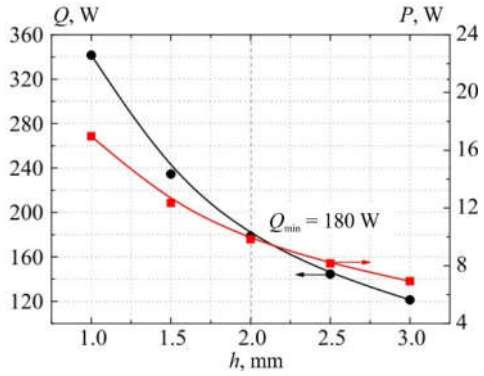

Fig. 8. Dependence of thermal Q and electric P power of module Altec-1061 on the leg height h.

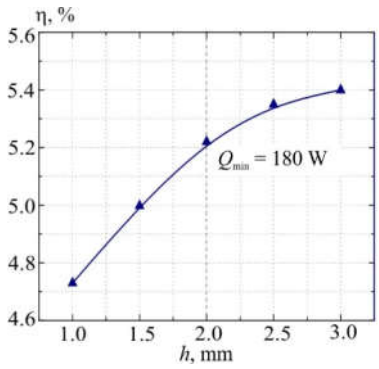

Fig. 9. Dependence of efficiency of module Altec-1061 on the leg height h.

From the represented data it follows that with decreasing the height of thermoelement leg, in the range of 3-1 mm there is increase in both thermal ($Q_{h=3}$ = 120 W – $Q_{h=1}$ = 340 W) and generated electric ($P_{h=3}$ = 7 W – $P_{h=1}$ = 17 W) of module power, which is caused by the reduction of its thermal resistance. In so doing, the necessary level of thermal power $Q_{\min}$ = 180 W is achieved with the height of thermoelement leg 2 mm. In this case the electric power of module is ~ 10 W (Fig. 8). Thus, to increase heat production, the heater must employ the design of module Altec-1061 with the legs the height of which does not exceed 2 mm. However, the reduction of height also leads to increased influence of contact electric and thermal resistances, which is visually demonstrated by the efficiency behavior (Fig. 9). Thus, in the range of heights (3-2) mm the efficiency of module is reduced from 5.4% to 5.2%, whereas in the range of h = (2-1) mm the reduction of η is more intensive: η = 5.2% at h = 2 mm, η = 4.4% at h = 1 mm.

So, in our opinion, the use in the heater of modules with the height of legs 2 mm is the most rational variant, since it enables one to ensure the level of thermal power necessary for start heating with the minimum losses of device efficiency.

The rationality of using legs with minimum losses of height is also quite justified in terms of reliability. With decreasing the height, owing to temperature gradient along the leg, the effect of thermal expansion is intensified, which causes deformation of the leg and, accordingly, reduces the mechanical strength of the module. This is particularly important under conditions of heater operation on transportation means during their motion, where the effect of vibrations, shocks and other loads is manifested simultaneously, increasing the risk of heater thermopile failure.

Based on the results of computer design a modified series of thermoelectric generator modules Altec-1061 was created with the height of thermoelement leg 2 mm that are intended for optimization of thermoelectric starting pre-heater. The results of experimental research on the energy characteristics of module at the hot side temperature 280°C and the range of cold side temperatures 30-70°C are represented in the table.

Table

Dependence of the energy characteristics of thermoelectric module Altec-1061 with the leg height 2 mm on the cold side temperature at T_h = 280°C

№	T_c, °C	U, V	I, A	P, W	Q, W	η, %
1	30	1.98	5.6	11.0	205	5.1
2	40	1.9	5.3	10.0	198	4.8
3	50	1.8	5.0	9.0	190	4.52
4	60	1.73	4.8	8.3	184	4.32
5	70	1.65	4.5	7.4	176	4.0

As is seen from the tabulated data, the experimental results correlate well with computer calculations (Fig. 8, 9). Thus, electric P and thermal Q power of module at T_h = 280°C and T_c = 50°C are 9 W and 190 W, respectively. The thermoelectric conversion efficiency η = 4.5%. The difference (~13%) between the calculated and obtained efficiency is most probably related to deviation of the values of material parameters α, σ, κ from standard temperature dependences, as well as to heat exchange of the lateral surfaces of legs with the environment.

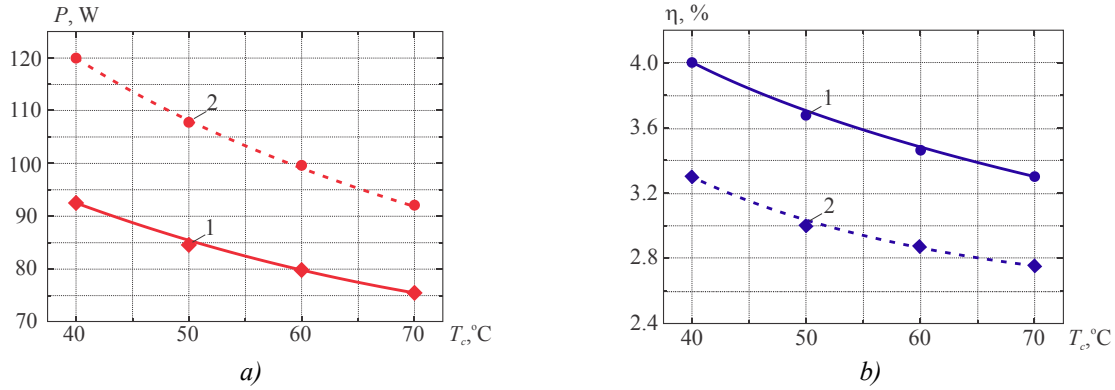

a) *b)*

Fig. 10. Dependence of maximum electric power P (a) and efficiency η (b) of thermoelectric heater on cold heat carrier temperature T_c: 1 – obtained in heater version I; 2 – predicted in heater version II.

Thus, the use of the developed modification of modules as a thermopile allows increasing the thermal power of thermoelectric starting pre-heater by a factor of ~ 1.5, to the level of 2.3 kW. In so doing, in the temperature range of the cold heat carrier (40 - 70)°C the generated electric power of the heater is expected to increase to (120 - 90) W (Fig. 10a), and the predicted range of efficiency values will be 3.3% - 2.75%, respectively (Fig. 10b).

Conclusions

1. It is shown that for start heating of automobile engine to optimal for its start temperature 70°C, the thermal power of thermoelectric heater must be at least 2.2 kW, as per one thermoelectric module of heater thermopile – at least 180 W of heat.

2. It is established that the most rational variant is to use in thermoelectric starting pre-heater of generator modules Altec-1061 with the height of legs 2 mm. It provides for the level of thermal power necessary for start heating with minimum losses of efficiency and device reliability.

3. It is established that at the hot side temperature 280°C and the cold side temperature range 30 - 70°C, the electric power of modified modules Altec-1061 is within 11 W - 7.4 W, the efficiency of thermoelectric conversion is 5.1% - 4%.

4. It is established that the use of the developed modification of modules as a thermopile allows increasing the thermal power of thermoelectric starting pre-heater to the level of 2.3 kW. In so doing, the generated electric power of the heater is expected to increase to 120 W - 90 W, and the predicted range of efficiency values is 3.3% - 2.75%, respectively.

References

1. Михайловський В.Я. Режими роботи автомобілів при понижених температурах. Необхідність використання нагрівачів та раціональність застосування термогенераторів для їх роботи. / Михайловський В.Я., Максимук М.В. // Термоелектрика. – 2015. – № 3. – С. 20 – 31.
2. Михайловський В.Я. Раціональні потужності термогенераторів для передпускових нагрівачів транспортних засобів. / Михайловський В.Я., Максимук М.В. // Термоелектрика. – 2015. – № 4. – С. 65 – 74.
3. Михайловський В.Я. Комп'ютерне проектування термоелектричного автомобільного передпускового нагрівача на дизельному паливі. / Михайловський В.Я., Максимук М.В. // Термоелектрика. – 2016. – № 1. – С. 52 – 65.
4. Анатичук Л.І. Експериментальні дослідження термоелектричного автомобільного передпускового нагрівача на дизельному паливі. / Анатичук Л.І., Михайловський В.Я., Максимук М.В., Андрусяк І.С. // Термоелектрика. – 2016. – № 4. – С. 84 – 94.
5. Максимук М.В. Електронний блок керування термоелектричним передпусковим автомобільним нагрівником. / Максимук М.В., Андрусяк І.С. // Термоелектрика. – 2016. – № 5. – С. 44 – 51.
6. Найман В.С. Все о предпусковых обогревателях и отопителях. / Найман В.С. Москва. – 2017. – 213 с.
7. Вихор Л.М. Оптимізація матеріалів та оцінка характеристик генераторних модулів для рекуператорів тепла. / Вихор Л.М., Михайловський В.Я., Мочернюк Р.М. // Фізика і хімія твердого тіла. – 2014. – № 1. – Т 15. – С. 206 – 213.
8. Термоелектричні генераторні модулі із матеріалів на основі *n-InSe* і *p-PbTe* для діапазону робочих температур 30 – 500 °С. / Михайловський В.Я., Кузь Р.В., Лисько В.В. [і. інш.]. // Термоелектрика. – 2014. – № 5. – С. 39 – 48.
9. Черкез Р.Г. Проектування термоелектричних проникних структур на основі силіцидів *Mg* і *Mn*. / Черкез Р.Г., Максимук М.В., Феняк П.П. // Термоелектрика. – 2013. – № 6. – С. 62 – 70.
10. Михайловський В.Я. Проектування термоелектричних каскадних модулів із секційними вітками на основі Bi_2Te_3-*PbTe-TAGS*. / Михайловський В.Я., Вихор Л.М., Максимук М.В., Мочернюк Р.М. // Термоелектрика. – 2015. – № 2. – С. 48 – 59.
11. Анатичук Л.І. Енергетичні й економічні показники термоелектричних генераторних модулів на основі *Bi-Te* для рекуперації відходів тепла. / Анатичук Л.І., Кузь Р.В., Хванг Дж.Д. // Термоелектрика. – 2012. – № 4. – С. 75 – 82.
12. http://inst.cv.ua
13. www.comsol.com

Submitted 15.03.17

Максимук М. В.

Інститут термоелектрики НАН і МОН України,
вул. Науки, 1, Чернівці, 58029, Україна,
e-mail: anatych@gmail.com

ПРО ОПТИМІЗАЦІЮ ТЕРМОЕЛЕКТРИЧНИХ ГЕНЕРАТОРНИХ МОДУЛІВ АВТОМОБІЛЬНОГО ПЕРЕДПУСКОВОГО НАГРІВНИКА

Наведено результати комп'ютерного проектування та експериментальних досліджень зі створення нової конструкції термоелектричного термопарного генераторного модуля «Алтек-1061» для підвищення теплопродуктивності термоелектричного автомобільного передпускового нагрівника. Проектування здійснено з урахуванням температурних залежностей параметрів матеріалів, теплових і електричних втрат на контактах і комутації модуля. Бібл. 13, рис. 10, табл. 1.
Ключові слова: передпусковий нагрівник, термоелектричний генератор, комп'ютерне проектування, фізична модель, термоелемент.

Максимук Н. В.

Институт термоэлектричества НАН и МОН Украины,
ул. Науки, 1, Черновцы, 58029, Украина
e-mail: anatych@gmail.com

ОБ ОПТИМИЗАЦИИ ТЕРМОЭЛЕКТРИЧЕСКИХ ГЕНЕРАТОРНЫХ МОДУЛЕЙ АВТОМОБИЛЬНОГО ПРЕДПУСКОВОГО НАГРЕВАТЕЛЯ

Приведены результаты компьютерного проектирования и экспериментальных исследований по созданию новой конструкции термоэлектрического термопарного генераторного модуля «Алтек-1061» для повышения теплопроизводительности термоэлектрического автомобильного предпускового нагревателя. Проектирование осуществлено с учетом температурных зависимостей параметров материалов, тепловых и электрических потерь на контактах и коммутации модуля. Библ. 13, рис. 10, табл. 1.
Ключевые слова: предпусковой нагреватель, термоэлектрический генератор, компьютерное проектирование, физическая модель, термоэлемент.

References

1. Mykhailovskyi V.Ya., Maksymuk M.V. (2015). Rezhymy roboty avtomobiliv pry ponyzhenykh temperaturakh. Neobhidnist vykorystannia nahrivachiv ta ratsionalnist zastosuvannia termoheneratoriv dlia yikh roboty [Automobile operating conditions at low temperatures. The necessity of applying heaters and the rationality of using thermal generators for their work]. *Termoelektryka - J.Thermoelectricity,* 3, 20 – 31 [in Ukrainian].

2. Mykhailovskyi V.Ya., Maksymuk M.V. (2015). Ratsionalni potuzhnosti termoheneratoriv dlia peredpuskovykh nahrivachiv transportnykh zasobiv [Rational powers of thermal generators for starting pre-heaters of vehicles]. *Termoelektryka - J.Thermoelectricity,* 4, 65 – 74 [in Ukrainian].
3. Mykhailovskyi V.Ya., Maksymuk M.V. (2016). Kompiuterne proektuvannia termoelektrychnoho avtomobilnoho peredpuskovoho nahrivacha na dyzelnomu palyvi [Computer design of thermoelectric automobile starting pre-heater operated with diesel fuel]. *Termoelektryka - J.Thermoelectricity,* 1, 52 – 65 [in Ukrainian].
4. Anatychuk L.I., Mykhailovskyi V.Ya., Maksymuk M.V., Andrusiak I.S. (2016). Eksperymentalni doslidzhennia termoelektrychnoho avtomobilnoho peredpuskovoho nahrivacha na dyzelnomu palyvi [Experimental research on thermoelectric automobile starting pre-heater operated with diesel fuel]. *Termoelektryka - J.Thermoelectricity,* 4, 84 – 94 [in Ukrainian].
5. Maksymuk M.V., Andrusiak I.S (2016). Eektronnyi blok keruvannia termoelektrychnym avtomobilnym peredpuskovym nahrivachem [Electronic control unit for thermoelectric automobile starting pre-heater]. *Termoelektryka - J.Thermoelectricity,* 5, 44 – 51 [in Ukrainian].
6. Naiman V.S. (2007). *Vse o predpuskovykh obogrevateliakh i otopiteliakh* [*All about Starting Pre-Heaters and Heaters*]. Moscow: ACT [in Russian].
7. Vykhor L.M., Mykhailovskyi V.Ya., Mochernyuk R.M. (2014). Optymizatsia materialiv ta otsinka kharakterystyk heneratornykh moduliv dlia rekuperatoriv tepla [Optimization of materials and evaluation of characteristics of generator modules for heat recuperators]. *Fizyka i khimia tverdoho tila - Physics and Chemistry of the Solid State,* 15 (1), 206 – 213 [in Ukrainian].
8. Mykhailovskyi V.Ya., Kuz R.V., Lysko V.V., Maksymuk M.V., Mocherniuk R.M. (2014). Termoelektrychni heneratorni mofuli iz materialiv na osnovi *n-InSe* i *p-PbTe* dlia diapazonu robochykh temperatur 30 – 500 °C [Thermoelectric generator modules of n-InSe and p-PbTe-based materials for the level of operating temperatures 30-500°C]. *Termoelektryka - J.Thermoelectricity,* 5, 39 – 48 [in Ukrainian].
9. Cherkez R.G., Maksymuk M.V., Feniak P.P. (2013). Proektuvannia termoelektrychnykh pronyknykh struktur na osnovi sylitsydiv *Mg* i *Mn* [Design of thermoelectric permeable structures based on *Mg* and *Mn* Silicides]. *Termoelektryka - J.Thermoelectricity,* 6, 62 – 70 [in Ukrainian].
10. Mykhailovskyi V.Ya., Vykhor L.M., Maksymuk M.V., Mocherniuk R.M. (2015). Proektuvannia termoelektrychnykh kaskadnykh moduliv iz sektsiinymy vitkamy na osnovi Bi_2Te_3-*PbTe-TAGS* [Design of thermoelectric staged modules with segmented legs based on Bi_2Te_3-*PbTe-TAGS*]. *Termoelektryka - J.Thermoelectricity,* 2, 48 – 59 [in Ukrainian].
11. Anatychuk L.I., Kuz R.V., Hwang J.D. (2012). Energetychni i ekonomichni pokaznyky termoelektrychnykh heneratornykh moduliv na osnovi *Bi-Te* dlia rekuperatsii vidkhodiv tepla [The energy and economic parameters of *Bi-Te* Based thermoelectric generator modules for waste heat recovery]. *Termoelektryka - J.Thermoelectricity,* 4, 75 – 82 [in Ukrainian].
12. http://inst.cv.ua
13. www.comsol.com

Subminited 15.03.2017

L.I. Anatychuk[1,2] *acad. National Academy of Sciences of Ukraine*,
R.R. Kobylianskyi[1,2] *Candidate fiz.-mat. Science*, **T.Ya. Kadenyuk**[1]

[1]Institute of Thermoelectricity of the NAS and MES Ukraine,
Nauky str., Chernivtsi, 58029, Ukraine,
e-mail: anatych@gmail.com;
[2]Yu. Fedkovich Chernivtsi National University,
Kotsyubynsky str., Chernivtsi, 58012, Ukraine
e-mail: anatych@gmail.com

COMPUTER SIMULATION OF LOCAL THERMAL EFFECT ON HUMAN SKIN

In this paper, the physical, mathematical and computer models of local thermal effect on human skin are constructed. Temperature distributions in different skin layers are determined for cooling mode. The results obtained allow optimization of a working tool of device for treatment of skin diseases in order to ensure the necessary depth of freezing of biological tissue and maximum effect when carrying out cryomassage. Bibl. 24, Fig. 7, Table. 1.
Key words: thermoelectric cooling, cryomassage, biological tissue, human skin, computer simulation.

Introduction

It is known [1 – 5] that temperature effect contributes to activation of processes in human organism and is an important factor for treatment of various diseases, namely dermatologic, allergic, gynecologic, diseases of cardio-vascular system, respiratory organs, locomotor system, etc. Cold activates metabolism, helps to slow down the process of skin aging, cleans and facilitates its breathing, accelerates blood circulation, removes from the surface layers of the skin the vital products of the body, supports muscle tone, etc. The therapeutic effect of the cold locally reduces the skin temperature, provides anti-inflammatory, antispastic, analgesic action, exfoliate the epidermis, and with prolonged exposure allows the removal of benign or malignant neoplasms, etc. [6 – 10].

The above information on the thermal effect on the surface of human skin testifies to the promising character of using thermoelectric cooling and heating in dermatology [11 – 13]. This is related to its advantages: possibility to precisely assign the necessary temperature of the tool surface, the time of temperature effect on the corresponding area of human body and to ensure cyclic change of cooling and heating modes [14 – 16]. However, the use of low and elevated temperatures in medical practice calls for a comprehensive study of the peculiarities of thermal effect on biological tissue, which is a complicated task requiring creation of precise physical and mathematical models (with regard to blood circulation, metabolic and heat exchange processes) and the use of computer simulation.

So, *the purpose of the work* is creation of computer simulation technique that will allow predicting the results of local thermal effect on human skin, including cryomassage in dermatology.

A physical model of biological tissue with a cooling element

The biological tissue of human body (Fig. 1) is a structure of three skin layers (epidermis 1,

dermis 2, subcutaneous tissue 3) and the internal tissue 4. The temperatures on the boundaries of the corresponding layers of biological tissue of thickness h_1, h_2, h_3, h_4 are T_1, T_2, T_3, T_4, and the specific heat fluxes inside are Q_1, Q_2, Q_3, Q_4. The free surface of skin area (epidermis 1) is in the state of heat exchange with the environment with temperature T_7. The specific heat flux from the free skin surface is Q_6, and the specific heat flux from the internal human organs is Q_5. Skin heat exchange due to radiation and sweating is disregarded.

Arranged on the surface of biological tissue (epidermis 1) with temperature T_5 is a cooling element 5 of height l, with contact surface temperature T_6.

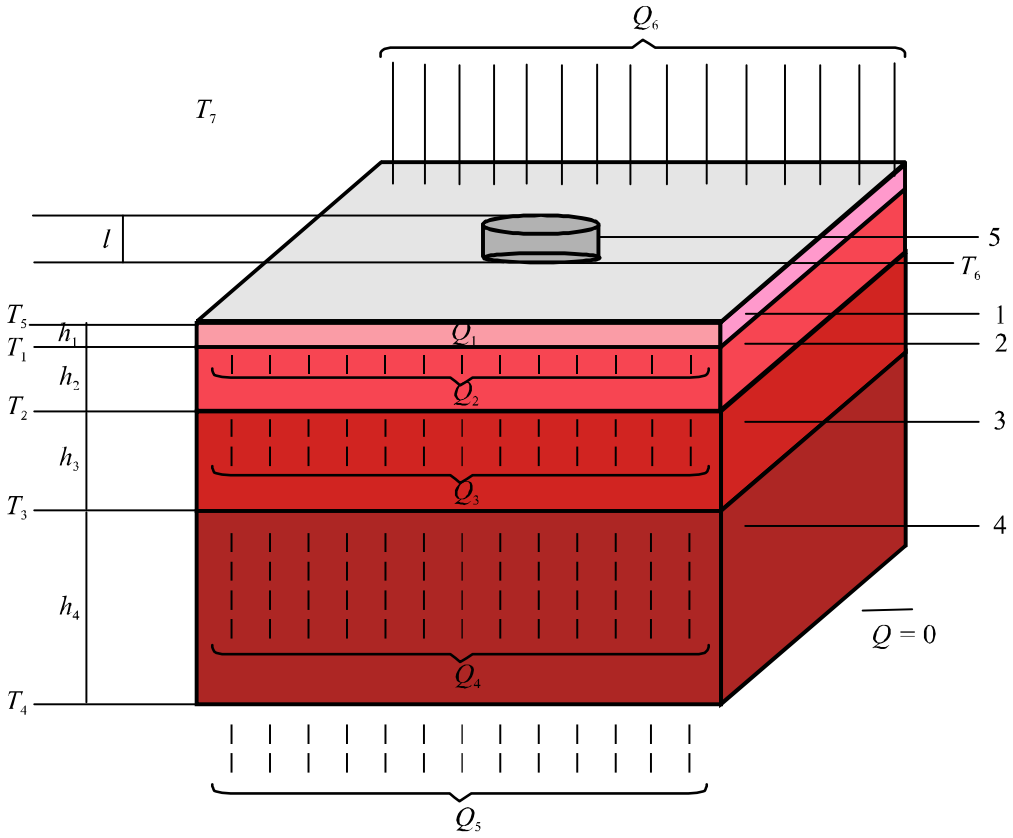

Fig. 1. Physical model of biological tissue with a cooling element: 1 – epidermis, 2 – dermis, 3 – subcutaneous tissue, 4 – internal tissue, 5 – cooling element.

As long as a physical model is an area of a four-layered biological tissue, with identical biochemical processes occurring in adjacent layers, it can be assumed that no heat overflow occurs through the lateral surfaces of biological tissue ($Q = 0$).

Mathematical description of the model

To describe the process of heat exchange in “living” biological tissues, the Pennes model is used [17]. The model is based on the four assumptions:

1. heat exchange between blood and biological tissue in prearteriolas and posyvenules is neglected;
2. blood flow in small capillaries is considered to be isotropic, the direction of blood flow is neglected;
3. large blood vessels in the immediate vicinity from capillaries do not contribute to energy exchange between biological tissue and capillary blood (that is, the Pennes model does not take into account

local geometry of vessels);

4. blood temperature in arteriolas is equal to body temperature. Energy exchange occurs immediately: blood temperature is equalized with local temperature of biological tissue.

Based on the above assumptions, Pennes simulated the effect of blood as isotropic heat source proportional to blood flow velocity and the difference between body temperature and local temperature of tissue [18 – 20]:

$$\rho_{skin} Cp_{skin} \frac{\partial T}{\partial t} = \nabla \cdot (\kappa_{skin} \nabla T) + (\rho Cp)_{blood} \omega_b (T_a - T) + q_m , \quad (1)$$

where ρ_{skin} is human skin density;

Cp_{skin} is specific heat of human skin;

k_{skin} is thermal capacity of human skin;

ρ_{blood} is human blood density;

Cp_{blood} is specific heat of human blood;

ω_b is human blood perfusion;

T_a is arterial blood temperature (T_a = 37°C);

T is biological tissue temperature;

q_m is heat released due to metabolism.

The generation of metabolic heat considered in this model is assumed to be uniformly distributed along the entire tissue, blood perfusion is also considered to be uniform and isotropic. According to the Pennes model, thermal equilibrium arises directly in the capillary circle of microcirculatory bloodstream (blood at temperature T_a comes to capillaries where heat exchange takes place and the temperature is reduced to the temperature of biological tissue *T*).

The summand in the left side of Eq. (1) is the rate of change in thermal energy located in the unit volume of biological tissue. Three summands in the right side of this equation are, accordingly, the rate of change in thermal energy due to thermal conductivity, blood perfusion and metabolic heat.

For the steady-state case $\frac{\partial T}{\partial t} = 0$, so Eq. (1) is simplified to:

$$\nabla \cdot (\kappa_{skin} \nabla T) + (\rho Cp)_{blood} \omega_b (T_a - T) + q_m = 0 . \quad (2)$$

The steady-state equation of heat exchange in biological tissue (2) is solved with the following boundary conditions (3), as a result of which the distribution *T(x, y, z)* is determined

$$\begin{cases} Q\big|_{x=0} = 0, \\ Q\big|_{x=a} = 0, \end{cases} \quad \begin{cases} Q\big|_{y=0} = 0, \\ Q\big|_{y=a} = 0, \end{cases} \quad \begin{cases} T\big|_{z=0} = 37°\text{C}, \\ q\big|_{z=b} = \alpha \cdot (T_0 - T), \end{cases} \quad (3)$$

where Q is heat flux density, T is absolute temperature, T_0 is ambient temperature, α is heat exchange coefficient.

The thermophysical properties of human skin layers are given in Table.

Table

Thermophysical properties of human skin layers [21 – 24]

Skin layers	*Property*	*Value*	*Measurement units*
Epidermis	Thermal conductivity, k_{skin}	0.24	W/m°K
	Density, ρ_{skin}	1200	kg/m^3
	Specific heat, Cp_{skin}	3590	J/kg°K
	Thickness, h	8×10^{-5}	m
	Perfusion, ω_b	0	s^{-1}
Dermis	Thermal conductivity, k_{skin}	0.45	W/m°K
	Density, ρ_{skin}	1200	kg/m^3
	Specific heat, Cp_{skin}	3300	J/kg°K
	Thickness, h	2×10^{-3}	m
	Perfusion, ω_b	0.00125	s^{-1}
Subcutaneous tissue	Thermal conductivity, k_{skin}	0.19	W/m°K
	Density, ρ_{skin}	1000	kg/m^3
	Specific heat, Cp_{skin}	2500	J/kg°K
	Thickness, h	1×10^{-2}	m
	Perfusion, ω_b	0.00125	s^{-1}
Internal tissue	Thermal conductivity, k_{skin}	0.5	W/m°K
	Density, ρ_{skin}	1000	kg/m^3
	Specific heat, Cp_{skin}	4000	J/kg°K
	Thickness, h	3×10^{-2}	m
	Perfusion, ω_b	0.00125	s^{-1}

Computer simulation results

In a cylinder coordinate system a 3D computer model of biological tissue was created with a cooling element arranged on its surface. The computer model was constructed with the use of Comsol Multiphysics applied software package [25], which allows simulation of thermophysical processes in biological tissue with regard to blood circulation and metabolism.

The distribution of temperature and heat flux density in biological tissue was calculated by the finite element method. According to this method, an object under study is split into a large number of finite elements, and in each of them the value of function is sought which satisfies given differential equations of second kind with the respective boundary conditions. The accuracy of solving the formulated problem depends on the level of splitting and is ensured by using a large number of finite elements [25].

Fig. 2 and Fig. 3 show temperature distributions in the bulk and cross-section of human body

biological tissue having on its surface a cooling element at temperature $T = -30$°C.

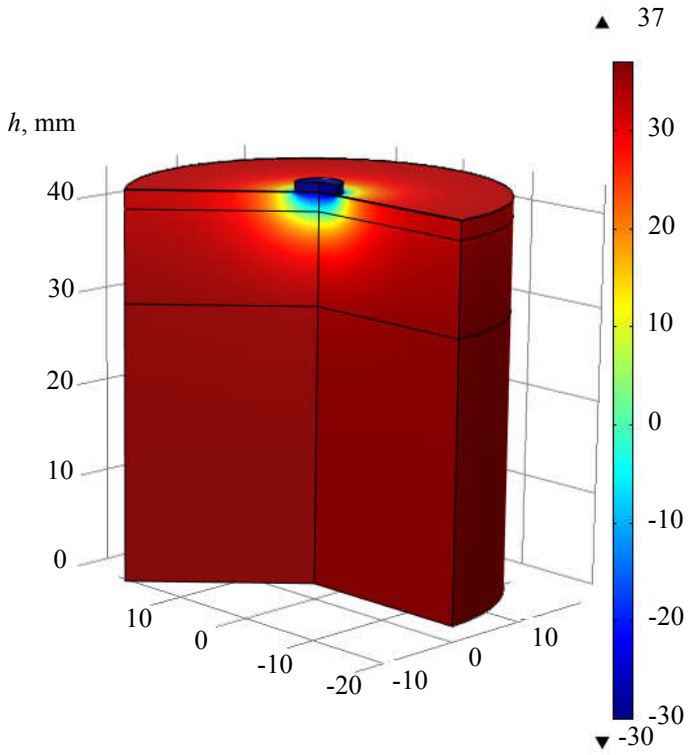

Fig. 2. Temperature distribution in the bulk of biological tissue having on its surface a cooling element at temperature $T = -30$°C.

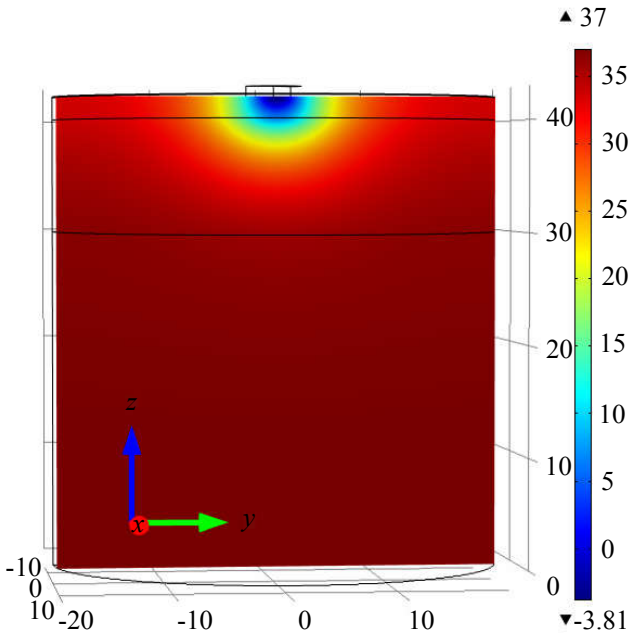

Fig. 3. Temperature distribution in the cross-section of biological tissue having on its surface a cooling element at temperature $T = -30$°C.

Computer simulation was also used to obtain the distribution of isothermal surfaces in biological tissue (Fig. 4) with regard to the boundary effects in the improved 3D computer model.

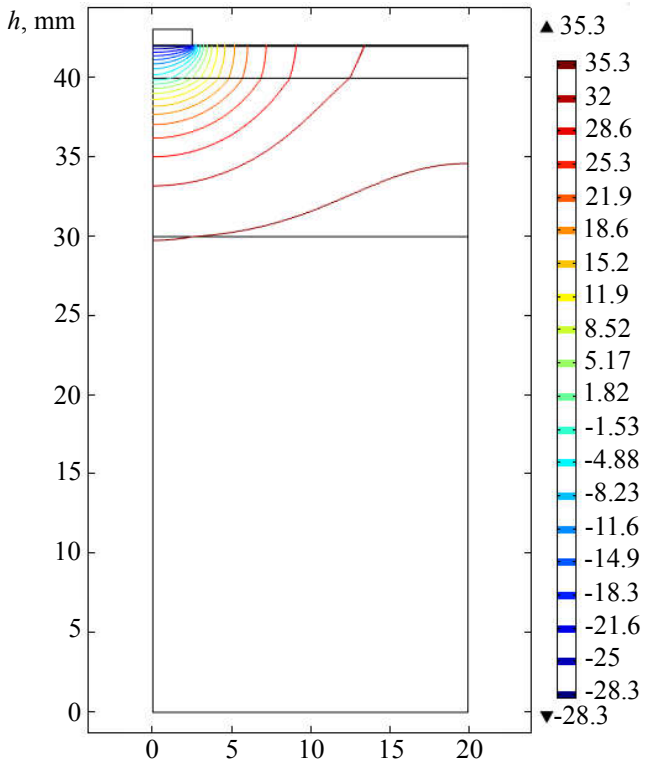

Fig. 4. Distribution of isothermal surfaces in biological tissue having on its surface a cooling element at temperature T = – 30°C.

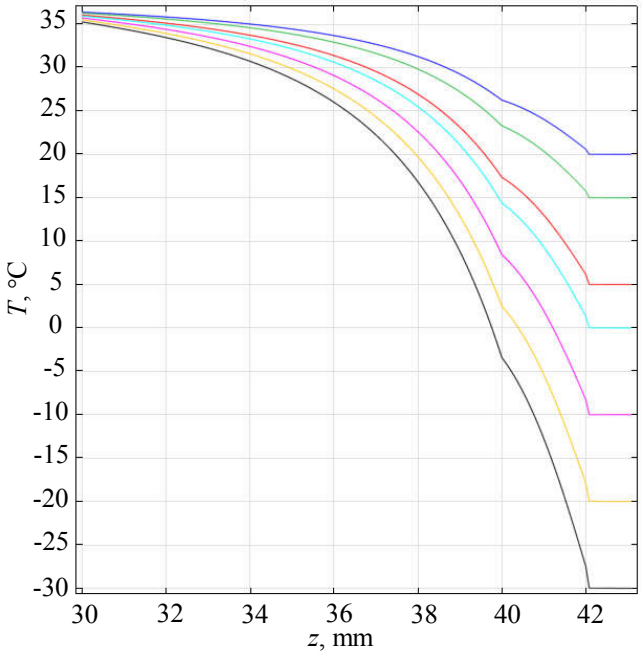

Fig. 5. Temperature distribution in biological tissue at cooling element temperatures in the range of T = +25 ÷ – 30°C.

Computer simulation was used to obtain temperature distribution in biological tissue. As an example, Fig. 5 shows the above temperature distribution in biological tissue at cooling element temperatures in the range of $T = +25 \div -30$°C.

Also, the relationship between the temperature of cooling element on the skin surface and the depth of freezing of biological tissue was determined (Fig. 6). It was established that to achieve freezing of biological tissue to the depth of 3 mm, it is necessary to provide skin surface temperature $T = -30$°C.

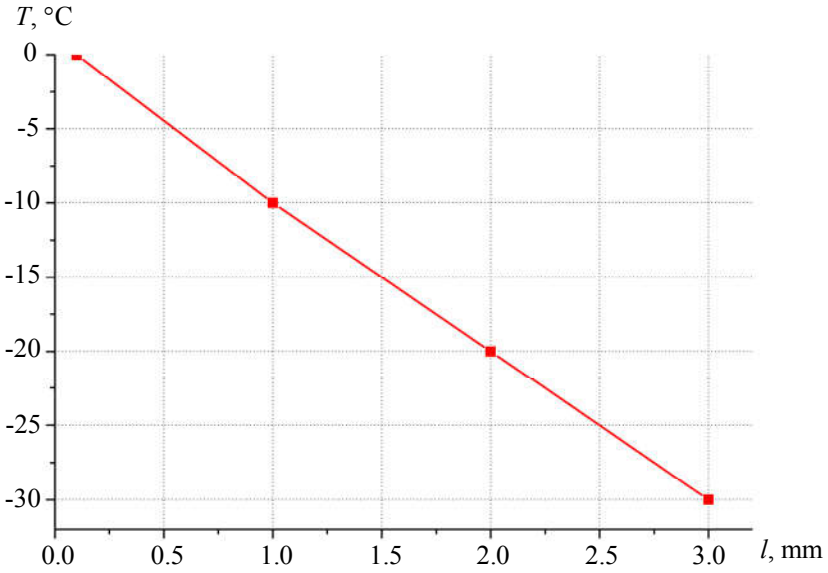

Fig. 6. Temperature of cooling element on the skin surface versus the depth of freezing of biological tissue.

Computer simulation was used to determine the dependence of cooling element temperature on the thermal power rejected from it to the environment (Fig. 7).

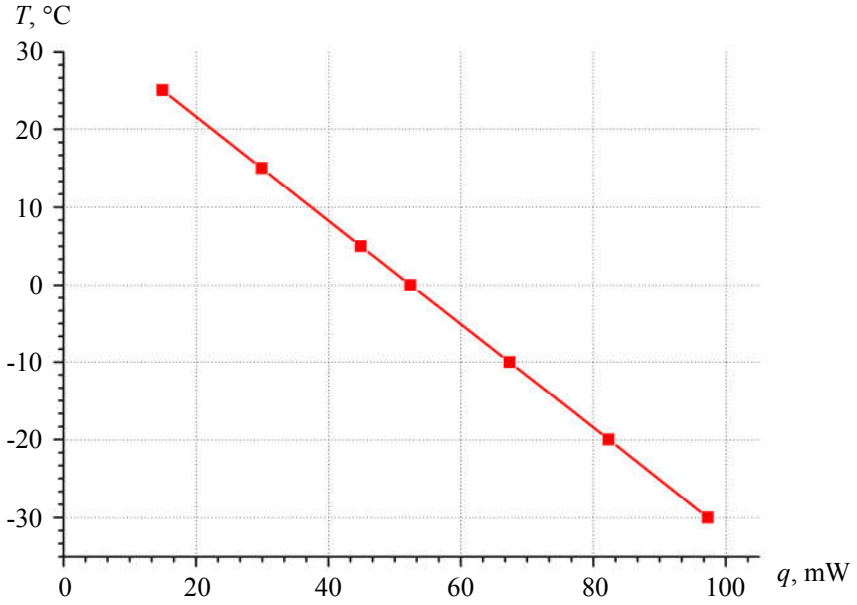

Fig. 7. Dependence of cooling element temperature on the thermal power rejected from it to the environment.

From Fig. 7 it is evident that to ensure the temperature $T = -30$°C on the skin surface, it is necessary to reject $W = 0.1$ W of heat. The results obtained enable one to determine cooling capacity of a working tool of device for treatment of skin diseases in order to ensure the necessary temperature mode of cryomassage (0 ÷ +5)°C in the near-surface layer of biological tissue. This, in turn, allows

design optimization of a working tool of device for treatment of skin diseases in order to ensure the necessary depth of freezing of biological tissue and to achieve maximum effect when carrying out cryomassage.

Conclusions

1. Computer simulation technique was developed which allows predicting the results of local thermal effect on human skin, including cryomassage in dermatology.
2. Computer simulation method was used to determine temperature distributions in different skin layers in cooling mode. It was established that the temperature of a working tool must be $T = -30$°C and cooling capacity must be $q = 0.1$ W in order to ensure the necessary temperature mode (0 ÷ +5)°C in the near-surface layer of biological tissue when carrying out cryomassage.

References

1. Машкиллейсон А.Л. Лечение кожных болезней. / Машкиллейсон А.Л. Москва. – 2000. – 250 с.
2. Грищенко В.И. Практическая криомедицина. / Грищенко В.И., Сандомирський Б.П., Колонтай Ю.Ю. Киев. – 1987. – 248 с
3. Дерматология, венерология. Учебник / Под редакцией. Степаненко В.И. Киев. – 2012. – 904 с.
4. Ахтямов С.Н. Практическая дерматокосметология. / Ахтямов С.Н., Бутов Ю.С. Учебное пособие. Москва. – 2003. – 394 с.
5. Буренина И.А. Современные методики криотерапиив в клинической практике. Вестник современной клинической медицины. 2014 Том 7. приложение 1. 57 – 61 с.
6. Mourot L. Jacques regnard hyperbaric gaseous cryotherapy: effects on skin temperature and systemic vasoconstriction. archives of physical medicine and rehabilitation, / Mourot L., Cluzeau C. // November 2007. – 1339 – 1343 p.
7. Deonizio J.Histological Comparison of Two Cryopeeling Methods for Photodamaged Skin. / Deonizio J., Werner B., Fabiane A. Mulinari-Brenner. // Hindawi Publishing Corporation. – 2014. – p. 1 – 5.
8. Задорожный Б.А. Криотерапия в дерматологии (Библиотека практического врача) / Задорожный Б.А. Киев. – 1985. – 72 с.
9. Земсков В.С. Низкие температуры в медицине / Земсков В.С., Гасанов Л.И. Киев. – 1988. – 278 с.
10. Анатичук Л.І. Про використання термоелектричного охолодження в дерматології та косметології. / Анатичук Л.І., Денисенко О.І., Кобилянський Р.Р., Каденюк Т.Я. Термоелектрика. – 2015. – № 3. – С. 57 – 71.
11. Кобилянський Р.Р., Каденюк Т.Я. Про перспективи використання термоелектрики для лікування захворювань шкіри холодом. Науковий вісник Чернівецького університету: збірник наук. праць. Фізика. Електроніка. Т. 5, Вип. 1. Чернівці: Чернівецький національний університет. 2016. С. 67 – 72.
12. Анатичук Л.І. Сучасні методи кріовпливу у дерматологічній практиці Клінічна та експериментальна патологія. - 2017. – Том XVI. – №1(59). – С. 150 –156.
13. Анатычук Л.И. Термоэлементы и термоэлектрические устройства / Анатычук Л.И. Киев. – 1979. – 768 с.

14. Анатычук Л.И. Термоэлектричество. Т.2. Термоэлектрические преобразователи энергии. / Анатычук Л.И. Киев, Черновцы: Институт термоэлектричества. – 2003. – 376 с.
15. Коленко Е.А. Термоэлектрические охлаждающие приборы. / Коленко Е.А. – Л.: Наука. – 1967. – 283с.
16. Pennes H.H. Analysis of tissue and arterial blood temperatures in the resting forearm / Pennes H.H. J. Appl. Physiol. – 1948. – Vol. 1. – no. 2. – P. 93 – 122.
17. Fan L.T. A review on mathematical models of the human thermal system / Fan L.T., Hsu F.T., Hwang C.L. // IEEE Trans on Bio-Med. Eng. – 1971. – 18. – № 3. – P. 218 – 234.
18. Zanchini E. Heat transfer in circulatory system / Zanchini E., Mariotti M., Salvini S. // Ras-segna di Bioingegneria. – 1979. – № 8. – P. 33 – 44.
19. Chato J.C. Heat transfer to blood vessels. / Chato J.C. // Trasns. ASME. J. Biomech. Eng. – 1980. – Vol. 102. – №2. – P. 110 – 118.
20. Gordon G. R. Mathematical model of the human temperature regulatory system. / Gordon G. R., Roemer R.B., Horvath S.M. // Transient cold expoasure response. IEEE Trans. Biomed. Eng. – 1976. – Vol. 23. – №5. – P. 434 – 444.
21. Jiang S.C. Effects of thermal properties and geometrical dimensions on skin burn injuries. / Jiang S.C., Ma N., Li H.J., Zhang X.X. // Burns. – 28. – 2002. – p. 713 – 717.
22. Cetingul M.P. Identification of skin lesions from the ransient thermal response using infrared ima-
23. ging technique / Cetingul M.P., Herman C. // IEEE. – 2008. – p. 1219 – 1222.
24. Ciesielski M. Numerical modeling of biological tissue heating. Admissible thermal dose. / Ciesielski M., Mochnacki B., Szopa R. // Scientific Research of the Institute of Mathematics and Computer Science. – 2011. – 1(10). – p. 11 – 20.
25. COMSOL Multiphysics User's Guide // COMSOLAB. 2010. 804 p.

Submitted 20.03.2017

Анатичук Л.І.[1,2] *ак. НАН України*,
Кобилянський Р.Р.[1,2] *канд. фіз.-мат. наук*,
Каденюк Т.Я.[1]

[1]Інститут термоелектрики НАН і МОН України, вул. Науки, 1,
Чернівці, 58029, Україна, *e-mail: anatych@gmail.com*;
[2]Чернівецький національний університет ім. Юрія Федьковича,
вул. Коцюбинського 2, Чернівці, 58012, Україна, *e-mail: anatych@gmail.com*

КОМП'ЮТЕРНЕ МОДЕЛЮВАННЯ ЛОКАЛЬНОГО ТЕПЛОВОГО ВПЛИВУ НА ШКІРУ ЛЮДИНИ

У роботі побудовано фізичну, математичну та комп'ютерну моделі локального теплового впливу на шкіру людини. Визначено розподіли температури у різних шарах шкіри в режимі охолодження. Отримані результати дають можливість оптимізувати конструкцію робочого інструменту приладу для лікування захворювань шкіри з метою досягнення необхідної глибини промерзання біологічної тканини та максимального ефекту при проведенні кріомасажу. Бібл. 24, рис. 7, табл. 1.

Ключові слова: термоелектричне охолодження, кріомасаж, біологічна тканина, шкіра людини, комп'ютерне моделювання.

Анатичук Л.И.[1,2] *ак. НАН Украины*,
Кобылянский Р.Р.[1,2] *канд. фіз.-мат. наук*,
Каденюк Т.Я.[1]
[1]Институт термоэлектричества, ул. Науки, 1, Черновцы, 58029, Украина;
e-mail: anatych@gmail.com;
[2]Черновицкий национальный университет им. Ю.Федьковича,
ул. Коцюбинского, 2, Черновцы, 58000, Украина
e-mail: anatych@gmail.com

КОМПЬЮТЕРНОЕ МОДЕЛИРОВАНИЕ ЛОКАЛЬНОГО ТЕПЛОВОГО ВЛИЯНИЯ НА КОЖУ ЧЕЛОВЕКА

В работе построены физическая, математическая и компьютерная модели локального теплового влияния на кожу человека. Определены распределения температуры в разных слоях кожи в режиме охлаждения. Полученные результаты дают возможность оптимизировать конструкцию рабочего инструмента прибора для лечения заболеваний кожи с целью достижения необходимой глубины промерзания биологической ткани и максимального эффекта при проведении криомассажа. Библ. 24, рис. 7, табл. 1.
Ключевые слова: термоэлектрическое охлаждение, криомассаж, биологическая ткань, кожа человека, компьютерное моделирование.

References

1. Mashkilleison A.L. (2000). *Lechenie kozhnykh boleznei [Treatment of skin diseases]*. *Moscow:* Kron-Pres [in Russian].
2. Hryshchenko V.I., Sandomyrskyi B.P., Kolontai Yu.Yu. (1987). *Prakticheskaia kriomeditsina [Practical cryomedicine]*. Kyiv: Zdorovie [in Russian].
3. *Dermatologia, venerologia. Uchebnik [Deramatology, venerology. Textbook]*. Stepanenko V.I. (Ed.). (2012). Kyiv:KIM [in Russian].
4. Akhtiamov S.N., Butov Yu.S. (2003). *Prakticheskaia dermatokosmetologia. Uchebnoe posobie. [Practical Dermacosmetology. Manual]*. Moscow: Meditsina [in Russian].
5. Burenina I.A. (2014). Sovremennye metodiki krioterapii v klinicheskoi praktike [Modern cryotherapy methods in clinical practice]. *Vestnik sovremennoi klinicheskoi meditsiny – Bulletin of modern clinical medicine*, 7, 1, 57 – 61 [in Russian].
6. Mourot L., Cluzeau C., Regnard J. (2007). Hyperbaric gaseous cryotherapy: effects on skin temperature and systemic vasoconstriction. *Archives of physical medicine and rehabilitation, November* 2007, 1339 – 1343.
7. Deonizio J., Werner B., Fabiane A. Mulinari-Brenner. (2014). *Histological comparison of two cryopeeling methods for photodamaged skin.* Hindawi Publishing Corporation*,* 2014, 1–5.
8. Zadorozhnyi B.A. (1985). *Krioterapia v dermatologii (Biblioteka practicheskogo vracha). [Cryotherapy in dermatology (Library of practicing physician)]*. Kyiv: Zdorovie [in Russian].

9. Zemskov V.S., Gasanov L.I. (1988). *Nizkie temperatury v meditsine [Low temperatures in medicine]*. Kyiv: Naukova dumka [in Russian].
10. Anatychuk L.I., Denisenko O.I., Kobylianskyi R.R., Kadeniuk T.Ya. (2015). Pro vykorystannia termoelektrychnoho okholodzhennia v dermatologii ta kosmetologii [On the use of thermoelectric cooling in dermatology and cosmetology]. *Termoelektryka - J.Thermoelectricity,* 3, 57 – 71 [in Ukrainian].
11. Kobylianskyi R.R., Kadeniuk T.Ya. (2016). Pro perspektyvy vykorystannia termoelektryky dlia likuvannia zakhvoriuvan shkiry kholodom [On the prospects of using thermoelectricity for treatment of skin diseases with cold]. *Naukovy visnyk Chernivetskogo universitetu: zbirnyk naukovykh ptrats. Fizyka. Eletronika - Scientific Bulletin of Chernivtsi University: Collection of Scientific Papers. Physics. Electronics,* 5, 1, 67 – 72 [in Ukrainian].
12. Anatychuk L.I., Denisenko O.I., Kobylianskyi R.R., Kadeniuk T.Ya. , Perepichka M.P. (2017). Suchasni metody kriovpluvu u dermatologichnii practytsi [Modern cryotherapy methods in dermatology practice]. *Klinichna ta eksperymentalna patologia – Clinical and Experimental Pathology,* XVI, 1(59), 150 –156 [in Ukrainian].
13. Anatychuk L.I. (1979). *Termoelementy i termoelektricheskie ustroistva [Thermoelements and thermoelectric devices]*. Kyiv: Naukova dumka [in Russian].
14. Anatychuk L.I. (2003). Termoelektrichestvo. T.2. Termoelektricheskie preobrazovateli energii [Thermoelectricity.Vol.2. Thermoelectric power converters]. Kyiv, Chernivtsi: Institute of Thermoelectricity [in Russian].
15. Kolenko E.A. (1967). *Termoelektricheskie okhlazhdaiushchie pribory [Thermoelectric cooling devices]*. Leningrad: Nauka [in Russian].
16. Pennes H.H. (1948). Analysis of tissue and arterial blood temperatures in the resting forearm *J. Appl. Physiol*., 1(2), 93 – 122.
17. Fan L.T., Hsu F.T., Hwang C.L. (1971). A review on mathematical models of the human thermal system *IEEE Trans on Bio-Med. Eng*., 18(3), 218 – 234.
18. Zanchini E., Mariotti M., Salvini S. (1979). Heat transfer in circulatory system *Ras-segna di Bioingegneria,* 8, 33 – 44.
19. Chato J.C. (1980). Heat transfer to blood vessels. *Trasns. ASME. J. Biomech. Eng*., 102(2), 110 – 118.
20. Gordon G. R., Roemer R.B., Horvath S.M. (1976). Mathematical model of the human temperature regulatory system. *Transient cold exposure response. IEEE Trans. Biomed. Eng*., 23(5), 434 – 444.
21. Jiang S.C., Ma N., Li H.J., Zhang X.X. (2002). Effects of thermal properties and geometrical dimensions on skin burn injuries *Burns,* 28, 713 – 717.
22. Cetingul M.P., Herman C. (2008). Identification of skin lesions from the ransient thermal response using infrared imaging technique *IEEE,* 1219 – 1222.
23. Ciesielski M., Mochnacki B., Szopa R. (2011). Numerical modeling of biological tissue heating. Admissible thermal dose. *Scientific Research of the Institute of Mathematics and Computer Science,* 1(10), 11 – 20.
24. COMSOL Multiphysics User's Guide. COMSOLAB. 2010. 804 p.

Subminited 20.03.2017

V. G. Rifert[1] *Doctor of Technical Sciences*,
L. I. Anatychuk[2] *acad. National Academy of Sciences of Ukraine*
P. A. Barabash[3] *Candidate of Technical Sciences*,
V. I. Usenko[3] *Doctor of Technical Sciences*,
A. P. Strikun[1], **A. V. Prybyla**[2] *Candidate fiz. – mat Science*

[1]Thermodistillation Co., Kyiv, Ukraine, *e-mail: v.grifert@ukr.net;*
[2]Institute of Thermoelectricity of the NAS and MES Ukraine,
Nauky str., Chernivtsi, 58029, Ukraine, *e-mail: anatych@gmail.com*
[3] National Technical University of Ukraine
"Kyiv Polytechnic Institute"

IMPROVEMENT OF THE DISTILLATION METHODS BY USING CENTRIFUGAL FORCES FOR WATER RECOVERY IN SPACE FLIGHT APPLICATIONS

Validation of waste water recovery and purification takes its place among the problems to be solved in long-term human space missions. Implementation of vacuum rotary distillation (VRD) is the most promising method of getting high quality water. This method gives a high degree of residue concentration in comparison with other technologies (reverse osmosis and evaporation on porous membranes). The methods of multi-stage distillation (MVRD) and of thermal-electric heat pump (THP) give good results as to power consumption index as well.

The report concerns the history and evolution of VRD and THP development starting from a 3-stage MVRD manufactured and tested in Kyiv Polytechnic Institute (KPI). In 1999 Thermodistillation Co., Ukraine, developed a 5-stage centrifugal distiller named cascade distiller (CD). The results of MVRD with 3 stages and CD are analyzed; the works of various authors who studied CDS characteristics are reviewed. New results demonstrating improved performance of MVRD with THP are represented. Bibl. 29, Fig. 4, Table. 5.

Key words: distiller, thermoelectric heat pump, hydraulic circuit.

Introduction

The technology based on the rotary distillation devices began in 1974 in the former Soviet Union at the Thermal Desalination Department, KPI. The first studies were directed to fundamental research of liquid film hydrodynamics and heat-and-mass transfer under condensation and evaporation on a rotating surface [1-7]. In collaboration with NIIKhimMash, Moscow, Russia, these studies led to the designing and testing of a series of rotary distillers [8-13]. These designs varied from a single-stage one to multi-stage versions to provide for internal heat recovery. The distillers were integrated with heat recovery devices, thermoelectric heat pumps included.

Three MVRD systems with a 5-stage MVRD cascade distiller CD were produced within the period from 2000 to 2006. They were tested at the test benches of the Thermodistillation Co. and Honeywell. In 2007 one of the CDS was mounted at NASA's test bench and beginning from 2009 until now about 20 reports and various kinds of information related to CDS were published. These publications mainly concerned such integral features as specific energy, capacity, and product quality. The attempts of

modelling CDS features were made.

In the present report the attention is drawn to CDS performance and the results of both capacity increasing and specific energy decreasing without CD design changes.

History and evolution of multi-stage vacuum rotary distillation

The rotary multi-stage distiller was developed and manufactured in 1988 and had three stages. A schematic representation of the MVRD is shown in Figure 1. It consists of a complex rotor assembly 20 on bearings 26, 27 and stationary shaft 25 mounted in housing 24. Evaporation and condensation occur within the rotor. Warm urine brine flows through connections 2 and 3 and cooled distillate flows through connections 22 and 23 mounted on the stationary shaft.

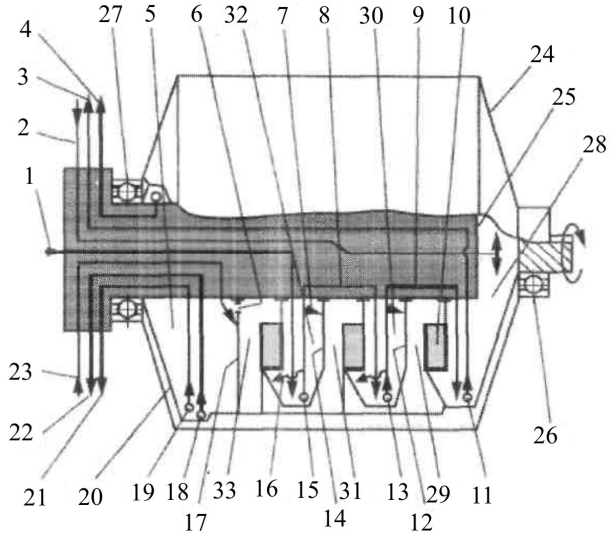

Fig. 1. Multi-stage Vacuum Distillation System Schematic (MVRD).

The MVRD consists of three stages of vacuum distillation connected in series with a thermoelectric heat pump for heating and cooling. There are three evaporation chambers 28, 30, and 32 and three condensation chambers 29, 31, and 33. The chambers are separated by baffles and separators. Alternating evaporation and condensation chambers make up the different stages. The first stage consists of chambers 28 and 29, the second stage consists of chambers 30 and 31, and the third stage consists of chambers 32 and 33. The surfaces 12, 14, and 17 separating the stages act as heat transferring surfaces. It is here where heat recovery occurs due to coincident evaporation and condensation on the opposite sides of the surfaces. This design permits heat recovery by placing vacuum distillation stages in series, so that the latent heat from the phase change can be reused several times and is the key feature for the outstanding performance of this technology.

The MVRD functions in the following manner: All noncondensable gases are removed through the vacuum port 4 prior to starting the operation. The rotational drive motor maintains a constant operating speed. Warm brine/urine from the external heat pump flows through the brine inlet connection 2 to the first-stage evaporation chamber 28. Centrifugal force causes the liquid to spread out into a thin film as it moves to the periphery of the chamber. Some of the water in the flowing thin film is evaporated into steam and flows through the mist separator to the first-stage condensing chamber 29. The brine is cooled as evaporation takes place. Most of the brine liquid travels to the outer edge of the evaporation chamber, where it forms a liquid layer on the inside of the chamber

drum and moves at rotational speed. The stationary Pitot tube (pump) 11 acts to pump the brine to the external heat pump through the outlet connection 3. The heat pump provides the thermal energy to the process as the brine is circulated. The steam from the first-stage evaporator is condensed on the heat

transfer surface 12 of the relatively cold second-stage evaporator. This, in turn, causes evaporation in the second-stage evaporator 30. The steam produced flows through a mist separator to the second- stage condenser 31. It is condensed on the heat transfer surface 14 of the relatively cold third-stage evaporator 32. Once again, evaporation occurs in the third stage evaporator partially due to the condensation in the adjacent chamber. The steam produced flows to the third stage condensing chamber 33 and is condensed on the primary condensing surface 17. This surface is cooled with the cold distillate.

The condensate formed at each of the stages 29, 31, and 33 flows to the outer drum owing to centrifugal forces. Once on the inside wall of the drum, it flows from one stage to the next until it collects in the final condenser chamber 5. Here, it is pumped by the distillate circulation Pitot tube 18 through the distillate outlet connection 22 to the cold side of the heat pump. After passing through a trim cooler, the cooled distillate enters through the connection 23 and sprays the primary condensing surface 17. The heat pump thus provides heating and cooling for the process at an efficiency measured by its coefficient of performance (COP). When the volume of distillate increases due to condensation, it is removed through the distillate product Pitot tube 19 and the distillate product connection 21.

When the volume of brine in the circulating loop decreases because of evaporation, fresh urine is supplied through the inlet connection 1 to the third-stage evaporator 32. This liquid flows to the periphery due to centrifugal forces and forms a liquid ring on the inside of the chamber drum. Some of the entering urine is evaporated and the liquid cooled. The steam produced flows through a mist separator to the condenser chamber 33. When the volume of liquid increases, the liquid layer becomes deeper and covers the third-stage Pitot brine pump 15. It is then pumped to the second-stage evaporator 30 through a passage 8 in the stationary shaft 25. While the brine is being pumped to the next stage, some of the liquid is sprayed on the heat transfer surfaces in the chamber by nozzles 7 and 16. This causes more evaporation by heating the condensate in the adjacent chamber. This process is repeated in the second-stage evaporator, where the entering brine forms a liquid layer that is pumped to the first-stage through passage 9. While being pumped, it is sprayed, evaporated, and cooled.

Technological uniqueness of multi-stage rotary distillation is protected by the patents of Russia [14], Ukraine [15], and USA [16] and is as follows:

- all processes running in MVRD (heat transfer, vapor separation, growth of concentration between the stages, pumping-over of liquid flows) are provided by centrifugal forces exceeding gravity by 100 and more times;
- thin films of evaporating liquid and condensate provide high heat transfer coefficients, low pressure and temperature drops in the stages and in distiller as a whole that is actual for higher efficiency of a thermoelectric heat pump;
- stage design specifics in the absence of gravity and rotor rotation prevent unauthorized migration of distillate and processed liquid in the distiller's cavities;
- evaporation in thin films moving with high velocity prevents formation of the deposits on heat exchanging surfaces; and low requirements to the preliminary treatment of waste water fed to the distiller.
- In Table 1 the results of MRD first model test performed in Thermodistillation Co. in 1991 and the test jointly performed by AlliedSignal Co. and NIIKhimMash (Moscow, Russia) in 1999 are given [17].

In early 2000, Thermodistillation Co. developed, manufactured, and tested a new rotary distillation Cascaded Distiller unit [19-21]. This new unit has five stages providing significantly improved performance. The principle of its operation completely coincides with that of MVRD described above.

Some design changes allowed increasing heat exchange surface of each stage by 17%. In 2009 USA patent [18], where only the layout of treated liquid circuit was of principal novelty, was obtained. In this case, the initial liquid was directed into the first stage, while the maximal concentration took place in the last stage.

Table 1

Results of 3-stage centrifugal distiller tests

Investigator	Liquid	Rotation speed, rpm	Power of THP, W	Capacity, kg/h	Specific power consumption, W·h/kg	Recovery, %
Thermodistillation Co., 1991	Water	1500	297	2.80	132	
	Urine	1550	310	2.50	154	91
NIIKhimMash + AlliedSignal Co., 1999	Urine	1400	293	2.56	144	88

Given in Fig. 2 is the schematic hydraulic representation of CD [22].

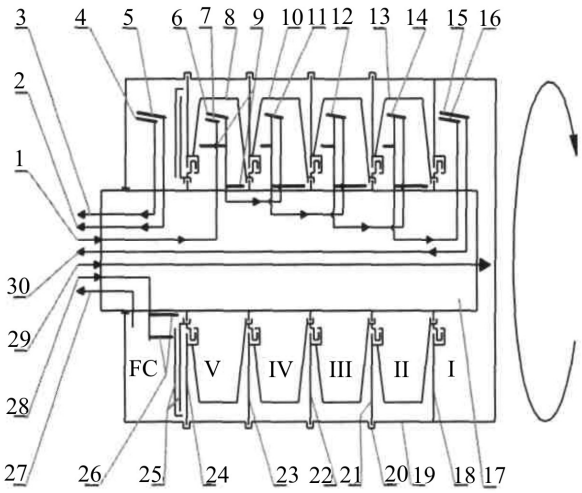

Fig. 2. Schematic hydraulic representation of CD.

Basic components of a distiller are as follows. The rotating part: rotor 19 subdivided by partitions 18, 21 – 24 into five stages (I through V) and a final condenser (FC); heat transfer surfaces 8, 10, 13, 24, 25. The stationary part are: inlet 17 containing passages for feeding and discharging both liquid and vapor; Pitot scoop pumps 4 – 7, 11, 12, 14 – 16 attached to a shaft inside each stage and the final condenser.

A new thermoelectric heat pump was also developed and manufactured by Altec Ltd. (Chernivtsi, Ukraine). Honeywell Inc. has sponsored and led development of the CD and THP. These two devices were tested at Thermodistillation's test facilities in Kyiv with participation of Honeywell personnel to evaluate water reclamation performance.

The ALTEC-7001 thermopile based on the Peltier and Joule effects serves as a heat pump [22, 23]. It provides heat removal from one object and transfer of it together with the Joule heat to another object. The ALTEC-7001 thermopile is comprised of special liquid heat exchangers, thermoelectric modules and liquid collectors forming motion of liquids along the heat exchangers. The heat exchangers meet high technical requirements, namely they must possess low thermal resistance and, on the other hand, must be made of materials resistant to aggressive liquids. Such materials generally possess increased thermal resistance.

Design optimization of heat exchangers was done by computer simulation. This resulted in heat exchanger designs consisting of titanium tubes and aluminum heat concentrators embracing them. To assure a turbulent mode of liquid motion, spiral titanium inserts are mounted into titanium tubes. High demands are imposed on thermoelectric modules, especially as regards reliability. In order to increase the heat pump service life, the module components were connected into parallel-in-series circuits, increasing mean time between failures (MTBF) by hundreds of times.

Figure 3 represents a typical pattern of the thermopile efficiency as a function of electric load and liquid temperature difference at the thermopile input.

The efficiency or heating coefficient has been calculated as the ratio of heat flux output from the thermopile heating cavity to electric power input:

$$Q_h / N_{ip} = G_h c_h (T_{hout} - T_{hin}) / (IU),$$

where: G_h is a mass liquid flow rate in "hot" loop, kg/h; c_h is a heat capacity of liquid in "hot" loop, J/kg-degree; T_{hout} is a liquid temperature in "hot" loop at thermopile heating cavity output, degree; T_{hin} is a liquid temperature in "hot" loop at thermopile heating cavity input, degree; I , U are the electric current and supply voltage of thermopile, respectively.

From Fig. 3 it follows that with increasing temperature difference $\Delta T_{in} = T_{hout} - T_{hin}$ and increasing electric load the efficiency is reduced. That is, the increase in each of these j factors results in growing temperature difference at thermoelement junctions and the degradation of their characteristics.

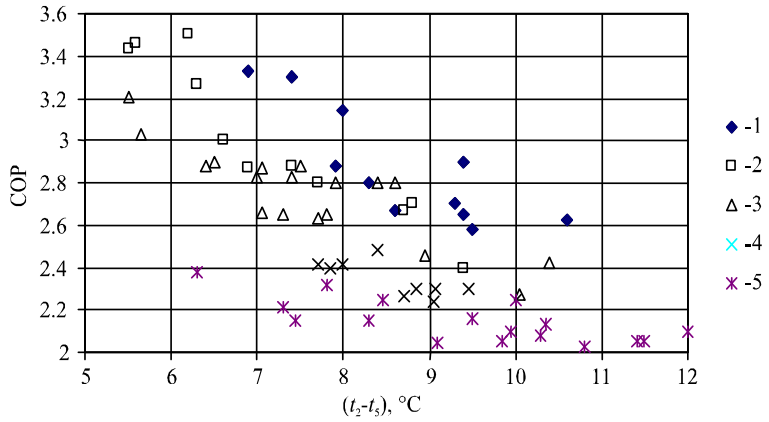

Fig. 3. Impact of electric load and difference in temperature of liquid flows at thermopile input on thermopile efficiency: N_{THP}, W: 1 – 100; 2 – 150; 3 – 200; 4 – 300; 5 – 400.

The cascade distillation system is shown in a simplified form in Fig. 4. The system consists of two main components: a multi-stage vacuum rotary distiller and a thermoelectric heat pump. The feed liquid, such as preserved urine, is fed to the multi-stage vacuum rotary distiller (cascade distiller) where evaporation and condensation of water take place. The multiple stages operate in parallel to provide a high rate of water production. The energy for the process comes from the heat pump, where the distilled water is cooled and the process liquid is heated. Both streams are pumped by the CD in loops to the heat pump and return to the CD. The temperatures of the process are 35°C to 45°C for the hot loop and 20°C to 25°C for the cold one. The other components of the system are used for the storage and control of the liquids used in the process. The feed and removal of liquids are controlled by pressure-controlled valves and do not require a digital controller. The feed liquid is held in a run tank and is delivered to the hot loop through a pressure-controlled valve. The system operates in vacuum and when the volume of the hot loop decreases due to

distillation, its pressure decreases and more feed is sucked into the CD. The product or condensate is delivered to a product tank through a pressure-controlled valve operating in the reverse direction. In this case, the product tank is also held under the system vacuum pressure. When the cold loop volume increases due to distillation, its pressure increases and the valve opens to deliver the product.

The process is operated as a batch process to obtain the maximum recovery of water from the feed liquid. The CD distills product water from the hot loop depleting the volume of the hot loop. The feed liquid is added to the hot loop to maintain constant volume in the hot loop. This process continues until the hot loop is filled with the concentrated brine and the distillation temperature increases. At this point the heat pump is turned off and pressure is restored to ambient. This usually occurs when over 90% of the feed water is distilled and collected in a product tank. The brine is then pumped out of the system to the brine tank and the CD is turned off. A typical batch consists of processing 10 liters of feed, producing 9 liters of the product water and one liter of brine.

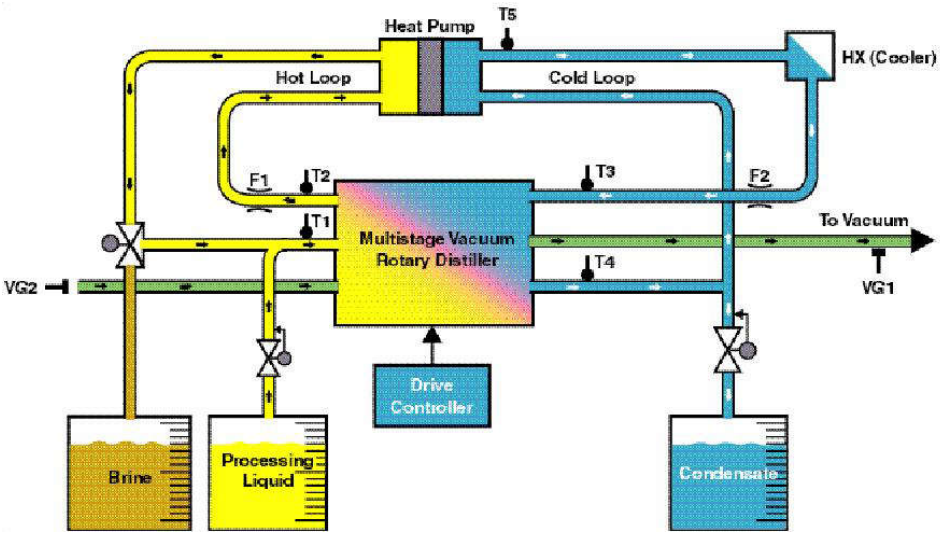

Fig. 4. Cascade Subsystem Functional Diagram.

In [27] the test bench made in Honeywell for JSC Advanced Water Recovery Systems Development Facility is described.

In 2007 Honeywell delivered to NASA the systems with CD and THP developed and manufactured by Thermodistillation RV Co. From 10.10.2007 to 02.08.2008 the Honeywell employees conducted tests of CDS with several liquids [26, 27]. In Tables 2 the averaged data on desalination of seven different liquids are given.

Three competing technologies were evaluated in 2009 for application in a closed loop system, including the Vapor Compression Distillation (VCD), CDS, and the Wiped-Film Rotating Disk (WFRD).

The Distillation Comparison Test evaluated these three distillation technologies at two NASA Centers: Marshall Space Flight Center (MSFC) tested the WFRD and the VCD, while the Johnson Space Center (JSC) tested the CDS according to the detailed test requirements. The test consisted in processing two different waste streams by each of the technologies for a period equivalent to 30 mission days. The objective of this test was to collect performance data sufficient for the adequate comparison of the three technologies. The first waste stream, Solution 1, consisted of pretreated urine and pretreated humidity condensate. The second waste stream, Solution 2, included pretreated hygiene wastewater (from showering, hand washing, brushing teeth, and wet shaving) plus the pretreated urine and pretreated humidity condensate.

Table 2

Summary of Thermodynamic Performance – Solution Verification Test

Solution Type	Batch, kg	Prod. rate, kg/h	Recovery, %	Sp. power, W·h/kg
DI water	6.10	4.53	91.3	93.2
Transit Ersatz	6.37	4.50	77.6	89.3
EPB, Ersatz	6.11	4.53	75.5	88.5
MSFC, Real	6.21	4.27	75.9	94.1
Pretreated Urine (UP)	9.11	4.10	84.4	99.9
TME	9.53	3.93	84.5	103.7
UP+HC	6.5	4.40	80.0	93.9

Quality data on the product obtained after desalination of these two solutions revealed better quality in CDS by all parameters. In Tables 3 and 4 the data on four parameters of specific energy for the three tested systems are shown [28].

Table 3

Summary of Solution №1 Analytical Data (all units are in mg/L, unless other noted)

	CDS			VCD			WFRD		
Parameter	Feed	Distillate	Brine	Feed	Distillate	Brine	Feed	Distillate	Brine
TOC	9.28	0.04	146.23	10.47	0.08	84	9.7	0.1	81
Conductivity, mS/cm	1586	18	25064	1417	24.5	21260	1428	25.5	21520
TIC	< 0.5	< 0.5	< 0.5	11.8	4.76	4.4	11.7	< 0.5	5.8
Ammonia	79	< 0.5	1048	175	0.5	2392	65.3	1.5	169

Table 4

Summary of Solution №2 Analytical Data (all units are in mg/L, unless other noted)

	CDS			VCD			WFRD		
Parameter	Feed	Distillate	Brine	Feed	Distillate	Brine	Feed	Distillate	Brine
TOC	5.33	0.03	54.9	5.56	0.05	38.7	8.7	0.11	29.7
Conductivity, mS/cm	817	9.03	8350	649	15.3	6852	1348	18.2	3250
TIC	<0.5	<0.5	<0.5	7.9	5.64	9.3	13.3	<0.5	10.4
Ammonia	24.7	<0.5	265.8	51	0.6	263	9.3	<0.5	178.5

In Tables 5 and 6 the data on specific energy for the three tested systems are shown.

It should be noted that WFRD, as shown in [28], is not available for operation under zero-gravity, since drain of brine in this distiller is possible due to gravity only.

In [29] such criteria of the system assessment, likely to be successful and risk, are also given.

The VCD was predicted likely to be 84 – 90% successful, with 3% risk in the result. The CDS technology was predicted to be 84 – 87% successful, with 5% risk in the result. The WFRD was predicted to have 52 to 61% of being successful with 7% risk.

For CDS with its history of development about 10 years such parameters are good enough and close to those for VCD with its history exceeding 50 years.

CDS improvement

In NASA and Honeywell plans there is development, manufacture, and test of Generation III CD in 2020. In order to achieve qualitative effect of updating CDS it is necessary to have deep understanding of the principles of its operation and impact of many factors on its efficiency. In all cited above sources analysis of CDS processes and their effect on the system's performance are not given. Besides, the same is with the data on specific power consumption, capacity, COP, the main parameters of distiller and THP. It should be clear that THP specific efficiency depends upon both CD performance (rotation speed, number of stages, configuration and size of heat-exchanging surface) and the parameters of electric and hydraulic circuits of THP.

In testing CD-1, CD-2, and CD-3 in Thermodistillation Co. all data required for the future predictions and analysis were measured. They are as follows:

- THP current and voltage to calculate its power;
- drive current and voltage to calculate drive power;
- quantity of initial liquid, product;
- quantity of removed liquid (drainage of distiller);
- THP hot liquid inlet and outlet temperatures;
- THP cold liquid inlet and outlet temperatures;
- flow rate of circulating liquid in hot loop, G_h;
- flow rate of circulating liquid in cold loop, G_c;
- steam temperature in condensation zone of the last stage;
- salt content in concentrate, C;
- temperature of cooling liquid entering condensation zone of the last stage.

All these data were fixed with a 6-min interval during the whole cycle of evaporation. The cycles of testing (vaporization) equaled to 60, 120, and 180 min.

Altogether, 240 cycles of testing with water, urine, and *NaCl* solution were performed.

For further analysis of the processes by the measured parameters the following parameters were calculated:

- power – N_{THP}, drive power – N_d;
- temperature difference in THP, $\Delta t_{in} = t_{h1} - t_{h2}$;
- hot line temperature difference (liquid overheating), $\Delta t_h = t_h - t_n$;
- cold line temperature difference, $\Delta t_c = t_{c2} - t_{c1}$;
- heat quantity released on hot side of THP, $Q_h = cG_h\Delta t_h$;
- heat quantity released on cold side of THP, $Q_c = cG_c\Delta t_c$;
- THP efficiency, $COP = Q_h / N_{THP}$; and

- specific energy $S_e = (N_{THP} + N_h) / G_d$.

As far back as in 1990 – 1995 we developed the design program of MRD with THP performance to evaluate both dynamic characteristics (temperature and pressure changes in specific points of distillation system, capacity, specific energy, temperature degradation versus time), as well as integral and average per cycle characteristics. Accuracy of the calculations of the expected characteristics first of all depends upon accuracy of the heat transfer coefficient U definition in the distiller stages. The value of U makes it possible to determine temperature drop ΔT in each of the stages and in the whole distiller. ΔT defines temperature drop between hot and cold sides of THP.

Parameter COP as a factor of THP efficiency depends upon ΔT_{in}. Heat transfer coefficient is defined as

$$U = \frac{1}{1/\alpha_c + 1/\alpha_i + \delta_u / \lambda_u}, \quad (1)$$

where α_c is the heat transfer coefficient in condensation on rotating elements of a stage; α_i is the heat transfer coefficient in liquid film evaporation on rotating elements of the stages; δ_u and λ_u are the thickness and heat conductivity of heat exchanging surfaces.

Heat transfer under condensation on the surface rotating disk or cone (95% of heat exchanging surface in MRD) was theoretically and experimentally studied in [1-7].

It is shown in [1, 2, 5, and 6] that the experimental data are in good agreement with Nusselt's theory for laminar film condensation:

$$Nu = \frac{\alpha_c}{\lambda_c}\left(\frac{\nu^2}{g}\right)^{1/3} = 0.66\,\mathrm{Re}_c^{-1/3}, \quad (2)$$

if to replace g in by centrifugal acceleration $\omega^2 R \sin\varphi$ (φ is the angle between the axis of rotation and surface of the heat transfer). In (2) $\mathrm{Re} = qR / (r\mu_c)$.

Heat transfer under liquid film evaporation on the rotating surface α_v can also be determined by (2), since on the main part of the heat-transferring surface $\mathrm{Re} = G_l / (2\pi r \mu_c) < 50$, i.e., a laminar flow of evaporating liquid takes place. Here G_v is the quantity of liquid, which sprinkles the evaporation surface of a stage by Pitot tube.

In the period of 2001 – 2008 several integral CDS characteristics, such as capacity *Gd* as a function of THP power, rotor speed n and system operation time, THP efficiency (COP as a function of N_{NHP}) were investigated. These data do not permit to analyze the impact of the following parameters of desalination: temperature drop at CD stages ΔT_{ef}, concentration degree C and temperature degradation $\Delta T_{\deg}$ related to it, as well as the flow rate of the circulating liquid in the cold and hot loops of the system Gc and Gh, respectively, on these main CDS characteristics.

In the program close to that described in the report [20] the model has been created for prediction of the liquid concentration degree at each stage of CD taking into consideration that the maximal concentration takes place in the first stage of distiller. This prediction results in determination of both temperature degradation $\Delta T_{\deg}$ in each stage and general temperature drop in 5 stages $\sum \Delta T_{\deg}$ in any cycle interval.

In Tables 5A and 5B, as an example, the experimental data relating to local characteristics of urine concentration process obtained in 2006 are presented. The estimated data on the general temperature drop

due to heat transfer $\sum \Delta T_{ef}$, experimental general temperature drop at the THP inlet $\Delta T_{in} = T_1 - T_5$, and estimated general temperature drop in distiller $\sum \Delta T_{incal} = \sum \Delta T_{ef} + \sum \Delta T_{\deg}$, where T_1 is the experimental value of liquid temperature at CD 1st stage outlet and T_5 is the temperature of condensate entering THP from the condensation chamber of the 5th stage.

$$\sum \Delta T_{ef} = \sum Q_d / (U \sum F),$$

where $\sum Q_d = G_d r$; $\sum F = 0.35\,\text{m}^2$ is a general evaporation surface of a CD.

Table 5

Summary of Experimental and predicted data

	φ_{THP}	φ_{SP}, Wh/kg	G_{pr}, kg/h	ΔT_{in}, °C	C, %	$\Delta T_{\deg}$, °C	$\sum \Delta T_{ef}$, °C	$\sum \Delta T_{cal}$, °C
A1	2.40	107	2.58	10.2	23	2.4	3.4	5.8
A2	2.02	116	4.26	14.4	26	2.6	5.5	8.1
B1	2.62	80	3.41	7.7	23	2.3	4.1	6.4
B2	2.35	94	5.40	10.8	18	1.8	6.4	8.2

In Table 5: A1, B1: N_{THP} = 200 W; A2, B2: N_{THP} = 400 W. n = 1100 to 1200 rpm. $G_h \approx G_c = 92$ l/h.

As seen from the table, in both cases, given for comparison, the experimental temperature drop at THP inlet ΔT_{in} is by several degrees above the estimated values.

As the distiller rotor speed increases, the flow rate of the liquid circulating in hot and cold CDS loops increases as well. It facilitates the enhancement of convective heat exchange in THP also and decreases the total temperature drop $\Sigma\Delta T_{THP}$ that, in its turn, increases COP. This increase equals to 6…8% under growth of n from 800 to 1100 rpm. In this case, N_d increases by 2 times. Therefore, it is reasonable to increase the flow rate in circulation loops under high loads of THP (> 400 W), when the drive power consumption is much lower than THP power.

Basing on the test results for three CDS systems we have verified several methods of CDS performance enhancement.

Decrease in temperature drop at THP inlet

The reasons for condensate temperature decrease at the last stage by 3 to 5°C below steam temperature in a final condenser were found and eliminated.

Tests shows that when the overcooling of condensate in the last stage (final condenser) is less and the condensate temperature t_5 is approaching the steam temperature in the last stage, the temperature drop at THP inlet is approaching the predicted value. As a result, under equal initial data THP capacity in the experiments is by 25 – 30% higher and specific flow rate by 15 – 20% lower.

Improvement of THP: electrohydraulic schematic

In 2015, jointly with ALTEC – 7001 (Chernivtsy, Ukraine), we developed a new two-cascade THP2. The main difference between THP2 and THP used by us together with Honeywell earlier in 2004 – 2010 consists in the about twice times decreased operating current at the same power of the THP.

Testing of the new THP2 was carried out at the beginning of 2016 at our test bench in Thermodistillation RV by using MVRD with three stage by evaporation water and *NaCl* solution with concentration of 2.8% under N_{THP} = 200 and 300 W.

The results of these tests revealed the COP increase by 30% and specific energy decrease by 20 - 25%.

In a 5-stage CD under capacity of 5 l/h in recovering urine application of THP2 will decrease specific energy consumption by 20 to 25% down to 80 to 85 W·h/l.

Increase in circulating liquid flow rate in hot and cold loops

The THP efficiency depends upon both inlet temperature difference ΔT_{in} and temperature drop $\Sigma\Delta T_m$ in the very THP module. This drop could be reduced by increasing the enhancement of the convective heat exchange from both sides of THP working modules. Under the turbulent motion of liquid heat transfer α_c is proportional to the circulating liquid flow rate in power of 0.8, i.e., $\alpha_c = f(G^{0.8})$. The flow rate in the loops could be increased in two ways: by updating the Pitot tube and by application of additional pumps.

Earlier in testing HVRD we used an additional pump that increased the liquid flow rate in the loop by 1.3 to 1.4 times under the power supply not exceeding 10 W. The COP was increased by 10 to 11%.

Reduction of thermal resistance on rotating heat-exchanging surface

This method allows reducing the temperature drop ΔT_{st} at the stages and, respectively, the temperature drop at the THP inlet that provides increasing the COP.

The design of the existing CD gives the possibility to increase heat-exchanging surface by 10 to 15% and to reduce the thickness of rotating heat-exchanging elements by 20%. It provides the reduction in $\Sigma\Delta T_{ef}$ by approximately 15%.

Conclusion

The history and evolution of the multi-stage centrifugal vacuum distillation (MRVD) technology for water recovery from waste in the space systems of life support are presented.

The development of this unique technology has been carried out in Kyiv Polytechnic Institute, Ukraine in 1988.

Then this technology was improved by using MRVD with 3 stages.

Since 2000 Thermodistillation RV Co. developed and manufactured three MRVD systems with five stages. These systems named CDS are investigated until now with the outlook of their application in space missions. The results of CDS performance enhancement reducing the specific energy consumption by 20 to 25% are reported.

References

1. Butuzov A.I. and Rifert V.G. An Experimental Study of Heat Transfer during Condensation of Steam at a Rotating Disk. *Heat Transfer-Soviet Research.* 1972. Vol.4. No. 6.November-December
2. Butuzov A.I. and Rifert V.G. Heat Transfer in Evaporation of Liquid from a Film on a Rotating Disk. *Heat Transfer-Soviet Research.* 1973. Vol. 5. No. 1. January-February.
3. Butuzov A.I., Pukhovoy I.I. and Rifert V.G. Experimental Determination of the Minimum Irrigation Density in a Thin-Film Rotating Disk Apparatus. *Fluid Mechanics-Soviet Research.* 1976. Vol. 5. No. 1. January-February.
4. Rifert V.G., Barabash P.A. and Goliyad N.N. Condensation of Steam on a Water Film Falling Down onto Rotating Surface. *Heat Transfer-Soviet Research.* 1984. Vol. 16 No. 3. May-June .
5. Rifert V.G., Intensification of Heat Exchange at Condensation and Evaporation of Liquid in 5 Flowing-Down Films. Proc. of the 9th International Conference Heat Transfer, Israel. 1990.

pp. 293 – 298.

6. Rifert V.G., Pukhovoy I.I., and Nikitenko E.I. Character and Intensity of Heat Exchange at Evaporation of the Fluid Film on the Rotation Disk. *Proc. of the 2nd European Thermal- Sciences and the 14th UIT National Heat Transfer Conference.* Rome, Italy. 1996. May 29 – 31. Vol. 1. pp. 249 – 252.
7. Rifert V.G., Barabash P.A., and Muzhilko A. Flow of Liquid Film over the Surface of a Rotation Disk. *Heat Transfer-Soviet Research.* 1983. Vol. 15. No. 5. pp. 1 – 6.
8. Samsonov, N.M., Bobe, L.S, Novikov, V., Rifert, V.G., et al. Systems for Water Reclamation from Humidity Condensate and Urine for Space Station. SAE Paper 941536, 24th International Conference on Environmental Systems, and 5th European Symposium on Space Environmental Control Systems, Friedrichshafen, Germany. 1994. June
9. Samsonov, N.M., Bobe, L.S, Novikov, V.M., Rifert V.G., Barabash P.A., et al. Development of Urine Processor Distillation Hardware for Space Stations. SAE Paper 951605, the 25th International Conference on Environmental Systems, San Diego. 1995. July.
10. Samsonov, N.M., Bobe, L.S, Novikov, V.M, Rifert V.G., et al. Problems of Developing Systems for Water Reclamation from Urine for Prospective Space Stations. SAE Paper 961409, the 26th International Conference on Environmental Systems, Monterey. 1996. July.
11. Samsonov, N.M., Bobe, L.S, Novikov, V., Rifert V.G., et al., "Updated Systems for Water Recovery from Humidity Condensate and Urine for the International Space Station," SAE Paper 972559, the 27th International Conference on Environmental Systems, Lake Tahoe, July 1997.
12. Samsonov, N.M., Bobe, L.S, Novikov, V.M,, et al. Experience in Development of Systems for Water Reclamation from Urine Based on Distillation with Heat Energy Recuperation. the 6th European Symposium on Space Environmental Control Systems, SP400. 1997. vol. 2.pp. 786 – 791. ESA.
13. Samsonov, N.M., Bobe, L.S, Novikov, V., Rifert V.G., et al. Rationale and Selection of a Distillation Subsystem for Water Reclamation from Urine. SAE Paper 981714, the 28th International Conference on Environmental Systems, Danvers, MA. 1998. July.
14. Samsonov, N.M., Bobe, L.S., Rifert, V.G., Barabash, P.A., et al. The system and Vacuum Centrifugal Distiller for Water Recovery from Urine Aboard of Spacecraft. Patent of Russia Federation for invention #2127627 of 21.07.1998.
15. Rifert, V.G., Usenko, V.I., Strikun, A.P., and Zolotukhin, I.V. Multi-stage Centrifugal Distiller. Patent of Ukraine for invention # 35941A of 16.04.2001.
16. Samsonov, N.M., Bobe, L.S., Rifert, V.G., Barabash, P.A., et al. System and Rotary Vacuum Distiller for Water Recovery from Aqueous Solutions, Preferably from Urine Aboard Spacecraft. Patent of US #6,258,215 B1. Date of Patent: Jul. 10, 2001.
17. Lubman, A, Macknight, A., Reddig, M., Bobe.S.L., Pinski, B.Y., Rakov, V.V., and Edeen, M., "Performance Evaluation of a Three-Stage Vacuum Rotary Distillation Processor", SAE Paper 00ICES-292, the 30th International conference Environmental Systems, Tolouse, France. 2000. July.
18. Apparatus and methods for water regeneration from waste. US Patent 7610768 -. November 4, 2009. Alex M. Lubman, Allen K. Macknight of Signal Hill, Calif, Volodimir G. Rifert, Ivan V. Zolotukhin, Vladimir I. Usenko, Petr A. Barabash and Aleksandr P. Strikun.
19. Rifert, V., V. Usenko, I. Zolotukhin, A. Macknight and A. Lubman, "Design Optimisation of Cascade Rotary Distiller with the Heat Pump for Water Reclamation from Urine", SAE Paper 2001-01-2248, the 31st International Conference on Environmental Systems, Orlando, July 2001.
20. Rifert, V. G., V. I. Usenko, I. V. Zolotukhin, L. I. Anatychuk, A. Macknight and A. Lubman. Development and Test Cascade Centrifugal Distiller for Regeneration of Water from Urine. *Industrial*

Heat Engineering, International Scientific and Applied Journal, National Academy of Sciences of Ukraine. 2001. Vol. 23. No. 4-5.

21. Rifert, V. G., Lubman, A. M., Macknight, A. K., Usenko, V. I. , and Zolotukhin, I. V. Water Recovery System from Brines and Wastewater for Extreme Living Conditions of the Man" – IDA World Congress on Desalination and Water Reuse. Manama, Bahrain. 2001. October 26 – 31.
22. Anatychuk, L.I., Zolotukhin, I.V., Rifert, V.G., Rozver, Yu.Yu., and Usenko, V.I. Use of Thermopile in Water Recovery System for Manned Space Vehicles. *Journal of Thermoelectricity*, 2002. p. 69 – 73.
23. Anatychuk, L.I., Barabash, P.A., Rifert, V.G., Rozver, Yu.Yu., Usenko, V.I., and Cherkez, R.G. Thermoelectric heat pump as a means of improving efficiency of water purification systems on space missions. *Journal of Thermoelectricity*. 2013. #6. pp. 72 – 76.
24. A. Lubman, A. Macknight, V. Rifert, I. Zolotukhin, and K. Pickering. Wastewater Processing Cascade Distillation Subsystem Design and Evaluation. *SAE International.* 2006. 01 – 2273. July.
25. A. Lubman, A. Macknight, V.Rifert, and P. Barabash. Cascade Distillation Subsystem Hardware Development for Verification Testing. *SAE International.* 2007. 01 – 3177. July.
26. M. Callahan, A. Lubman, A. Macknight, H. Thomas, and K. Pickering. Cascade Distillation Subsystem Development Testing. *SAE International.* 2008. 01 – 2195. July.
27. M. Callahan, A. Lubman, and K. Pickering, Cascade Distillation Subsystem Development: Progress toward a Distillation Comparison Test. *SAE International.* 2009. 01 -2401. July.
28. Jeff Mcquillan, Karen D. Pickering, Molly Anderson, Layne Carter, Michael Flynn, Michael Callahan, Leticia Vega, Rama Allada and Jannivine Yeh. Distillation Technology Down-selection for the Exploration Life Support (ELS) Water Recovery Systems Element. *The 40th International Conference on Environmental Systems.* AIAA 2010 – 6125.
29. M. Callahan, V. Patel, and K. Pickering, Cascade Distillation Subsystem Development: Early Results from the Exploration Life Support Distillation Technology Comparison Test. American Institute of Aeronautics and Astronautics, 2010 – 6149. July 2010.

Submitted 16.02.2017.

Ріферт В. Г.[1] *докт. техн. наук*, **Анатичук Л. І.**[2] *акад. НАН України*,
Барабаш П. А.[3] *канд. техн. наук*, **Усенко В. І.**[3] *докт. техн. наук*,
Стрикун А. П.[1], **Прибила А. В.**[2] *канд.фіз.-мат. наук*

[1]Компанія «Термодистилляция», Київ, Україна, *e-mail: v.grifert@ukr.net;*
[2]Інститут термоелектрики НАН і МОН України, вул. Науки, 1,
Чернівці, 58029, Україна, *e-mail: anatych@gmail.com*
[3]Національний технічний університет України
«Київський політехнічний інститут, ім. І. Сікорського», Київ, Україна

ПОКРАЩЕННЯ МЕТОДІВ ДИСТИЛЯЦІЇ ПРИ ВИКОРИСТАННІ ВІДЦЕНТРОВИХ СИЛ ДЛЯ РЕГЕНЕРАЦІЇ ВОДИ ПІД ЧАС КОСМІЧНИХ ПОЛЬОТІВ

Оцінка регенерації й чистоти відпрацьованої води належить до проблем, які необхідно

розв'язати під час довгострокових польотів людини в космос. Найбільш перспективним методом одержання високоякісної води є імплементація вакуумної роторної дистиляції (VRD). Даний метод забезпечує високий ступінь концентрації залишку в порівнянні з іншими технологіями (зворотний осмос і випар на пористих мембранах). Також гарні результати відносно індексу споживання електроенергії дають методи багатокаскадної дистиляції (MVRD) і термоелектричного теплового насоса (THP). Даний звіт присвячений історії й еволюції розробки VRD та THP, починаючи із трьохкаскадного MVRD, розробленого й випробуваного в Київському політехнічному інституті (КПІ). В 1999 році компанія «Термодистилляция» (Україна) розробила 5-каскадний відцентровий дистилятор, який одержав назву каскадного дистилятора (CD). Приводиться аналіз результатів MVRD з 3 каскадами й CD; розглянуті роботи різних авторів, що вивчали характеристики CD. Представлені нові результати, що демонструють поліпшені характеристики MVRD з THP. Бібл. 29, рис. 4, табл. 5.

Ключові слова: дистилятор, термоелектричний тепловий насос, гідравлічна схема.

Риферт В. Г.[1] *докт. техн. наук*, **Анатычук Л. І.**[2] *акад. НАН Украины*,
Барабаш П. А.[3] *канд. техн. наук*, **Усенко В. И.**[3] *докт. техн. наук*,
Стрикун А. П.[1], **Прибыла А. В.**[2] *канд.физ.-мат. наук*

[1]Компания «Термодистилляция», Киев, Украина, *e-mail: v.grifert@ukr.net;*
[2]Институт термоэлектричества НАН и МОН Украины,
ул. Науки, 1, Черновцы,58029, Украина, *e-mail: anatych@gmail.com*
[3]Национальный технический университет Украины
«Киевский политехнический институт», Киев, Украина

УЛУЧШЕНИЕ МЕТОДОВ ДИСТИЛЛЯЦИИ ПРИ ИСПОЛЬЗОВАНИИ ЦЕНТРОБЕЖНЫХ СИЛ ДЛЯ РЕГЕНЕРАЦИИ ВОДЫ ВО ВРЕМЯ КОСМИЧЕСКИХ ПОЛЕТОВ

Оценка регенерации и чистоты отработанной воды относится к числу проблем, которые необходимо решить во время долгосрочных полетов человека в космос (пилотируемых космических полетов). Наиболее перспективным методом получения высококачественной воды является имплементация вакуумной роторной дистилляции (VRD). Данный метод обеспечивает высокую степень концентрации остатка по сравнению с другими технологиями (обратный осмос и испарение на пористых мембранах). Также хорошие результаты в отношении индекса потребления электроэнергии дают методы многокаскадной дистилляции (MVRD) и термоэлектрического теплового насоса (THP). Данный отчет посвящен истории и эволюции разработки VRD and THP, начиная с трехкаскадного MVRD, разработанного и испытанного в Киевском политехническом институте (КПИ). В 1999 году компания «Термодистилляция» (Украина) разработала 5-каскадный центробежный дистиллятор, который получил название каскадного дистиллятора (CD). Приводится анализ результатов MVRD с 3 каскадами и CD; рассмотрены работы различных авторов, изучавших характеристики CD. Представлены новые результаты, демонстрирующие улучшенные характеристики MVRD с THP. Библ. 29, рис. 4, табл. 5.

Ключевые слова: дистиллятор, термоэлектрический тепловой насос, гидравлическая схема.

References

1. Butuzov A.I. and Rifert V.G. (1972). An experimental study of heat transfer during condensation of steam at a rotating disk. *Heat Transfer-Soviet Research,* 4(6), November-December.
2. Butuzov A.I. and Rifert V.G. (1973). Heat transfer in evaporation of liquid from a film on a rotating disk. *Heat Transfer-Soviet Research,* 5(1), January-February.
3. Butuzov A.I., Pukhovoy I.I. Rifert V.G. (1976). Experimental determination of the minimum irrigation density in a thin-film rotating disk apparatus. *Fluid Mechanics-Soviet Research,* 5(1), January-February.
4. Rifert V.G., Barabash P.A., Goliyad N.N. (1984). Condensation of steam on a water film falling down onto rotating surface. *Heat Transfer-Soviet Research,* 16 (3), May-June .
5. Rifert V.G.. (1990). Intensification of heat exchange at condensation and evaporation of liquid in 5 flowing-down films. *Proc. of the 9th International Conference Heat Transfer* (Israel, 1990) (pp. 293 – 298).
6. Rifert V.G., Pukhovoy I.I., Nikitenko E.I. (1996). Character and intensity of heat exchange at evaporation of the fluid film on the rotation disk. *Proc. of the 2nd European Thermal- Sciences and the 14th UIT National Heat Transfer Conference* (Rome, Italy, May 29 – 31, 1996). (Vol. 1. pp. 249 – 252).
7. Rifert V.G., Barabash P.A., and Muzhilko A. Flow of Liquid Film over the Surface of a Rotation Disk. *Heat Transfer-Soviet Research.* 1983. Vol. 15. No. 5. pp. 1 – 6.
8. Samsonov, N.M., Bobe, L.S, Novikov, V., Rifert, V.G., et al.(1994). Systems for water reclamation from humidity condensate and urine for space station. *SAE Paper 941536, 24th International Conference on Environmental Systems, and 5th European Symposium on Space Environmental Control Systems* (Friedrichshafen, Germany, June 1994).
9. Samsonov, N.M., Bobe, L.S, Novikov, V.M., Rifert V.G., Barabash P.A., et al.(1995). Development of urine processor distillation hardware for space stations. *SAE Paper 951605, the 25th International Conference on Environmental Systems* (San Diego, July 1995).
10. Samsonov, N.M., Bobe, L.S, Novikov, V.M, Rifert V.G., et al. Problems of developing systems for water reclamation from urine for prospective space stations. SAE Paper 961409. *The 26th International Conference on Environmental Systems* (Monterey, July 1996).
11. Samsonov, N.M., Bobe, L.S, Novikov, V., Rifert V.G., et al., Updated systems for water recovery from humidity condensate and urine for the international space station, SAE Paper 972559. *The 27th International Conference on Environmental Systems* (Lake Tahoe, July 1997).
12. Samsonov, N.M., Bobe, L.S, Novikov, V.M, et al. (1997). Experience in development of systems for water reclamation from urine based on distillation with heat energy recuperation. *The 6th European Symposium on Space Environmental Control Systems* (Noordwijk, The Netherlands, 20-22 May 1997) (vol. 2, pp. 786 – 791).
13. Samsonov, N.M., Bobe, L.S, Novikov, V., Rifert V.G., et al. (1998). Rationale and selection of a distillation subsystem for water reclamation from urine. SAE Paper 981714. *The 28th International Conference on Environmental Systems* (Danvers, MA, July 1998).
14. *Patent of RF № 35941A* (1998). Samsonov, N.M., Bobe, L.S., Rifert, V.G., Barabash, P.A., et al. The system and vacuum centrifugal distiller for water recovery from urine aboard of spacecraft.
15. *Patent of Ukraine № 35941A* (2001). Rifert, V.G., Usenko, V.I., Strikun, A.P., Zolotukhin, I.V. Multi-stage centrifugal distiller.
16. *Patent of US № 6,258,215 B1* (2001). Samsonov, N.M., Bobe, L.S., Rifert, V.G., Barabash, P.A., et al. System and rotary vacuum distiller for water recovery from aqueous solutions, preferably from urine

aboard spacecraft.

17. Lubman, A, Macknight, A., Reddig, M., Bobe.S.L., Pinski, B.Y., Rakov, V.V., et al. Performance evaluation of a three-stage vacuum rotary distillation processor. SAE Paper 00ICES-292, *30th International Conference Environmental Systems* (Tolouse, France, July 2000).
18. *US Patent № 7610768* (2009). Apparatus and methods for water regeneration from waste. Alex M. Lubman, Allen K. Macknight, Volodimir G. Rifert, Ivan V. Zolotukhin, Vladimir I. Usenko, Petr A. Barabash, Aleksandr P. Strikun.
19. Rifert, V., Usenko V., Zolotukhin I., Macknight A., Lubman A. Design optimisation of cascade rotary distiller with the heat pump for water reclamation from urine. SAE Paper 2001-01-2248, *31st International Conference on Environmental Systems* (Orlando, Florida, July 2001).
20. Rifert, V. G., Usenko V.I., Zolotukhin I.V., Anatychuk L.I., Macknight A., Lubman A. (2001) Development and test cascade centrifugal distiller for regeneration of water from urine. *Industrial Heat Engineering, International Scientific and Applied Journal, National Academy of Sciences of Ukraine,* 23 (4-5).
21. Rifert, V. G., Lubman, A. M., Macknight, A. K., Usenko, V. I., Zolotukhin, I. V. (2001). Water recovery system from brines and wastewater for extreme living conditions of the man. *IDA World Congress on Desalination and Water Reuse* (Manama, Bahrain, October 26 – 31, 2001).
22. Anatychuk, L.I., Zolotukhin, I.V., Rifert, V.G., Rozver, Yu.Yu., Usenko, V.I. (2002). Primenenie termoelektricheskoi batarei v sisteme rekuperattsii vody dlia pilotiruemykh kosmicheskikh korablei [Use of thermopile in water recovery system for manned space vehicles]. *Termoelektryka – J. Thermoelectricity*, №1, 69 – 73 [in Russian].
23. Anatychuk, L.I., Barabash, P.A., Rifert, V.G., Rozver, Yu.Yu., Usenko, V.I., Cherkez, R.G.(2013) Termoelektricheskii teplovoi nasos kak sredstvo povyshchenia effektivnosti sistemy ochistki vody dlia biologicheskikh nuzhd pri kosmicheskikh polyotakh [Thermoelectric heat pump as a means of improving efficiency of water purification systems on space missions]. *Termoelektryka – J. Thermoelectricity,* 6, 72 – 76 [in Russian].
24. Lubman A., Macknight A., Rifert V., Zolotukhin, I., Pickering K. (2006). Wastewater processing cascade distillation subsystem design and evaluation. *SAE International,* 2006 01 – 2273, July 2006.
25. Lubman A., Macknight A., Rifert V., Barabash P. (2007). Cascade distillation subsystem hardware development for verification testing. *SAE International,* 2007-01 – 3177, July 2007.
26. Callahan M., Lubman A., Macknight A., Thomas H., Pickering K. (2008). Cascade distillation subsystem development testing. *SAE International,* 2008. 01 – 2195, July 2008.
27. Callahan M., Lubman A., Pickering K.. (2009). Cascade distillation subsystem development: progress toward a distillation comparison test. *SAE International,* 2009. 01 -2401, July 2009.
28. Mcquillan Jeff, Pickering Karen D., Anderson Molly, Carter Layne, Flynn Michael, Callahan Michael, Vega Leticia, Allada Rama, Yeh Jannivine. (2010). Distillation technology down-selection for the exploration life support (ELS) water recovery systems element. *The 40th International Conference on Environmental Systems* (Barcelona, Spain, 11-15 July 2010).
29. Callahan M., Patel V., Pickering K.. Cascade distillation subsystem development: early results from the exploration life support distillation technology comparison test, *American Institute of Aeronautics and Astronautics,* 2010 – 6149, July 2010.

Subminited 16.02.2017

ARTICLE SUBMISSION GUIDELINES

For publication in a specialized journal, scientific works are accepted that have never been printed before. The article should be written on an actual topic, contain the results of an in-depth scientific study, the novelty and justification of scientific conclusions for the purpose of the article (the task in view).

The materials published in the journal are subject to internal and external review which is carried out by members of the editorial board and international editorial board of the journal or experts of the relevant field. Reviewing is done on the basis of confidentiality. In the event of a negative review or substantial remarks, the article may be rejected or returned to the author(s) for revision. In the case when the author(s) disagrees with the opinion of the reviewer, an additional independent review may be done by the editorial board. After the author makes changes in accordance with the comments of the reviewer, the article is signed to print.

The editorial board has the right to refuse to publish manuscripts containing previously published data, as well as materials that do not fit the profile of the journal or materials of research pursued in violation of ethical norms (for instance, conflicts between authors or between authors and organization, plagiarism, etc.). The editorial board of the journal reserves the right to edit and reduce the manuscripts without violating the author's content. Rejected manuscripts are not returned to the authors.

Submission of manuscript to the journal

The manuscript is submitted to the editorial office of the journal in paper form in duplicate and in electronic form on an electronic medium (disc, memory stick). The electronic version of the article shall fully correspond to the paper version. The manuscript must be signed by all co-authors or a responsible representative.

In some cases it is allowed to send an article by e-mail instead of an electronic medium (disc, memory stick).

English-speaking authors submit their manuscripts in English. Russian-speaking and Ukrainian-speaking authors submit their manuscripts in English and in Russian or Ukrainian, respectively. Page format is A4. The number of pages shall not exceed 15 (together with References and extended abstracts). By agreement with the editorial board, the number of pages can be increased.

To the manuscript is added:

1. Official recommendation letter, signed by the head of the institution where the work was carried out.

2. License agreement on the transfer of copyright (the form of the agreement can be obtained from the editorial office of the journal or downloaded from the journal website – Dohovir.pdf). The license agreement comes into force after the acceptance of the article for publication. Signing of the license agreement by the author(s) means that they are acquainted and agree with the terms of the agreement.

3. Information about each of the authors – full name, position, place of work, academic title, academic degree, contact information (phone number, e-mail address), ORCID code (if available). Information about the authors is submitted as follows:

authors from Ukraine - in three languages, namely Ukrainian, Russian and English;

authors from the CIS countries - in two languages, namely Russian and English;

authors from foreign countries – in English.

4. Medium with the text of the article, figures, tables, information about the authors in electronic

form.

5. Colored photo of the author(s). Black-and-white photos are not accepted by the editorial staff. With the number of authors more than two, their photos are not shown.

Requirements for article design

The article should be structured according to the following sections:

- *Introduction*. Contains the problem statement, relevance of the chosen topic, analysis of recent research and publications, purpose and objectives.
- *Presentation of the main research material* and the results obtained.
- *Conclusions* summing up the work and the prospects for further research in this direction.
- *References*.

The first page of the article contains information:

1) in the upper left corner – UDC identifier (for authors from Ukraine and the CIS countries);

2) surname(s) and initials, academic degree and scientific title of the author(s);

3) the name of the institution where the author(s) work, the postal address, telephone number, e-mail address of the author(s);

4) article title;

5) abstract to the article – not more than 1 800 characters. The abstract should reflect the consistent logic of describing the results and describe the main objectives of the study, summarize the most significant results;

6) key words – not more than 8 words.

The text of the article is printed in Times New Roman, font size 11 pt, line spacing 1.2 on A4 size paper, justified alignment. There should be no hyphenation in the article.

Page setup: "mirror margins" – top margin – 2.5 cm, bottom margin – 2.0 cm, inside – 2.0 cm, outside – 3.0 cm, from the edge to page header and page footer – 1.27 cm.

Graphic materials, pictures shall be submitted in color or, as an exception, black and white, in .opj or .cdr formats, .jpg or .tif formats being also permissible. According to author's choice, the tables and partially the text can be also in color.

Figures are printed on separate pages. The text in the figures must be in the font size 10 pt. On the charts, the units of measure are separated by commas. Figures are numbered in the order of their arrangement in the text, parts of the figures are numbered with letters – a, b, .. On the back of the figure, the title of the article, the author (authors) and the figure number are written in pencil. Scanned images and graphs are not allowed to be inserted.

Tables are provided on separate pages and must be executed using the MSWord table editor. Using pseudo-graph characters to design tables is inadmissible.

Formulae shall be typed in Equation or MatType formula editors. Articles with formulae written by hand are not accepted for printing. It is necessary to give definitions of quantities that are first used in the text, and then use the appropriate term.

Captions to figures and tables are printed in the manuscript after the references.

Reference list shall appear at the end of the article. References are numbered consecutively in the order in which they are quoted in the text of the article. References to unpublished and unfinished works are inadmissible.

Attention! In connection with the inclusion of the journal in the international bibliographic abstract database, the reference list should consist of two blocks: CITED LITERATURE and REFERENCES (this requirement also applies to English articles):

CITED LITERATURE – sources in the original language, executed in accordance with the Ukrainian standard of bibliographic description DSTU 8302:2015. With the aid of VAK.in.ua (http://vak.in.ua) you can automatically, quickly and easily execute your "Cited literature" list in conformity with the requirements of State Certification Commission of Ukraine and prepare references to scientific sources in Ukraine in understandable and unified manner. This portal facilitates the processing of scientific sources when writing your publications, dissertations and other scientific papers.

REFERENCES – the same cited literature list transliterated in Roman alphabet (recommendations according to international bibliographic standard APA-2010, guidelines for drawing up a transliterated reference list "References" are on the site http//www.dse.org.ua, section for authors).

To speed up the publication of the article, please adhere to the following rules:

- in the upper left corner of the first page of the article – the UDC identifier;
- family name and initials of the author(s);
- academic degree, scientific title;

begin a new line, Times New Roman font, size 12 pt, line spacing 1.2, center alignment;

- name of organization, address (street, city, zip code, country), e-mail of the author(s);

begin a new line 1 cm below the name and initials of the author(s), Times New Roman font, size 11 pt, line spacing 1.2, center alignment;

- the title of the article is arranged 1 cm below the name of organization, in capital letters, semi-bold, font Times New Roman, size 12 pt, line spacing 1.2, center alignment. The title of the article shall be concrete and possibly concise;
- the abstract is arranged 1 cm below the title of the article, font Times New Roman, size 10 pt, in italics, line spacing 1.2, justified alignment in Ukrainian or Russian (for Ukrainian-speaking and Russian-speaking authors, respectively);
- key words are arranged below the abstract, font Times New Roman, size 10 pt, line spacing 1.2, justified alignment. The language of the key words corresponds to that of the abstract. Heading "Key words" - font Times New Roman, size 10 pt, semi-bold;
- the main text of the article is arranged 1 cm below the abstract, indent 1 cm, font Times New Roman, size 11 pt, line space spacing 1.2, justified alignment;
- formulae are typed in formula editor, fonts Symbol, Times New Roman. Font size is "normal" – 12 pt, "large index" – 7 pt, "small index" – 5 pt, "large symbol" – 18 pt, "small symbol" – 12 pt. The formula is arranged in the text, center aligned and shall not occupy more than 5/6 of the line width, formulae are numbered in parentheses on the right;
- dimensions of all quantities used in the article are represented in the International System of Units (SI) with the explication of the symbols employed;
- figures are arranged in the text. The figures and pictures shall be clear and contrast; the plot axes – parallel to sheet edges, thus eliminating possible displacement of angles in scaling; figures are submitted in color, black-and-white figures are not accepted by the editorial staff of the journal;
- tables are arranged in the text. The width of the table shall be 1 cm less than the line width. Above the table its ordinary number is indicated, right alignment. Continuous table numbering

throughout the text. The title of the table is arranged below its number, center alignment;

- references should appear at the end of the article. References within the text should be enclosed in square brackets behind the text. References should be numbered in order of first appearance in the text. Examples of various reference types are given below.

Examples of LITERATURE CITED

Journal articles

Anatychuk L.I., Mykhailovsky V.Ya., Maksymuk M.V., Andrusiak I.S. Experimental research on thermoelectric automobile starting pre-heater operated with diesel fuel. *J.Thermoelectricity*. 2016. №4. P.84–94.

Books

Anatychuk L.I. *Thermoelements and thermoelectric devices. Handbook.* Kyiv, Naukova dumka, 1979. 768 p.

Patents

Patent of Ukraine № 85293. Anatychuk L.I., Luste O.J., Nitsovych O.V. Thermoelement.

Conference proceedings

Lysko V.V. *State of the art and expected progress in metrology of thermoelectric materials.* Proceedings of the XVII International Forum on Thermoelectricity (May 14-18, 2017, Belfast). Chernivtsi, 2017. 64 p.

Authors' abstracts

Kobylianskyi R.R. *Thermoelectric devices for treatment of skin diseases*: extended abstract of candidate's thesis. Chernivtsi, 2011. 20 p.

Examples of REFERENCES

Journal articles

Gorskiy P.V. (2015). Ob usloviakh vysokoi dobrotnosti i metodikakh poiska perspektivnykh sverhreshetochnykh termoelektricheskikh materialov [On the conditions of high figure of merit and methods of search for promising superlattice thermoelectric materials]. *Termoelektrichestvo - J.Thermoelectricity,* 3, 5 – 14 [in Russian].

Books

Anatychuk L.I. (2003). *Thermoelectricity. Vol.2. Thermoelectric power converters*. Kyiv, Chernivtsi: Institute of Thermoelectricity.

Patents

Patent of Ukraine № 85293. Anatychuk L. I., Luste O.Ya., Nitsovych O.V. Thermoelements [In Ukrainian].

Conference proceedings

Rifert V.G. Intensification of heat exchange at condensation and evaporation of liquid in 5 flowing-down films. In: *Proc. of the 9th International Conference Heat Transfer*. May 20-25, 1990, Israel.

Authors'abstracts

Mashukov A.O. *Efficiency hospital state of rehabilitation of patients with color carcer.* PhD (Med.) Odesa, 2011 [In Ukrainian].